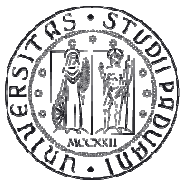

UNIVERSITÀ
DEGLI STUDI
DI PADOVA

Università degli Studi di Padova

Dipartimento di Chimica Biologica

Scuola di dottorato di ricerca in: Biochimica e Biotecnologie

Indirizzo: Biochimica e Biofisica

Ciclo XXIII

Skeletal muscle analysis by two different approaches:
- an *in vivo* model to study the physiology of cellular prion protein
- proteomics to identify biomarkers of illicit animal treatments

Direttore della Scuola: Ch.mo Prof. Giuseppe Zanotti

Coordinatore d'indirizzo: Ch.mo Prof. Maria Catia Sorgato

Supervisore: Ch.mo Prof. Maria Catia Sorgato

Dottorando: Roberto Stella

CONTENTS

LIST OF PAPERS

The following papers which are the main outcome of the present PhD thesis, are enclosed and referred to by Roman numerals (I, II, III).

I Stella R, Massimino ML, Sandri M, Sorgato MC, and Bertoli A.
Cellular prion protein promotes regeneration of adult muscle tissue.
Molecular and Cellular Biology, 2010, 30: 4864-4876.

II Stella R, Massimino ML, Sorgato MC, and Bertoli A.
Prion and TNF-α: TAC(E)it agreement between the prion protein and cell signaling.
Cell Cycle, 2010, 9: 4616-4621.

III Stella R, Biancotto G, Krogh M, Angeletti R, Pozza G, Sorgato MC, James P, and Andrighetto I.
Proteomic profiling of skeletal muscle for discovering biomarkers for growth promoters abuse in beef cattle.
Submitted to Journal of Proteome Research.

Brief summary of other publications in which R. Stella has contributed:

Bendz M, Möller MC, Arrigoni G, Wåhlander A, Stella R, Cappadona S, Levander F, Hederstedt L, and James P.
Quantification of membrane proteins using nonspecific protease digestions.
Journal of Proteome Research, 2009, 8: 5666-5673.

Approximately 30% of all translated genes code for integral membrane proteins. However, despite recent advances in protein technology, membrane proteins still represent one of the most difficult classes of proteins to be studied. There are three main reasons accounting for this problem: (i), the solubilisation and separation difficulties associated with large hydrophobic domains; (ii), the refractory nature toward digestion of this class of proteins; (iii), the large average size of peptides produced by specific endoproteases. Of consequence, the majority of proteins that are generally identified and quantified by current procedures are indeed either membrane associated proteins, or have large extra-membrane domains that behave like soluble proteins. The paucity of digestion sites for sequence-specific proteases close to the membrane domains and the general refractory nature toward digestion due to steric hindrance requires the use of strong denaturing agents that are incompatible with protease activity. Moreover, none of the methods explored so far have proven to be as effective as 1D SDS-PAGE combined to in-gel digestion.

In this work, we used a 1D SDS-PAGE electrophoresis for optimal protein fractionation and denaturation, the latter achievement increasing the accessibility to proteases during the following enzymatic digestion with proteinase-K. Digestion at pH 11 decreased protease activity, thus generating “ragged” peptides with many overlaps that allowed efficient identification and quantification of several membrane proteins. In this study, I was involved in the development of the high pH in-gel digestion protocol using a modified, more stable, acrylamide monomer (i.e. acryloyl-aminopropanol) for the suppression of proteinase-K exopeptidase activity.

Scholz B, Sköld K, Kultima K, Fernandez C, Waldemarson S, Savitski MM, Svensson M, Boren M, Stella R, Andren PE, Zubarev R, and James P.
Impact of temperature dependent sampling procedures in proteomics and peptidomics - A characterization of the liver and pancreas post mortem degradome.
Molecular & Cellular Proteomics, 2010, in press (doi: 10.1074/mcp.M900229-MCP200).

As the accuracy and efficiency of proteome analysis increase, there is an increasing demand for sampling procedures and preparation methodologies that minimize the effect of post-mortem protein degradation. The technical variability caused by protein handling and storage before the proteomic analysis greatly increases the number of samples that need to be processed to achieve statistically relevant results. This is especially true for complex human tissue samples obtained under clinical conditions. A few previous proteomic studies have faced this problem by exploiting 2DE-based protocols.

This is one of the first studies specifically dealing with protein degradation in liver and pancreatic tissues during proteomic procedures. By using 2D-differential in-gel electrophoresis (DIGE) for protein analysis, in combination with label free LC-MS for peptide analysis, we demonstrated that both mouse liver and pancreas are very sensitive to the choice of sampling procedure. This is particularly true for the protease-rich pancreas tissue. A comparison between rapid heat stabilization and snap freezing of fresh tissue samples showed that rapid heat stabilization is much more suited for sample preservation, given that rapidly-frozen samples displayed a larger amount of degradation products. In this project I was mainly involved in the 2D-gel processing of pancreatic and liver samples for the subsequent protein analysis by MALDI-TOF.

Lazzari C, Peggion C, Stella R, Massimino ML, Lim D, Bertoli A, and Sorgato MC.
Cellular prion protein is implicated in the regulation of local Ca^{2+} movements in cerebellar granule neurons.
Journal of Neurochemistry, 2011, in press (doi: 10.1111/j.1471-4159.2010.07015.x).

PrP^C is a cell-surface glycoprotein mainly expressed in the CNS. The structural conversion of PrP^C generates the prion, the infectious agent causing transmissible spongiform

encephalopathies, which are rare and fatal diseases affecting animals and humans. Despite decades of intensive research, the mechanism of prion-associated neurodegeneration and the physiologic role of PrP^C are still obscure. Recent evidence, however, supports the hypothesis that PrP^C may be involved in the control of Ca^{2+} homeostasis. Given the universal significance of Ca^{2+} as an intracellular messenger for both the life and death of cells, this possibility may help explain the complex, often controversial, dataset accumulated on PrP^C physiology, and the events leading to prion-associated neuronal demise.

In this study we have examined the possible involvement of PrP^C in the control of Ca^{2+} homeostasis by analyzing local Ca^{2+} movements in cerebellar granule neurons (CGN) derived from WT and PrP-KO mice. To this end we employed Ca^{2+}-sensitive photo-proteins delivered to CGN by use of Lentiviral expression vectors, and compared the expression levels of major Ca^{2+}-transporting systems in CGN with the two PrP genotypes. We found a dramatic increase of store-operated Ca^{2+} entry in PrP-KO CGN with respect to WT neurons. Notably, this phenotype was rescued upon restoring PrP^C expression. The Ca^{2+}-phenotype of PrP-KO neurons can in part be explained by the lower expression of two major Ca^{2+}-extruding proteins that transport the ion out of the cell, and/or into intracellular stores, namely the plasma membrane (PMCA) and the sarco-endoplasmic reticulum Ca^{2+}-ATPases (SERCA). The lower SERCA content may also contribute to explain why PrP-KO CGN accumulated less Ca^{2+} in the endoplasmic reticulum than the WT counterpart. In this study I was mainly involved inWestern blot analyses of the Ca^{2+}-transporting proteins in purified membrane preparations.

ABBREVIATIONS

2D	two dimensional
2DE	two dimensional gel electrophoresis
bHLH	basic helix-loop-helix
BSE	bovine spongiform encephalophathy
CAM	cell adhesion molecules
cAMP	cyclic adenosine monophosphate
CHAPS	3-[(3-cholamidopropyl)-dimethylammonio]-1-propane-sulfonate
CID	collision induced dissociation
CJD	Creutzfeldt Jacob disease
CNS	central nervous system
CWD	chronic wasting disease
DIGE	differential in gel electrophoresis
DNA	deoxyribonucleic acid
DTT	dithiothreitol
ECM	extra cellular matrix
ELISA	enzyme-linked immunosorbent assay
ER	endoplasmic reticulum
Erk	extracellular signal-regulated kinases
ESI	electrospray ionization
EU	European union
FFI	fatal familial insomnia
FT	Fourier transform
GAGs	glycosamminoglycans
GC	gas chromatography
GPA	growth promoting agent
GPI	glycosyl-phosphatidylinositol
GSS	Gerstmann-Sträussler-Scheinker
HPLC	high performance liquid chromatography
ICAT	isotope coded affinity tags
IEF	isoelectric focusing
IPG	immobilized pH gradient
iTRAQ	isobaric tagging for relative and absolute quantification
KO	knock-out
LC	liquid chromatography
MALDI	matrix-assisted laser desorption ionization
MAPK	mitogen-activated protein kinase
MCK	muscle creatine kinase
MRF	myogenic regulatory factor
MRM	multiple reaction monitoring
mRNA	messenger ribonucleic acid
MS	mass spectrometry
MS/MS	tandem mass spectrometry
m/z	mass-to-charge ratio
NADPH	nicotinamide adenine dinucleotide phosphate (reduced form)
NMR	nuclear magnetic resonance

ORF	open reading frame
pI	isoelectric point
PI3K	phosphoinositide 3-kinase
PK	proteinase K
PKA	protein kinase A
PM	plasma membrane
Prnp	prion protein gene
PrP	prion protein
PrP^{C}	cellular prion protein
PrP^{Sc}	scrapie prion protein (infective isoform of PrP)
Q	quadrupole
RNA	ribonucleic acid
ROS	reactive oxygen species
RP	reversed phase
SCX	strong cation exchange
SDS	sodium dodecyl sulphate
SDS-PAGE	sodium dodecyl sulphate polyacrylamide gel electrophoresis
SILAC	stable isotope labelling with amino acids in cell culture
SP	signal peptide
SPE	solid phase extraction
Tg	transgenic
TMT	tandem mass tags
TNF-α	tumor necrosis factor-alpha
TOF	time of flight
TSE	transmissible spongiform encephalopathies
WT	wild-type

ABSTRACT

Data reported in the present thesis were obtained in two different projects. Accordingly, the thesis is divided into two chapters. The first chapter, which refers to papers I and II, reports a study aimed at unravelling the physiologic role of the cellular prion protein (PrP^C) using an *in vivo* model of skeletal muscle regeneration. The second chapter refers to paper III in which the two dimensional electrophoresis (2DE) approach in combination with tandem mass spectrometry was used to identify potential biological markers of the illegal treatment of bulls with growth promoting agents (GPA).

By focusing on the relationship between PrP^C and skeletal muscle regeneration in a live model, in the first research line (Chapter I) we investigated if and how the protein influences the proliferation and the differentiation of muscle precursor cells. PrP^C is a cell surface glycoprotein involved in the onset of rare and fatal neurodegenerative disorders, known as transmissible spongiphorm encephalopathies (TSE) or prion diseases. TSE occur when PrP^C converts into a conformationally modified isoform that originates the prion, a novel infectious and neuro-pathogenic agent. Although much information is now available on the different routes of prion infection, both the mechanisms underlying prion neurotoxicity and the physiologic role of PrP^C remain unclear. Nonetheless, use of different animal and cell models has suggested a number of putative functions for the protein, ranging from cell protection against oxidative and apoptotic challenge, to cell adhesion, proliferation and differentiation. Skeletal muscles express significant amounts of PrP^C, and have been related to PrP^C pathophysiology by several findings. Therefore, in order to clarify the physiologic role of PrP^C, we employed a degeneration/regeneration protocol to the *tibialis anterior* muscle, which allowed us to compare the regeneration in mice expressing, or not, PrP^C. The analyzed histological and biochemical parameters provided proof for the physiologic relevance of PrP^C commitment in signalling events involved in muscle regeneration. Indeed, we observed that the absence of PrP^C significantly delayed the regenerative process compared to WT muscles. In particular, we found that the lack of PrP^C caused attenuation of the signalling pathway triggered by TNF-α, which in turn decreased the

activation of the p38 kinase pathway, and – consequently – later exit from the cell cycle, and differentiation, of myogenic precursor cells. Importantly, restoring PrP^C expression completely rescued the PrP-KO muscle phenotype, highlighting that regulation of signalling pathways by PrP^C has clear physiologic importance in an extraneural tissue.

The second research line, described in Chapter II, was aimed at setting up a proteomic-based strategy to identify illicit drug treatments in bulls. Classical assays for detecting this kind of illegal practice are not suited to detect compounds either of unknown chemical structure, or present at levels below the quantification threshold of the presently used analytical techniques. The successful application of histological analyses of target organs, which are indirectly modified following these treatments, has suggested that approaches based on the biological effects of the molecules under consideration, rather than the direct detection of their residues, could be potentially valuable in the field. The most relevant advantage of this methodology is that cellular or tissue modifications by drugs remain evident long time after the end of illicit treatments, when chemical residues are no longer, or hardly detectable. On the other hand, this approach is significantly limited by subjective experience and evaluation skill of technicians. Thus new strategies are needed for detecting indirect biomarkers in animal fluids or tissues. These biomarkers can be naturally occurring molecules, such as proteins that are modified in structure, or in concentration, following variations of the normal condition of the animal.

To identify possible biologic markers of illicit drug treatments of beef cattle, we adopted a proteomic approach, including 2D differential in gel electrophoresis (DIGE) and mass spectrometry analysis, to compare the protein expression pattern of muscle specimen from experimentally treated bulls and control animals. To this aim, bulls belonging to the treated cohort were subjected to three different pharmacological protocols, including use of growth promoting agents (GPA). Two of these treatments showed a remarkable anabolic effect compared to untreated animals, resulting in an altered skeletal muscle proteome. 2DE protein maps from treatment and control groups were compared using the DeCyder software for 2D-DIGE maps analysis. We then set out to

identify, using a MALDI-tandem mass spectrometry (MS/MS) approach, all proteins showing a significant alteration in their expression levels following administration of GPA. Among differentially expressed 169 proteins, 29 were identified, most of which were found to be involved in muscle contraction and energy metabolism. These results corroborate previous findings on the mechanism of action of GPA, and may be useful to design new strategies for the discovery of illicit pharmacological treatments in bulls.

RIASSUNTO

I dati riportati nella presente tesi sono stati ottenuti in due diversi progetti. Pertanto, la tesi è divisa in due distinti capitoli. Il primo capitolo, che si riferisce agli articoli I e II, riporta uno studio volto a chiarire il ruolo fisiologico della proteina prionica cellulare (PrP^C) utilizzando un modello *in vivo* di rigenerazione del muscolo scheletrico. Il secondo capitolo si riferisce all'articolo III, in cui si è cercato di individuare possibili marcatori biologici di trattamento illecito di vitelloni con agenti promotori della crescita (GPA), utilizzando un approccio di elettroforesi bidimensionale (2DE), in combinazione con spettrometria di massa.

Focalizzando l'attenzione sul rapporto tra PrP^C e la rigenerazione del muscolo scheletrico in un modello *in vivo*, nella prima linea di ricerca (Capitolo I) abbiamo indagato se e come la proteina influenza la proliferazione e la differenziazione delle cellule precursori del muscolo. PrP^C è una glicoproteina ancorata alla membrana esterna delle cellule coinvolta nella comparsa di malattie neurodegenerative rare e mortali, conosciute con il nome di encefalopatie spongiformi trasmissibili (EST) o malattie da prioni. L'evento alla base delle EST è la conversione della PrP^C in una isoforma con una modificata conformazione che dà origine al prione, un agente infettivo neurotossico. Anche se ora sono disponibili molte informazioni sulle diverse vie di infezione da parte del prione, sia i meccanismi alla base della neurotossicità, sia il ruolo fisiologico della PrP^C rimangono poco chiari. Tuttavia, l'uso di diversi modelli animali e cellulari ha suggerito molteplici funzioni putative per la PrP^C, che vanno dalla protezione cellulare contro lo stress ossidativo e stimoli apoptotici, all'adesione, proliferazione e differenziazione cellulare. Il muscolo scheletrico esprime quantità significative di PrP^C, e molti studi l'hanno correlato alla fisiopatologia della proteina. Pertanto, al fine di chiarire il ruolo fisiologico della PrP^C in questo tessuto, abbiamo impiegato una protocollo di degenerazione/rigenerazione del muscolo tibiale anteriore, che ci ha permesso di confrontare il processo rigenerativo in topi che esprimono, o meno, PrP^C. I parametri istologici e biochimici analizzati hanno fornito prove della rilevanza fisiologica della PrP^C e del suo coinvolgimento negli eventi di segnalazione coinvolti nella rigenerazione muscolare. Infatti, è stato osservato che l'assenza della PrP^C ritarda

significativamente il processo di rigenerazione rispetto ai muscoli WT. In particolare, abbiamo trovato che la mancanza di PrP^C causa un'attenuazione della via di segnalazione attivata dal TNF-α, che porta ad una ridotta attivazione della chinasi p38, e - conseguentemente - ritarda l'uscita dal ciclo cellulare e la differenziazione dei precursori miogenici. È importante sottolineare che il ripristino dell'espressione della PrP^C abolisce completamente il fenotipo osservato nei muscoli di topi PrP-KO, sottolineando che la regolazione delle vie di segnalazione da parte PrP^C ha una chiara importanza fisiologica anche in tessuti extraneuronali.

La seconda linea di ricerca, descritta nel capitolo II, è stata volta a creare una strategia basata su tecniche di proteomica per l'identificazione di trattamenti farmacologici illeciti in vitelloni. L'approccio classico per la rilevazione di questa pratica illegale non è adatto ad individuare composti sia di struttura chimica sconosciuta, sia di farmaci presenti a livelli inferiori alla soglia di quantificazione delle tecniche analitiche attualmente impiegate. Il successo delle analisi istologiche di organi bersaglio, che vengono indirettamente modificati a seguito di questi trattamenti, ha suggerito che gli approcci basati sulla ricerca degli effetti biologici delle molecole in esame, piuttosto che sulla rilevazione diretta dei loro residui, potrebbero essere molto utili. Il vantaggio più rilevante di questa metodologia è che le modificazioni del tessuto indotte da un trattamento farmacologico rimangono evidenti molto tempo dopo la fine dei trattamenti illeciti, quando i residui chimici non sono più, o quasi, rilevabili. D'altra parte, questo approccio è notevolmente limitato dalla capacità di valutazione dei tecnici e l'analisi e influenzata dalla soggettività. Per questo, sono necessarie nuove strategie per il rilevamento dei biomarcatori indiretti presenti nei fluidi animali o nei tessuti. Questi biomarcatori possono essere molecole naturalmente presenti, come ad esempio proteine che abbiano subito modifiche nella struttura, o nella concentrazione, a seguito di variazioni della condizione fisiologica dell'animale.

Per identificare tali marcatori biologici di trattamenti farmacologici illeciti nei bovini da carne, abbiamo adottato un approccio proteomico, mediante elettroforesi differenziale su gel in due dimensioni (2D-DIGE) e analisi in

spettrometria di massa, al fine di confrontare i pattern di espressione proteica di muscolo scheletrico tra animali trattati farmacologicamente e di controllo. A questo scopo, i vitelloni appartenenti al gruppo di trattamento sono stati sottoposti a tre differenti protocolli farmacologici, mediante l'impiego di agenti promotori della crescita. Due di questi trattamenti hanno portato ad un notevole effetto anabolico rispetto agli animali non trattati, mostrando di conseguenza un'alterazione del proteoma del muscolo scheletrico. Le mappe proteiche dei campioni appartenenti ai gruppi di trattamento e di controllo sono state confrontate utilizzando il software DeCyder per analisi di dati derivanti da 2D-DIGE. Si è poi cercato di identificare, con un approccio di spettrometria di massa (MALDI) in tandem (MS/MS), tutte le proteine che mostrano una significativa alterazione nei loro livelli di espressione in seguito a somministrazione di agenti promotori della crescita. Tra le 169 proteine che cambiano in espressione in seguito al trattamento farmacologico, sono state identificate 29 proteine diverse, la maggior parte delle quali è coinvolta nella contrazione muscolare e nel metabolismo energetico. Questi risultati confermano i precedenti risultati sul meccanismo d'azione degli agenti promotori della crescita, e possono essere utili per sviluppare nuove strategie per l'identificazione di trattamenti farmacologici illeciti nei bovini da carne.

CHAPTER I

INVESTIGATING THE PHYSIOLOGIC ROLE OF THE CELLULAR PRION PROTEIN USING A SKELETAL MUSCLE REGENERATION PARADIGM

INTRODUCTION

The prion protein (PrP) was discovered while trying to identify the elusive etiological agent of a group of rare fatal neurodegenerative diseases, known as transmissible spongiform encephalopathies (TSE). Such agents, later termed “prions”, were found in men and animals affected by TSE. Prions are insoluble β-amyloid aggregates that are mainly composed of the aberrant conformer (PrP^{Sc}) of the cellular prion protein (PrP^{C}). PrP^{C} is a highly conserved cell surface sialo-glycoprotein, physiologically expressed – in a non-aggregated form – in all mammalian tissues, particularly in the central nervous system (CNS). The implication of PrP^{Sc} in the onset and transmission of TSE is now well recognised although – despite decades of intensive research – the mechanisms of prion-associated neurodegeneration and the physiologic role of PrP^{C} are still unclear.

Prions and prion disease

TSE can be of infectious, genetic, or sporadic nature, and are characterized by protein aggregation and neurodegeneration (Prusiner, 1998). These diseases include Creutzfeldt-Jakob disease (CJD), Gerstmann-Sträussler-Scheinker (GSS), fatal familial insomnia (FFI), and kuru in humans, scrapie in sheep, chronic wasting disease (CWD) in cervids, and bovine spongiform encephalopathy (BSE), also known as “mad cow disease” in cattle. In 1967, for the first time J.S. Griffith proposed for the first time the concept that a sole protein, without the action of nucleic acid, could “replicate”, thus spreading biological information in other organisms (Griffith, 1967). This proposal was confirmed by several studies demonstrating that the transmissible agent resisted doses of radiation, which easily inactivate both viruses and bacteria

(Alper, 1967), and that its profile of sensitivity of the infectious agent to various chemicals differed from both viruses and viroids (Bellinger-Kawahara *et al*., 1987). Afterwords, Prusiner demonstrated that an unusually protease resistant proteinaceous extract from diseased brains was required for transmitting the disease without the need for other molecules including nucleic acids (Prusiner *et al*., 1984). This and other findings brought Prusiner to reformulate Griffith's hypothesis as the "prion only hypothesis", where the term prion (the acronym for "proteinaceous infectious particle") indicated the novel pathogen (Prusiner 1998). According to this concept, TSE pathogenesis is not determined by a common infectious agent (bacteria, virus), but is caused by a conformational conversion of a normal protein (PrP^{C}) into an aberrant isoform (PrP^{Sc}). PrP^{Sc} is indeed the major component of prions, the suffix "Sc" standing for scrapie (the first "prion disease" to be historically identified). Within the tenets of Prusiner's hypothesis, the most remarkable feature of prions is their capacity to self-propagate into host organisms (i.e., to be infectious), through an auto-catalytic mechanism in which pre-formed PrP^{Sc} seeds promote the structural conversion of other PrP^{C} molecules.

In light of these observations, prions are unique elements in the world of proteins, being able to transmit a biological function, a property that, so far, has been attributed only to nucleic acids. This hypothesis was subsequently supported by the discovery of prions in yeast and fungi, in which they act as heritable protein-based elements that cause biologically important phenotypic changes without, however, any underlying nucleic acid modification (Uptain and Lindquist, 2002).

The cellular prion protein (PrP^{C})

Mammalian PrP^{C} is a sialo-glycoprotein of about 210 aminoacids (a.a.). In its mature glycosilated form, it has an apparent mass of 35-36 kDa. Although expressed in almost all tissues, it is particularly abundant in the CNS.

The PrP gene (*Prnp*), identified in 1986 (Basler *et al*., 1986), is well conserved among mammalian species, and in humans it is localized in the short branch of chromosome 20 (Sparkes *et al*., 1986). The gene is composed by three exons,

although the open reading frame (ORF) is contained entirely in the third exon. For this reason the origin of the two PrP isoforms (PrP^{C} and PrP^{Sc}) from an alternative splicing event was excluded. In humans, the ORF codifies for a 253 a.a. long polypeptide that is subsequently processed in the endoplasmatic reticulum (ER). In the ER, the nascent protein is cleaved at the N-terminus to remove the signal peptide (a.a. 1-22) and at the C-terminus to remove the sequence following the attachment site (a.a. 231-253) for a glycosyl-phosphatidyl-inositol (GPI) anchor (Stahl *et al*., 1987; Rudd *et al*., 1999). The protein is also subjected to N-glycosilation processes on Asn^{181} and Asn^{197} (Figure 1). In the Golgi apparatus, glycans are processed by the removal of mannose residues and the addition of complex oligosaccharidic chains. The mature protein then moves along the secretory pathway to eventually reach the plasma membrane (PM). PrP^{C} is bound to the external leaflet of the PM through the GPI moiety. Like other GPI-anchored proteins, PrP^{C} resides in sphingolipid- and cholesterol-rich microdomains, known as detergent-resistant membranes, or lipid rafts (Taylor and Hooper, 2006), which are considered centres for signal transduction events (Kabouridis, 2006). During its turnover, PrP^{C} is internalized to be either recycled to the PM, or degraded in acidic compartments (Vey *et al*., 1996; Peters *et al*., 2003).

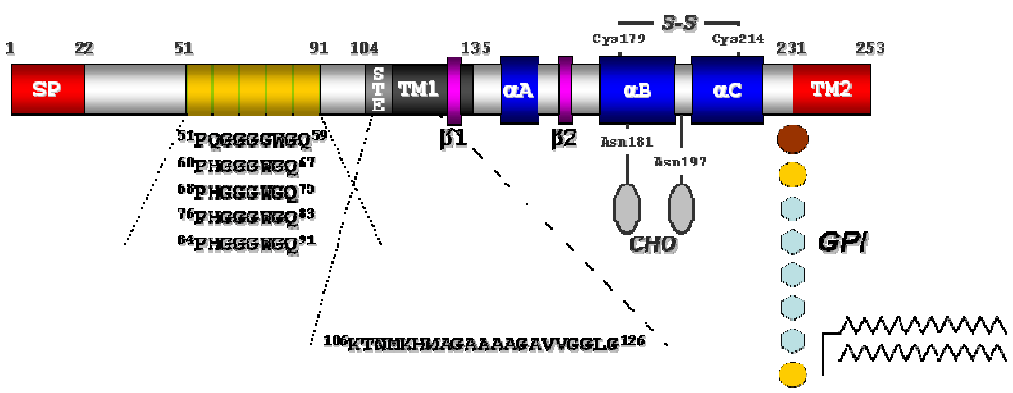

Figure 1. Schematic representation of human PrP^{c}. Mature PrP^{c} (23-230) comprises an unstructured N-terminus (amino acids 23- ~127) and a globular C-domain (residues ~128-230). The following domains are highlighted: the signal peptide (SP, 1-22) for ER import, and the C-end (231-253) (dark-striped boxes), either of which is removed during PrP^{c} maturation; the conserved octapeptide repeat region (51-91) (light-striped box) (the aminoacid sequence of each repeat is reported in the inset); the stop transfer effector (104-111) (STE, light grey box) and the putative transmembrane domain (112-135) (TM, dark grey box); β1 (128-131), and β2 (161-164) β-strands (white dotted boxes); the α-helical region composed of helices αA (144-

154), αB (173-194), and αC (200-220) (grey dotted boxes); Asn^{181} and Asn^{197} for glycans (CHO) attachment; the disulfide bridge (S-S) between Cys^{179} and Cys^{214}; the attachment of the glycosylphosphatidylinositol (GPI) moiety at residue 230. Proteolytic cleavage sites at residue around 90 and at residues 110-111/112, generating the C2 and C1 N-terminally truncated fragments, respectively, are also indicated.

PrP^C is an intriguing protein also from the structural point of view. It is composed of a flexible N-terminus (of about 100 a.a.) and of a globular C-terminus. This latter globular domain, which was studied extensively by NMR (Riek *et al*., 1996), is arranged in three α-helices, interspersed with two short anti-parallel β-strands (Figure 2).

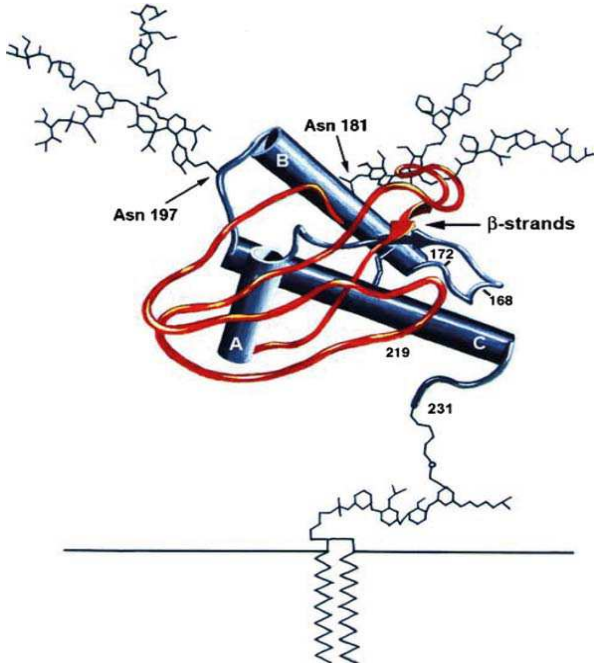

Figure 2. Tri-dimensional structure of the prion protein. The three α-helix and the two short β-strands, composing the structured C-terminus of PrP^C, are shown in the figure. The protein is anchored to outer leaflet of the plasma-membrane through a GPI extension, and contains two N-glycosilation.

The structure is stabilized by a single disulfide bond between two cysteine residues (Cys^{179} and Cys^{214} in the human sequence). Despite the apparent unstructured feature, the N-terminus contains interesting domains: five repetitions of eight aminoacids (PHGGGWGQ) (octarepeats) that can coordinate up-to six copper ions (Brown *et al*., 1997), and a hydrophobic region, located between the octarepeat region and the first α-helix (a.a. 106-126),

which is considered a possible trans-membrane domain, and is likely to exert neurotoxic functions (Forloni *et al*., 1993). Notably, despite the low sequence identity between PrP^{C} in chicken, turtle, frog, or fish, and the mammalian proteins, the major structural features of PrP^{C} are remarkably preserved in those non-mammalian species, suggesting evolutionarily conserved functions of the protein.

The *scrapie* prion protein (PrP^{Sc}) and its conversion from PrP^{C}

PrP^{C} and its aberrant isoform share the same aminoacidic sequence, and undergo identical post-translational modifications. The two isoforms, however, have a different content of secondary structure. The α-helix and β-strands content of PrP^{C} is about 30% and 3%, respectively, while in PrP^{Sc} the percentage of β-strands is as high as 45% (Figure 3). Because it is aggregated and insoluble, PrP^{Sc} structure cannot be studied by conventional methods, but analysis of the PrP sequence has suggested that is part of the N-terminus that is converted into β-structure (Pan *et al*., 1993; Safar *et al*., 1993). The conformational switch confers to PrP^{Sc} novel physico-chemical and biological properties, such as detergent insolubility, propensity to aggregate, resistance to proteolytic digestion, the ability to self-propagate in a host-organism, and, possibly, neurotoxic potentials (Caughey *et al*., 1991; Prusiner, 1984). In particular, the presence of proteinase K (PK)-resistant PrP in brain extracts is often taken as a proof of prion infection. The conversion of PrP^{C} into PrP^{Sc} can be initiated spontaneously, as is likely the case in sporadic or genetic TSEs, or triggered by exogenous prions, as in the case of the infectious forms (for a recent review on prion properties and the putative mechanisms of prion toxicity, see Aguzzi and Calella, 2009).

Although several models have been proposed to account for the formation of PrP^{Sc} aggregates, the basic proposal is that, following infection with PrP^{Sc} seeds, their binding to PrP^{C} leads to further conversion, thus resulting in accumulation of PrP^{Sc} at the expense of normal PrP^{C} molecules. This hypothesis is consistent with the progressive nature of all variants of prion diseases, as well as with the resistance of *Prnp*-KO mice to prion infection

(Brandner *et al*., 1996; Steele *et al*., 2007; Weissmann and Flechsig, 2003). It is also thought to underlie the predominant sporadic forms, in which pathogenesis might start with spontaneous conversion of a fraction of PrP^{C} by hitherto unknown reasons (Fornai *et al*., 2006), and genetic forms associated with certain mutations that destabilize the protein structure (Cohen *et al*., 1994).

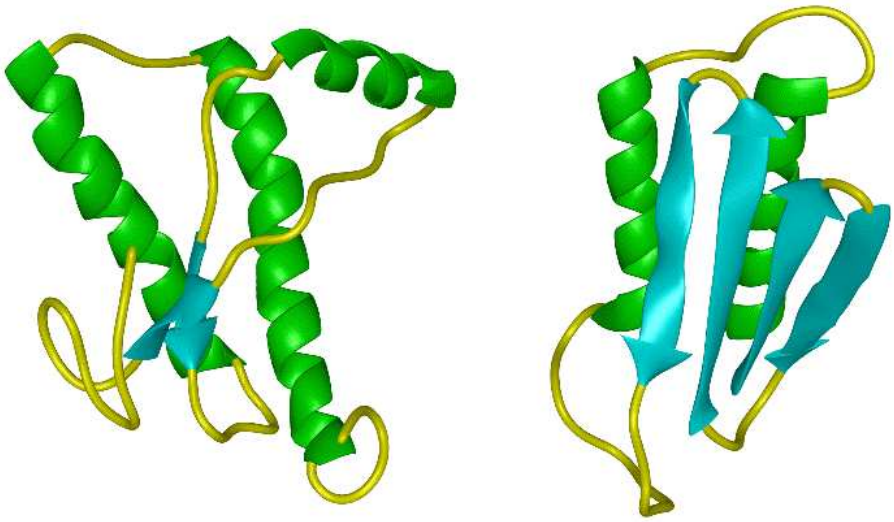

Figure 3. Ribbon drawing of the NMR structure model of PrP^{C} and of the hypotetical structure of PrP^{Sc}. The α-helical regions are shown in green, β-strands in blue, and the unstructured regions in yellow. To be noted the conversion from the prevalent α-helical structure, in PrP^{C} (on the left), to the β-enriched structure, in PrP^{Sc} (on the right) (adapted from Cohen *et al*., 1999).

Despite compelling evidence for the conformational conversion of PrP^{C} in the course of the disease, the molecular mechanisms of neurodegeneration leading to TSE are still unclear. For example, although it is widely assumed that a direct link exists between of PrP^{Sc} accumulation and neuronal demise, systematic examination of deceased patient's brain revealed no spatial correlation between neuronal apoptosis and PrP^{Sc} deposition (Chretien *et al*., 1999; Dorandeu *et al*., 1998). Also arguing against a direct cytotoxic effect of PrP^{Sc} is the report that accumulated PrP^{Sc} within PrP^{C}-expressing tissue grafted into the brains of *Prnp*-KO mice does not damage neighbouring PrP^{C}-null cells (Brandner *et al*., 1996), nor that it is toxic the progressive accumulation of PrP^{Sc} in glial cells around PrP^{C}-null neurons (Mallucci and Collinge, 2004). Moreover, subclinical forms of prion diseases have been observed in experimentally, or naturally,

infected animals that harbour high levels of PrP^{Sc}, but are asymptomatic during a normal life-span (Race and Chesebro, 1998; Hill *et al.*, 2000). Conversely, WT mice inoculated with BSE prions showed no detectable PK-resistant PrP in the brain, despite the presence of neurological symptoms and neuronal death (Lasmezas *et al.*, 1997). These conditions were observed not only in animals but also in humans. FFI, or GSS with A117V substitution revealed striking clinical manifestations but little, or undetectable, PK-resistant PrP (Collinge *et al.*, 1990; Medori *et al.*, 1992).

Thus, the pervasive gain-of-toxic-function hypothesis is still to be fully proven (Samaia and Brentani, 1998), thereby giving strength to the alternative "loss of function hypothesis" implying either PrP^{C} itself or pathways closely associated with the function of PrP^{C} as critical factor in TSE pathogenesis.

Biological functions of PrP^{C}

Initially, the discovery that PrP was the major, if not the only, component of the TSE causative agent has placed the protein in an extremely unfavourable light, but soon after, a wealth of evidence has supported the notion that the protein may positively influence several aspects of the cell physiology. Yet, the physiologic function actually performed by PrP^{C} in the cell still remains enigmatic. A plausible conceptual obstacle to this issue is the lack of serious alterations in lifespan, development, or behaviour of genetically modified mice with the targeted (also post-natal) disruption of the *Prnp* gene (Büeler *et al*., 1992; Manson, 1994; Mallucci *et al*., 2002). Recently, however, mild vacuolar brain degeneration has been observed in PrP-KO mice with FVB genotype. These animals show no prion-like clinical manifestation, but sensorimotor deficits are clearly evident long before the vacuolization stage (Nazor *et al*., 2007). Another current hypothesis proposes that PrP^{C} deficiency provokes subtle changes, whose manifestation needs, however, defined cell stress conditions (reviewed in Steele *et al*., 2007). This notion has recently been supported *in vivo*, in that PrP-KO mice show a defective response to hematopoietic cell depletion (Zhang *et al*., 2006). This result is particularly relevant with respect to the present work, since it is the first example in which

the combination of stress conditions and analysis of extra-neuronal cells provided a clear insight into the functions of PrP^C.

The search for the physiologic role of PrP^C is further confounded by the unrealistic number of functions that have been ascribed to the protein. Indeed, the extensive research devoted in last years to this issue, by means of several cellular and animal models, has resulted in the proposition that PrP^C may play multiple, sometime contrasting, cellular actions, possibly by interacting with extracellular partners, or by taking part in multi-component signaling complexes at the cell surface (for comprehensive reviews see Aguzzi *et al*., 2008; Linden *et al*., 2008).

Nonetheless, there is now a general consensus that PrP^C protects cells from different types of death signals, including serum deprivation (Kim *et al*., 2004), Bax overexpression (Bounhar *et al*., 2001), and anisomycin (Zanata *et al*., 2002). The neuroprotective potentials of PrP^C have also been underscored by studies on ischemic brain injury in rodents. PrP^C is up-regulated after cerebral ischemia, and this correlates with a reduced damage severity (Weise *et al*., 2004; Shyu *et al*., 2005). Accordingly, adenovirus-mediated PrP^C overexpression reduces infarct size and neurological impairment in rat brain (Shyu *et al*., 2005), while – conversely – a more severe ischemic brain injury is observed in PrP-KO mice (McLennan *et al*., 2004; Spudich *et al*., 2005; Weise *et al*., 2006; Mitteregger *et al*., 2007; Steele *et al*., 2009).

PrP^C has been also implicated in cell adhesion, recognition and differentiation. In this case, PrP^C would bind to cell adhesion molecules (CAMs), responsible for cell growth and differentiation (Hansen *et al*., 2008), or other extracellular matrix (ECM) proteins, causing the activation of downstream signalling pathways, thereby explaining the capacity of PrP^C to mediate neuritogenesis and neuronal differentiation, observed in several cell model systems (Steele *et al*., 2006). A case in point is the interaction, with the neuronal adhesion protein N-CAM (Schmitt-Ulms *et al*., 2001) that led to neurite outgrowth (Santuccione *et al*., 2005). N-CAM belongs to the CAM superfamily, which can not only mediate adhesion of cells, or link ECM proteins to the cytoskeleton, but also, following homo- or hetero-phylic interactions, act as a receptor to transduce signals

ultimately resulting in neurite outgrowth, neuronal survival and synaptic plasticity (Hansen *et al*., 2008). Another example is the binding of PrP^C to laminin, an heterotrimeric glycoprotein of the ECM, which induced neuritogenesis together with neurite adhesion and maintenance (Graner *et al*., 2000), but also learning and memory consolidation (Coitinho *et al*., 2006). Further, it has been described that PrP^C interacts with the mature 67 kDa-receptor (67LR) (and its 37 kDa-precursor) for laminin, and with glycosamminoglycans (GAGs), each of which is involved in neuronal differentiation and axon growth (Caughey *et al*., 1994; Rieger *et al*., 1997; Gauczynski *et al*., 2001; Hundt *et al*., 2001; Pan *et al*., 2002). More recently, Hajj *et al*. (2007) have reported that the direct interaction of PrP^C with another ECM protein, vitronectin, could accomplish the same process, and that the absence of PrP^C could be functionally compensated by the overexpression of integrin, another laminin receptor (McKerracher et al., 1996). Incidentally, the latter finding may provide a plausible explanation for the absence of clear phenotypes in mammalian PrP-KO paradigms. By exposing primary cultured neurons to recombinant PrPs, others have shown that homophylic trans-interactions of PrP^Cs are equally important for neuronal outgrowth (Chen et al., 2003; Kanaani *et al*., 2005), including the formation of synaptic contacts (Kanaani *et al*., 2005). Finally, it has been demonstrated that the binding of PrP^C with the secreted co-chaperone stress-inducible protein 1 (STI1) stimulated neuritogenesis (Lopes *et al*., 2005). However, this same interaction had also a pro-survival effect, as did the interaction of PrP^C with its recombinant form (Chen *et al*., 2003).

More recently, by using zebrafish as an experimental paradigm, a lethal developmental phenotype linked to the absence of PrP^C was unravelled. Zebrafish expresses two PrP^C isoforms (PrP1 and PrP2) that, similarly to mammalian PrP^C, are glycosylated and attached to the external leaflet of the plasma membrane through a glycolipid anchor. PrP1 and PrP2 are, however, expressed in distinct time frames of the zebrafish embryogenesis. Accordingly, the knockdown of the PrP1, or PrP2, gene very early in embryogenesis impaired development at different stages (Málaga-Trillo *et al*., 2009). By focusing on PrP1, this study showed that the protein was essential for cell

adhesion, and that the event occurred through PrP1 homophilic trans-interactions and signaling. This comprised activation of the Src-related tyrosine (Tyr) kinase $p59^{fyn}$, and, possibly, Ca^{2+} metabolism, leading to the regulation of the trafficking of E-cadherin, another member of CAMs superfamily. It was also reported that overlapping PrP1 functions were performed by PrP^C from other species, while the murine PrP^C was capable to replace PrP1 in rescuing, at least in part, the PrP1-knockdown developmental phenotype. Apart from providing the long-sought proof for a vital role of PrP^C, the demonstration that a mammalian isoform corrected the lethal zebrafish phenotype strongly reinforces the notion of a functional interplay of PrP^C with CAMs or ECM proteins, and cell signaling, to promote neuritogenesis and neuronal survival (Málaga-Trillo *et al*., 2009).

The most sensible hypothesis for the multifaceted behaviour of PrP^C is that the protein participates in signal transduction centres at the cell surface, as already suggested for other GPI-anchored proteins (Simons and Ikonen, 1997). Accordingly, several putative partners of PrP^C have been proposed (recently reviewed in Aguzzi *et al*., 2008). If one assumes that these interactions are all functionally significant, the most immediate interpretation of this “sticky” behaviour entails that PrP^C acts as a scaffolding protein in different ECM/membrane protein complexes. Each complex could then activate a specific signaling pathway depending on the type and state of the cell, the expression and glycosylation levels of PrP^C, and availability of extra- and/or intra-cellular signaling partners. In line with this proposition, several intracellular effectors of PrP^C-mediated signalling events have been proposed, including $p59^{fyn}$, mitogen-activated kinases (MAPK) Erk1/2, PI3K/Akt, and cAMP-PKA.

For example, it has been shown – by antibody-mediated cross-linking of PrP^C – that activation of the protein in bioaminergic neurons converged to Erk1/2 through $p59^{fyn}$ signalling (Mouillet-Richard *et al*., 2000; Schneider *et al*., 2003). In the same experimental model, antibody ligation of PrP^C also resulted in $p59^{fyn}$-dependent NADPH oxidase activation (Schneider *et al*., 2003), and subsequent production of reactive oxygen species (ROS), ultimately resulting in ROS-mediated downstream signalling (Pradines *et al*., 2009). A PrP^C-

dependent activation of $p59^{fyn}$ (Kanaani *et al*., 2005; Santuccione *et al*., 2005), and Erk1/2 (but also of PI3K and cAMP-PKA) (Chen *et al*., 2003), was evident in other neuronal cell paradigms, and, consistent with the almost ubiquitous expression of PrP^C, in non-neuronal cells such as Jurkat and T cells (Stuermer *et al*., 2004). In addition, it has been proposed that the interaction of PrP^C with STI1 can either lead to neuritogenesis, through the activation of the ERK1/2 pathway, or promote neuronal survival, by impinging on the cAMP/PKA pathway (Lopes *et al*., 2005). Interestingly, this is not the only example reporting that engagement of PrP^C activates simultaneously two independent pathways. In fact, possibly after trans-activating the receptor for the epidermal growth factor, the antibody-mediated clustering of PrP^C was shown to impinge on both the Erk1/2 pathway, and on a protein (stathmin) involved in controlling microtubule dynamics (Monnet *et al*., 2004). It must also be noted that, in line with the alleged role of PrP^C in mediating signal transduction events, perturbations of the ERK1/2 (Spudich *et al*., 2005) and Akt (Weise *et al*., 2006) signalling pathways have been reported upon ischemic challenge in PrP-KO brains with respect to the wild-type counterparts, with consequent increased post-ischemic caspase-3 activation, and exacerbation of neuronal damage. (Spudich *et al*., 2005; Weise *et al*., 2006).

In conclusion, regardless of the still uncertain molecular and cellular mechanisms, a mosaic of experimental data is accumulating that convincingly assign to PrP^C benign functions. This also reinforces the notion that a clear PrP-KO phenotype, which is probably masked by compensative systems in normal circumstances, could emerge under specific stress conditions, and that a loss of function of PrP^C may cause, or take part to, prion-induced neurodegeneration.

The prion protein and muscle tissues

As outlined more extensively in the *Aim* section, to study the involvement of PrP^C in the regenerative process we have used live adult mice subjected to an acute skeletal muscle degenerative injury. Hence, the biology of skeletal muscle regeneration, and the link between PrP^C and muscle, are now briefly reported.

Although neurons are generally regarded as the model of choice for unravelling the function of PrP^C, the expression of the protein in several other organs suggests that PrP^C has a conserved role in different tissues. Thus, important insight into PrP^C function may also be provided from the analysis of extra-neural tissues. One such tissue is skeletal muscle, in which PrP^C is expressed at significant levels (Miele *et al*., 2003; Massimino *et al*., 2006), and upregulated under stress conditions (Zanusso *et al*., 2001). On the other hand, ablation of the *Prnp* gene has been shown to directly affect skeletal muscles, by enhancing, for example, oxidative damage (Klamt *et al*., 2001), or by diminishing tolerance to physical exercise (Nico *et al*., 2005). The skeletal muscle can also be affected by prions. The involvement of peripheral tissues increases the risk of accidental transmission. On the other hand, detection of PrP^{Sc} in non-neuronal easy-accessible compartments such as muscle may offer a novel diagnostic tool. PrP^{Sc} accumulates in the skeletal muscle of individuals (humans and animals) naturally, or experimentally, affected by TSEs (Bosque *et al*., 2002; Glatzel *et al*., 2003; Andreoletti *et al*., 2004; Thomzig *et al*., 2004; Angers *et al*., 2006; Peden *et al*., 2006; Cardone *et al*., 2009; Krasemann *et al*., 2010). In the latter study, it was observed that PrP^{Sc} built up exponentially in the CNS of vCJD infected primates, but that it was preclinically detectable in both CNS and the muscular compartment. Moreover, transgenic (Tg) mouse models of some inherited TSEs, show specific muscular pathological changes. An example is Tg mice expressing the murine homologue of a nine-octapeptide insertional mutation (PG14), where necrotic fibres and accumulation of a PrP^{Sc}-like form in the skeletal muscle were observed (Chiesa *et al*., 2001). Recently, a primary myopathy has been found in a Tg mouse with muscle-specific 40 fold-overexpression of PrP^C, together with abnormal processing of the protein (Huang *et al*., 2007). Notably, skeletal muscle myositis, accompanied by PrP^{Sc}-rich inclusion bodies (Kovacs *et al*., 2004), have been described in two cases of sporadic CJD.

In light of these notions, the skeletal muscle appears a suitable tissue in which studying PrP^C pathophysiology.

Skeletal muscle and satellite cells

Skeletal muscles derive from somites, segments of paraxial mesoderm that form on either side of the axial structures in the vertebrate embryo (Buckingham *et al*., 2003). As somites mature, the dorsal part retains an epithelial structure, known as the dermomyotome, which is the source of myogenic progenitor cells. During the course of muscle development, a distinct subpopulation of myoblasts fails to differentiate, and remains associated with the surface of the developing myofibre as quiescent muscle progenitors, known as satellite cells.

From the time of their initial description in 1961 (Mauro, 1961), satellite cells were credited to be responsible for the growth and maintenance of skeletal muscle. In the adult, satellite cells are mitotically quiescent, and reside in a niche under the basal lamina of the multinucleated muscle fibre. In this state, they exhibit limited gene expression and protein synthesis, but they become readily activated in response to stress conditions, such as those induced by weight bearing, or trauma, and in the context of myodegenerative diseases (reviewed in Chargè and Rudnicki, 2004). The descendants of activated satellite cells, called myogenic precursor cells, or myoblasts, undergo multiple divisions before terminal differentiation. Activated satellite cells, however, can also generate a progeny that restore the pool of quiescent satellite cells (a process known as self-renewal), as demonstrated by the maintenance of satellite cell number in aged muscles after repeated cycles of degeneration and regeneration (Zammit *et al*., 2006). Many molecular processes and signals from the adjacent myofibre, microvasculature, basal membrane, the satellite cell itself, inflammatory cells, and motor neurons may be involved in determining satellite cell quiescence, activation, proliferation, and the subsequent choice between self-renewal and differentiation (Gopinath and Rando, 2008). Although the molecular mechanisms determining satellite cell fate are still largely unknown, it is clear that these cells are the main source of myogenic progenitors involved in the maintenance of adult skeletal muscles, and play key physiologic roles in normal post-natal growth of muscle fibres and regeneration after injuries.

Although there are some marginal discrepancies among the individual markers that identifies satellite cells, there is an overall agreement that the majority of

quiescent satellite cells in the mouse express myostatin, a negative regulator of myogenesis, which leads to a down-regulation of the paired-box proteins Pax3 and Myf5, and prevents the expression of MyoD (Amthor *et al*., 2002). Furthermore, most of them are positive for Pax7, another paired-box transcription factor that seems to be crucial for the maintenance of the satellite cell population during post-natal life (Relaix *et al*., 2006). Several additional novel genes have been recently identified, including CD34, neuritin, and MEGF10, which are expressed in satellite cells *in vivo*, but are not present in primary cultured myoblasts. Importantly, some of these markers are expressed at different levels in quiescent and activated satellite cells.

Pax7 is specifically expressed in satellite cells and their progeny of myogenic precursors in adult muscle, and in primary myoblasts cultured *in vitro*. Pax7 has an essential role in specifying the satellite cell myogenic lineage upstream of the MyoD family of transcription factors. $Pax7^{-/-}$ muscles are reduced in size, the fibres being significantly reduced in diameter and containing approximately 50% of the normal number of nuclei (Seale *et al*., 2000). An extensive analysis of $Pax7^{-/-}$ mice has confirmed the progressive ablation of the satellite cell lineage in multiple muscle groups.

Accordingly, Pax7 is required for the myogenic specification of muscle-derived adult stem cells during regenerative myogenesis. It regulates the process by driving the upregulation of the basic helix-loop-helix (bHLH) transcriptional activators MyoD and Myf5, belonging to the myogenic regulatory factor (MRF) family (Parker *et al*., 2003). Proliferative MyoD- and/or Myf5-positive myogenic cells are termed myoblasts. Proliferating myoblasts eventually exit the cell cycle to become terminally differentiated myocytes that express the late MRFs, myogenin and MRF4, and subsequently muscle-specific genes such as myosin heavy chain (MHC) and muscle creatine kinase (MCK). Finally, mononucleated myocytes fuse with each other to form the multinucleated syncytium, which eventually mature into contracting muscle fibres (Figure 4). The muscle fibres are the basic contractile units of skeletal muscles. They are individually surrounded by a connective tissue layer and grouped into bundles to form a skeletal muscle.

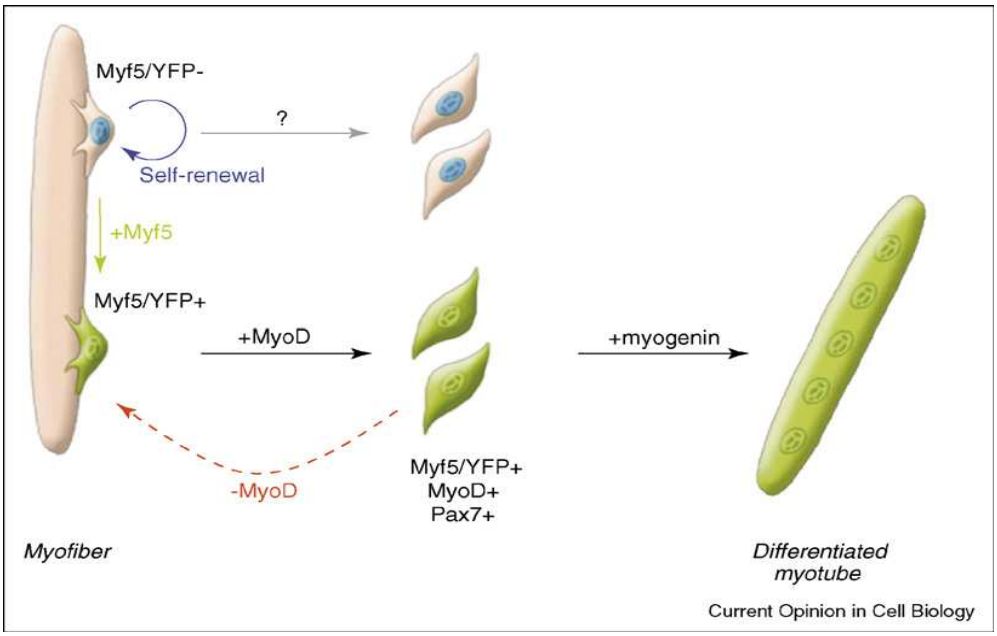

Figure 4. Schematic representation of adult myogenesis. Quiescent skeletal muscle satellite cell can become activated following stimuli from the micro-environment. Their proliferating myoblasts express the paired-box transcriptions factors Pax7 and Pax3, as well as the myogenic regulatory factors Myf5 and MyoD. Once committed to differentiation, myoblasts stop cycling and lose expression of Pax7, Pax3, and Myf5. Differentiating myogenin positive myocytes will then align and fuse to form multinucleated myofibres. MRF4 is further required for hypertrophy of the new fibres (Le Grand and Rudnicki, 2007).

Skeletal muscle regeneration

Adult mammalian skeletal muscle is a stable tissue, and minor lesions inflicted by daily wear and tear elicit only a slow turnover of its constituent multinucleated muscle fibres (Schmalbruch and Lewis, 2000). Nonetheless, mammalian skeletal muscle has the ability to undergo a rapid and extensive regeneration in response to severe damage. Many regulatory processes are involved in skeletal muscle regeneration, among which the specific microenvironment of the satellite cells, the niche, and different growth factors play a major role. In addition, a wide range of other multipotent stem cells has been suggested to take part to the regenerative process (Ten Broek *et al*., 2010).

Whatever the muscle injury, the regeneration process consists of three sequential and partially overlapping steps: i) the inflammatory reaction, dominated by the invasion of macrophages; ii) the activation, differentiation and

fusion of satellite cells; iii) the maturation of newly formed myofibres and remodeling of regenerated muscle. All these stages are in part regulated by the activity of muscle-specific transcription factors of the MRF family (for review see Le Grand and Rudnicki, 2007). These bHLH proteins include MyoD, myogenin, MRF4, and Myf5, each of which can heterodimerize with enhancer proteins, thereby enabling their binding to the regulatory sequences of muscle-specific genes to activate transcription. The initial event of muscle degeneration is necrosis of the muscle fibres. This event is characterized by disruption of the myofibre sarcolemma, that lead to haematoma formation, and is usually accompanied by the activation of mononucleated inflammatory cells and myogenic cells. The inflammatory response is initiated by the release of factors by the injured muscle that activate inflammatory cells residing within the muscle, which in turn provide the chemotactic signals to circulating inflammatory cells (reviewed by Tidball, 1995). During the early phases of the repair process, the necrotic debris is phagocytosed, and regeneration of myofibres begins through the activation of satellite cells (Zammit *et al*., 2006). Firstly, quiescent satellite cells expressing Pax7 migrate to the site of injury, up-regulate the MRFs MyoD and Myf5, and become proliferative (Smith *et al*., 1994; Cooper *et al*., 1999). Subsequently, most of proliferating satellite cells (myoblasts) enter the differentiation program, which is marked by the down-regulation of Pax7 (Zammit *et al*., 2004) and up-regulation of the MRFs MRF4, myogenin (Smith *et al*., 1994) and the transcription factors of myocyte enhancer binding factor-2 (MEF-2) family (Cornelison *et al*., 2000). Cell cycle arrest and chromatin remodeling are key events that allow MEF-2 and MRFs transcription factors to bind to DNA driving the expression of muscle-specific genes that are necessary for the transition to terminal differentiation. Finally, differentiated myocytes either fuse with each other to form multinucleated myofibres, or fuse to damaged myofibres (Chargé and Rudnicki, 2004). It has to be noted, however, that some of the activated satellite cells do not proliferate or differentiate, but self-renew and replenish the satellite cell niche by maintaining Pax7 expression while down-regulating MyoD expression.

The first stages of muscle regeneration after injury, including activation, proliferation, differentiation and fusion of myogenic precursors, can take place in

the absence of the nerve. However, the subsequent growth and maturation of newly formed myofibres requires the presence of the nerve. If neuromuscular connections are not re-established, regenerating myofibres remain atrophic. The demonstration that nerve activity is the crucial factor was achieved by electrical stimulation to promote muscle growth in denervated regenerating muscle (Kalhovde *et al*., 2005).

Inflammation and skeletal muscle regeneration

In general, the program of satellite cell activation and differentiation in regenerating muscles recapitulates embryonic myogenesis. The microenvironment in which myogenesis occurs, however, varies dramatically between embryonic myogenesis and muscle regeneration. In particular, while immune cells are relatively scarce in developing skeletal muscle, they can be present in the regenerative muscle at considerably high concentrations. Because of their capacity to release complex mixtures of proteins that affect the transcriptional activity of target cells, their importance in muscle repair has been recently become matter of interest (Villalta *et al*., 2009; Tidball and Wehling-Henricks, 2007). Although *in vitro* studies showed that the sequence of expression of developmentally regulated, myogenic genes occurs in the absence of myeloid cells, myeloid cells can clearly influence the magnitude and perhaps the timing of expression of at least some of these genes both *in vitro* and *in vivo*. For example, it was reported that conditioned media from J774 macrophage cultures increased the expression of MyoD in primary cycling myoblasts, and of myogenin in differentiating cultured myocytes expression (Cantini *et al*., 2002), indicating that macrophages may promote both proliferation and differentiation of muscle cells. Furthermore, depletion of intramuscular macrophages positive for F4/80 (a marker whose expression increases with macrophage differentiation), during the phase of muscle repair, resulted in a decreased diameter of regenerating myofibres, corroborating the involvement of macrophages in muscle cell differentiation and/or fibre growth (Arnold *et al*., 2007).

As in other tissues, neutrophils are the first responders after muscle injury. Following the onset of neutrophil invasion, phagocytic macrophages (M1 phenotype) begin to accumulate, increasing in number until the second day post injury (Tidball *et al*., 1999). M1 macrophages are a pro-inflammatory cell population implicated in the very early stages after muscle damage that are important to mediate cell debris removal and induction of myogenic precursor cell proliferation. After M1 macrophages reach their concentration peak in injured and regenerative muscle, they are replaced by a population of macrophages (M2) that can attenuate the inflammatory response and promote tissue repair inducing differentiation and fusion of muscle precursors (Villalta *et al*., 2009).

Recent studies showed that the macrophages play a double role in muscle regeneration because they both secrete cytokines affecting satellite cells, and interact with satellite cells protecting them from apoptosis (Chazaud *et al*., 2003). Cytokines are crucial in satellite cells regulation due to the activation of intracellular signaling pathways. These molecules are mostly secreted by active immune cells but also by activated muscle precursor cells after injury. In addition, the vasculature and motor neurons are also responsible for the production and release of soluble factors (Hawke and Garry, 2001).

Among these cytokines, interleukin-6 (IL-6) and tumor necrosis factor-alpha (TNF-α) may be particularly important in contributing to muscle regeneration. Application of IL-6 to cultured myoblasts increases their proliferation but not cell fusion rate (Serrano *et al*., 2008). In line with this observation, the IL-6 null mutant muscle showed slower growth reflecting, at least in part, loss of normal muscle cell differentiation due to an impaired transition from the proliferative stage to the early differentiation stage of myogenesis (Wang *et al*., 2008).

As a later consequence of injury, the expression of TNF-α receptors by muscle cells increases during the regenerative process and enables the direct influence of TNF-α on muscle cells to modulate their proliferation and differentiation. TNF-α and TNF-α receptor null mutants show lower levels of MyoD and MEF-2 expression than wild-type controls following acute injury, suggesting that TNF-α may promote muscle regeneration by positively influencing both the proliferative

and early differentiation stages of regeneration (Chen *et al*., 2005). TNF-α can promote muscle differentiation instead of proliferation through the activation of p38 MAPK. The ability of p38 to promote myogenesis relies, in part, on its ability to phosphorylate MEF-2,thereby increasing its transcriptional activity (Han *et al*., 1997), and in the induction of p21 that - by inhibiting cyclin dependent kinases - eventually accomplishes cell cycle arrest and terminal differentiation (Cabane *et al*., 2003). In particular, increased activation of p38 enhances the activity of MyoD, while p38 inhibition (*in vitro*), prevents myotubes formation and reduces the expression of MEF-2, myogenin, and myosin light chain kinase (Wu *et al*., 2000).

AIM OF THE STUDY

Although various functions have been ascribed to PrP^C, the true physiologic role of the protein is still unclear. Given that PrP^C is abundant in skeletal muscles, and it is upregulated in this tissue during differentiation and in response to cellular stress, we aimed at evaluating if and how PrP^C had an effect in the myogenic process of adult mice. To this end, we analysed the regeneration of the *tibilais anterior* (TA) hindlimb skeletal muscle in adult PrP-KO mice. Both wild-type (WT) and PrP-KO mice reconstituted with transgenic PrP^C served as controls. The applied protocol consisted in first degenerating the muscle with a myotoxin, and then evaluating the myogenic process - from the response to inflammation to the full muscle recovery - using morphometric and biochemical parameters. In particular, we focused on the role of PrP^C in cell proliferation and differentiation, given that this function has been previously suggested by (mainly *in vitro*) studies on neuronal cells. By combining acute insult and adult age, this strategy also had the potential to bypass possible compensatory mechanisms that might have masked until now PrP-KO phenotypes during embryogenesis and/or in adulthood under normal conditions.

The choice of this experimental paradigm was successful given that, using this *in vivo* approach, we provided clear evidence of the physiologic relevance of PrP^C commitment in signaling events involving the release of TNF-α, and in regulating the activation of p38 and Akt kinase pathways.

paper I

MOLECULAR AND CELLULAR BIOLOGY, Oct. 2010, p. 4864–4876 Vol. 30, No. 20
0270-7306/10/$12.00 doi:10.1128/MCB.01040-09
Copyright © 2010, American Society for Microbiology. All Rights Reserved.

Cellular Prion Protein Promotes Regeneration of Adult Muscle Tissue▽†

Roberto Stella,[1] Maria Lina Massimino,[2] Marco Sandri,[3,4] M. Catia Sorgato,[1,2] and Alessandro Bertoli[1]*

Department of Biological Chemistry,[1] CNR Institute of Neuroscience,[2] and Department of Biomedical Sciences,[3] University of Padova, Viale G. Colombo 3, 35131 Padua, Italy, and Dulbecco Telethon Institute-Venetian Institute of Molecular Medicine, Via G. Orus, 2, 35129 Padua, Italy[4]

Received 6 August 2009/Returned for modification 2 September 2009/Accepted 22 July 2010

It is now well established that the conversion of the cellular prion protein, PrP^C, into its anomalous conformer, PrP^{Sc}, is central to the onset of prion disease. However, both the mechanism of prion-related neurodegeneration and the physiologic role of PrP^C are still unknown. The use of animal and cell models has suggested a number of putative functions for the protein, including cell signaling, adhesion, proliferation, and differentiation. Given that skeletal muscles express significant amounts of PrP^C and have been related to PrP^C pathophysiology, in the present study, we used skeletal muscles to analyze whether the protein plays a role in adult morphogenesis. We employed an *in vivo* paradigm that allowed us to compare the regeneration of acutely damaged hind-limb tibialis anterior muscles of mice expressing, or not expressing, PrP^C. Using morphometric and biochemical parameters, we provide compelling evidence that the absence of PrP^C significantly slows the regeneration process compared to wild-type muscles by attenuating the stress-activated p38 pathway, and the consequent exit from the cell cycle, of myogenic precursor cells. Demonstrating the specificity of this finding, restoring PrP^C expression completely rescued the muscle phenotype evidenced in the absence of PrP^C.

The cellular prion protein (PrP^C) is a glycoprotein, prominently expressed in the mammalian central nervous system (CNS) and lymphoreticular system, that is anchored to the cell external surface through a glycolipidic moiety. The bad reputation acquired by PrP^C originates from the notion that an aberrant conformer of it (PrP^{Sc}) is the major component of the prion, the unconventional infectious particle that causes fatal neurodegenerative disorders, i.e., transmissible spongiform encephalopathies (TSE) or prion diseases (56). A wealth of evidence has suggested that the function of PrP^C is beneficial to the cell, but currently, our detailed comprehension of its physiology remains poor. In this respect, the availability of knockout (KO) paradigms for PrP^C has provided less crucial information than expected. Subtle phenotypes, e.g., mild neuropathologic, cognitive, and behavioral deficits, have been described in PrP-KO mice (17, 50), but these animals generally live a normal life span without displaying obvious developmental defects (8, 42). Importantly, the same holds true when the expression of PrP^C is postnatally abrogated (40). The extensive search for PrP^C's *raison d'être* has ascribed to the protein a plethora of functions (for updated reviews, see references 1 and 35); among these, roles in cell adhesion, migration, and differentiation have been proposed whereby PrP^C could act by modulating different cell-signaling pathways (63). In this framework, a variety of neuronal proteins have been hypothesized to interact with PrP^C (reviewed in references 1 and 11), for example, cell adhesion molecules or extracellular matrix proteins, which could explain the capacity of PrP^C to mediate the neuritogenesis and neuronal differentiation observed in several cell model systems (13, 22, 23, 27, 36, 59, 64).

Although neurons are generally regarded as the model of choice for unraveling the function of PrP^C, the expression of the protein in several other organs suggests that PrP^C has a conserved role in different tissues. Thus, important insight into PrP^C function may also be provided by the analysis of extraneural tissues. One such tissue is skeletal muscle, which has been shown to express PrP^C at significant levels (43, 46) and has been found to upregulate PrP^C levels under stress conditions (71). On the other hand, ablation of the PrP gene has been shown to directly affect skeletal muscles, for example, by enhancing oxidative damage (30) or by diminishing tolerance for physical exercise (51). Skeletal muscles have also been associated with prion pathology, as evidenced by the accumulation of PrP^{Sc} (or PrP^{Sc}-like forms) in the muscles of TSE-affected humans and animals (2, 3, 6, 21, 53, 67) and by transgenic-mouse models of some inherited TSEs (16). In addition, overexpression of wild-type (WT) PrP^C (25, 68), or expression of TSE-associated mutants of the protein (16, 66), generates myopathic traits in transgenic mice.

In light of these notions, and because intact muscle tissues are more amenable to *in vivo* manipulations than neural tissue, we set out to analyze the potential role of PrP^C in tissue morphogenesis (38, 41, 46) using an *in vivo* skeletal-muscle paradigm from two congenic mouse lines expressing (WT) or not expressing (PrP-KO) PrP^C. Importantly, to verify that the PrP-KO muscle phenotype was specifically dependent on the absence of PrP^C, we used PrP-KO mice reconstituted with a PrP transgene (PrP-Tg). The applied protocol consisted of first characterizing the degeneration of the hind-limb tibialis

* Corresponding author. Mailing address: University of Padua, Department of Biological Chemistry, Viale G. Colombo, 3, 35131 Padua, Italy. Phone: 39 049 8276150. Fax: 39 049 8073310. E-mail: alessandro.bertoli@unipd.it.

† Supplemental material for this article may be found at http://mcb.asm.org/.

▽ Published ahead of print on 2 August 2010.

anterior (TA) muscle and then evaluating the myogenic process from the response to inflammation to the full recovery of the muscle. By combining acute insult with adult age, this strategy also had the potential to bypass possible compensatory mechanisms that might mask PrP-KO phenotypes during embryogenesis and/or in adulthood under normal conditions (65).

In this study, we provide evidence that, compared to animals expressing PrP^C (WT and PrP-Tg), recovery from damage of adult skeletal muscles was significantly slower in PrP-KO mice. Analysis of the different stages of muscle regeneration allowed us to conclude that PrP^C is one of the factors that govern the early phases of this process, in which the proliferation and differentiation of myogenic precursor cells take place.

MATERIALS AND METHODS

Animal models and degeneration-regeneration protocol. We used 3-month-old male WT mice with the FVB genotype (Harlan) and congenic (FVB) PrP-KO mice (line F10, kindly provided by the MRC Prion Unit, London, United Kingdom) (40), and PrP-Tg mice (39) (line Tg37, kindly provided by Imperial College, London, United Kingdom). Some preliminary experiments were carried out using the *Zrchl* line of PrP-KO mice (8) (kindly provided by A. Aguzzi, University Hospital, Zurich, Switzerland) and WT C57BL/6 mice (Harlan). The TA muscles of these animals were used for the cardiotoxin (CTx)-induced injury model (18, 24). After the animals were anesthetized with isoflurane, the TA muscle of the right hind limb was injected with a single shot of CTx (80 μl of 10 μM Latoxan in sterile phosphate-buffered saline [PBS]). As a control, the contralateral left TA muscle was injected with an equal volume of sterile PBS. The syringe needle (30 gauge) was inserted longitudinally deep into the muscle and was then slowly withdrawn with a little pressure to allow full permeation of the liquid. To assess muscle regeneration on different days post-treatment (p.t.), the mice were euthanized, and their TA muscles were dissected from the hind limb, flash frozen in liquid nitrogen, and stored at −80°C for subsequent analyses.

All aspects of animal care and experimentation were performed in compliance with European and Italian (D.L. 116/92) laws concerning the care and use of laboratory animals. The authors' institution has been authorized by the Italian Ministry of Health for the use of mice for experimental purposes.

Histochemical parameters of muscle regeneration. (i) Fiber dimensions. TA muscle fibers can be classified based on their contractile and metabolic properties, i.e., glycolytic (type 2B) and oxidative (types 2A and 2X) fibers (60), which are characterized by different cross-sectional areas and by a low and a high content of mitochondria, respectively. The dimensions of fibers in control and regenerating muscles were determined separately for the two fiber populations by relating the production of a colored (reduced) ditetrazolium derivative to their contents of mitochondrial succinate dehydrogenase (SDH) (20, 49). Four to six serial 10-μm-thick TA muscle cryosections were treated (30 min; 37°C) with 0.5 ml of phosphate buffer (0.2 M; pH 7.6) containing nitroblue tetrazolium (1.2 mM; Sigma) and sodium succinate (0.2 M). After extensive rinsing, the cryosections were dehydrated using a graded series of ethanol washes (30%, 50%, 70%, 96%, and 100%), washed with xylene, and mounted with Canada balsam (Merck) for image processing. Digitized images were taken of each muscle cross section and stored as gray-level pictures. Image-processing software (Scion Image 0.4.0.3; Scion Corporation) was used to quantify the light transmittance for each pixel of the digitized images, which was subsequently converted to optical density (OD). Each OD reading was calculated by averaging all pixels within the fiber boundaries and was used to determine the OD of SDH staining. Accordingly, we arbitrarily classified muscle fibers as (mitochondrion-rich) oxidative fibers when the OD value was higher than 135 and (mitochondrion-poor) glycolytic fibers when the OD value was lower than 135. At least 200 fibers per muscle section were analyzed.

(ii) H&E staining. Four to six cryosections of each TA muscle were treated (10 min) with a hematoxylin (H) solution (Fluka) to stain nuclei, rinsed for 10 min under running tap water, and then rinsed briefly with distilled water before incubation (10 min) in an eosin (E) solution (Fluka) to stain cytosols. Staining was arrested by multiple washings with distilled water. The cryosections were dehydrated and mounted as described above. The percentage of fibers with 3 or more central nuclei was evaluated as the percentage ratio of the number of fibers with ≥3 central nuclei over the total number of regenerating fibers. Fibers with peripheral nuclei were regarded as being undamaged by the toxin (and hence nonregenerating) and thus were not considered in the calculation. Because this parameter was statistically identical at 9 and 16 days p.t. for each individual mouse line, the reported values (see Fig. 4) are derived from the cumulative counts of 3 fields of each H&E-stained cryosection, using a total of 8 independently treated muscles at 9 and 16 days p.t.

***In vivo* cell proliferation assay.** To determine the extent of proliferation of muscle precursor cells in regenerating TA muscles, the thymidine analogue 5′-bromodeoxyuridine (BrdU) (Sigma) was administered intraperitoneally (50 mg/kg body weight) to CTx-treated mice, either as a single pulse 18 h before the animals' sacrifice (at 5 days p.t.) or, starting from 2 days p.t., as multiple pulses every 48 h before the animals' sacrifice (at 9 days p.t.). Transverse TA muscle cryosections (10 μm) were then fixed with 2% (wt/vol) paraformaldehyde in PBS (10 min; 4°C) on glass coverslips. The sections were treated with proteinase K (Roche; 20 μg/ml in 10 mM Tris-HCl [pH 7.4]; 20 min; 37°C), dipped in HCl (4 M; 30 min; room temperature [RT]), and then washed with PBS. After nonspecific binding sites were blocked with bovine serum albumin (BSA) (1% [wt/vol] in PBS supplemented with 0.1% [wt/vol] Tween 20 [PBS-T]) for 15 min at RT, the sections were incubated with an anti-BrdU monoclonal antibody (MAb) conjugated to the fluorochrome Alexa-488 (Invitrogen; catalog no. A21303) (1:40 in PBS-T containing 0.5% [wt/vol] BSA; 18 h; 4°C). After extensive washing in PBS, the sections were incubated with a rabbit antilaminin polyclonal antibody (PAb) (Sigma; catalog no. L9393) (1:100 in PBS-T; 1 h; 37°C) to discriminate muscle precursors/fibers from nonmuscle cells. After being washed with PBS, the sections were treated with a tetramethyl rhodamine isocyanate (TRITC)-conjugated anti-rabbit secondary antibody (BD Biosciences) (1:100 in PBS-T; 1 h; 37°C) and extensively washed with PBS. The immunostained sections were observed with an inverted fluorescence microscope (Axiovert 100; Zeiss) equipped with a computer-assisted charge-coupled device (CCD) camera (AxioCam; Zeiss), and 6 fields from each section were digitized and stored for subsequent analysis. The proliferation index was calculated as the ratio between the number of BrdU-positive nuclei in laminin-positive cells/fibers and the total number of laminin-positive cells/fibers.

Western blotting and densitometric analyses. (i) Western blotting. TA muscle samples were homogenized in lysis buffer (62.5 mM Tris-HCl [pH 6.8], 10% glycerol, 2.3% sodium dodecyl sulfate [SDS], and protease inhibitors [Roche]) and centrifuged (16,000 × *g*; 10 min; 4°C) to remove cell debris. When samples were used for analyzing phosphorylated proteins, a cocktail of phosphatase inhibitors (25 mM sodium fluoride, 5 mM sodium orthovanadate, 0.5 μM okadaic acid) was added to the lysis buffer. After the total protein content was determined (BCA assay kit; Invitrogen), tissue homogenates were diluted in Laemmli sample buffer (LSB) and boiled (5 min). SDS-PAGE was carried out using (i) 12% acrylamide and 20 μg of proteins per lane (resuspended in LSB with no reducing agents) for detecting PrP^C; (ii) 10% acrylamide and 40 μg of proteins per lane (resuspended in LSB with no reducing agents) for determining Pax7; (iii) 7% acrylamide and 5 μg of proteins per lane (resuspended in LSB with 5% [vol/vol] β-mercaptoethanol as a reducing agent) for analyzing neonatal/developmental myosin heavy chain (neo-MHC); and (iv) 4 to 12% gradient precast acrylamide gels (Invitrogen) and 30 μg of proteins per lane (resuspended in LSB with 50 mM dithiothreitol as a reducing agent) for detecting F4/80, p38, and Akt (total or phosphorylated) and tumor necrosis factor alpha (TNF-α). The proteins were then electroblotted onto nitrocellulose membranes (Bio-Rad), which were stained with Ponceau red (Ponceau S; Sigma) to verify equal loading and transfer. The membranes were incubated (1 h at RT) with a blocking solution that, depending on the antibody used, contained either nonfat dry milk (5% [wt/vol]; Bio-Rad) (for neo-MHC and F4/80) or BSA (3% [wt/vol]; Sigma) (for PrP^C, Pax7, p38, Akt, and TNF-α) in PBS-T. The membranes were then incubated with the desired primary antibody (1 h at RT) diluted in the blocking solution. After being washed three times with PBS-T (10 min each time), the membranes were incubated (1 h at RT) with the following horseradish peroxidase-conjugated secondary antibody: anti-mouse IgG or anti-rabbit IgG (Santa Cruz Biotechnology; 1:3,000 in the blocking solution) or anti-rat IgG (Sigma; 1:10,000 in the blocking solution), according to the primary antibody (see below). After the membranes were washed, immunoreactive bands were visualized on a digital Kodak Image Station, using an enhanced-chemiluminescence reagent kit (Millipore).

(ii) Densitometric analysis. For densitometric analysis, band intensities were evaluated with the Kodak 1D image analysis software. In some cases, to compare different gels for quantifying the expression of a given protein, the intensities of the immunoreactive bands were normalized to that of a unique standard sample loaded into each gel. Standard samples were produced by pooling equal amounts of protein from regenerating TA muscle samples.

(iii) Antibodies. For immunoblotting, the following antibodies were used (dilutions are in parentheses): anti-PrP mouse MAb 8H4 (1:6,000) (a kind gift from

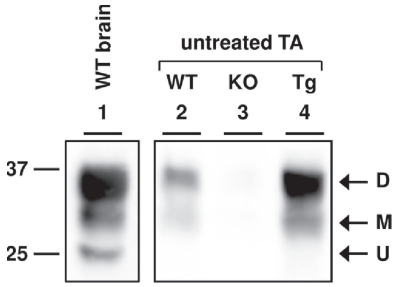

FIG. 1. Immunodetection of PrP^C in untreated TA muscles of different mouse strains. TA samples from 3-month-old WT, PrP-KO, and PrP-Tg male mice were homogenized, and proteins (20 μg per lane) were resolved in a 12% SDS-PAGE gel under nonreducing conditions, electroblotted onto a nitrocellulose membrane, and then probed with anti-PrP MAb 8H4. The PrP^C immunosignal was readily appreciable in the muscle from WT mice (lane 2) and was significantly increased in the PrP-Tg TA muscle (lane 4). Conversely, no signal was evident in the PrP-KO sample (lane 3). Equal protein loading in each lane was verified by Ponceau red staining of the nitrocellulose membrane. For comparison, the immunosignal of a WT brain homogenate (5 μg of proteins) is also shown (lane 1). The arrows on the right indicate the different PrP^C glycoforms, i.e., unglycosylated (U), monoglycosylated (M), and diglycosylated (D). Molecular mass standards (kDa) are shown on the left. The blot is representative of 8 independent experiments that yielded comparable results.

M. S. Sy, Case Western University, Cleveland, OH), anti-neo-MHC mouse MAb BF-34 (1:1,000) (a kind gift from S. Schiaffino, University of Padua, Padua, Italy), anti-Pax7 mouse MAb (1:300) (a kind gift from L. Vitiello, University of Padua, Padua, Italy), anti-F4/80 rat MAb (1:500) (AbCam; catalog no. AB6640), anti-p38 rabbit PAb (1:1,000) (Cell Signaling Technology; catalog no. 9212), anti-phosphorylated (at both Thr180/Tyr182)-p38 rabbit MAb (1:1,000) (Cell Signaling Technology; catalog no. 9211), anti-Akt rabbit PAb (1:1,500) (Santa Cruz Biotechnology; catalog no. sc-8312), anti-phosphorylated (at Ser473)-Akt rabbit PAb (1:1,500) (Santa Cruz Biotechnology; catalog no. sc-7985R), and anti-TNF-α rabbit PAb (1:1,000) (Cell Signaling Technology; catalog no. 3707).

Statistics. Values are reported as means ± standard errors of the mean (SEM); *n* indicates the number of biological replicates. Given that we always compared pairs of samples (i.e., PrP-KO and WT; PrP-KO and PrP-Tg), statistical analysis was performed using a two-sample Student's *t* test, with a *P* value of <0.05 considered statistically significant.

RESULTS

To investigate the contribution of PrP^C to muscle cell maturation during adulthood, we adopted a protocol (18, 24) that allowed us to compare the *in vivo* regeneration of the hindlimb TA muscles of PrP-KO and PrP^C-expressing (WT and PrP-Tg) mice. To achieve this, we first severely damaged the skeletal muscles of 3-month-old male mice by injecting a myotoxin (CTx) and then analyzed the contribution of PrP^C to the reestablishment of muscle integrity by using histochemical and biochemical tools. It is important to note that CTx specifically provokes necrosis of all muscle fibers, leaving nerves, the blood supply, and satellite cells intact (18). Satellite cells are the major stem cells of adult skeletal muscles, which account for the remarkable capacity of this tissue for maintenance and repair. Immediately after damage, satellite cells, which normally reside between the basal lamina and the sarcolemma of myofibers, migrate to the lesion center, where they extensively proliferate and originate into cycling myoblasts that eventually differentiate into mononucleated myocytes. After approximately 4 to 5 days p.t., these myocytes start to fuse to generate polynucleated myofibers that progressively accomplish full muscle maturation (12, 24).

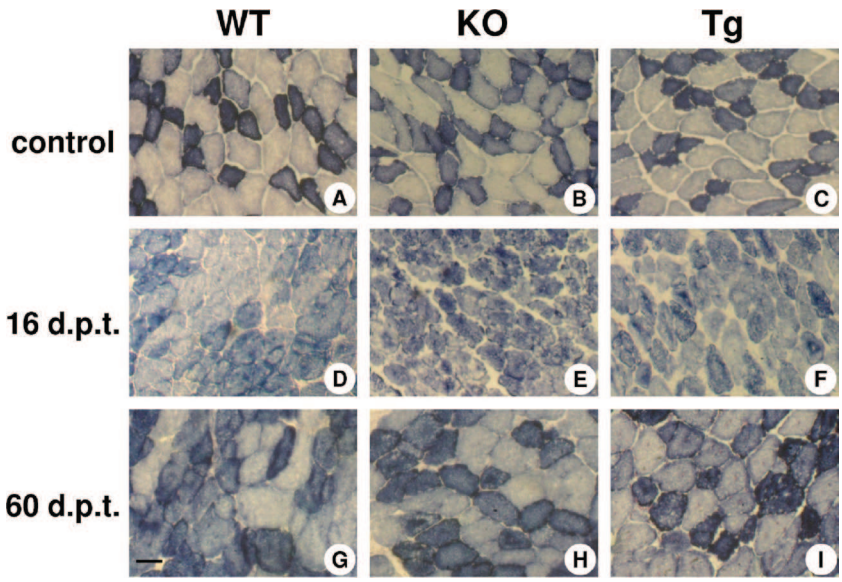

FIG. 2. SDH staining of cryosections of control and regenerating TA muscles. Shown are transverse cryosections of nondegenerated TA muscles (control) (A to C) and CTx-treated TA muscles at 16 (D to F) and 60 (G to I) days p.t. (d.p.t.) from 3 month-old WT (A, D, and G), PrP-KO (B, E, and H), and PrP-Tg (C, F, and I) male mice that were stained for their SDH contents to discriminate between oxidative (high SDH content; dark) and glycolytic (low SDH content; light) fibers. The photomicrographs were acquired with a digital-camera-equipped microscope. There was no appreciable difference in the dimensions and the relative numbers of the two fiber types in control TA muscles with or without PrP^C (A to C) or at 60 days p.t. (G to I), when the muscles had completely recovered from damage. Conversely, at 16 days p.t. (D to F), both oxidative and glycolytic fibers appeared smaller in the PrP-KO TA muscle than in the PrP^C-expressing muscles. Each photograph is representative of at least 4 independent experiments. Scale bar, 50 μm.

TABLE 1. Mean areas of glycolytic and oxidative fibers in the TA of control (non-CTx-treated) 3-month-old male mice with different PrP^C amounts

Fiber type	Mouse strain	Fiber area (10^3 μm^2)[a]
Glycolytic	WT	2.53 ± 0.05 (n = 8)
	KO	2.56 ± 0.04 (n = 7)
	Tg	2.56 ± 0.06 (n = 9)
Oxidative	WT	1.32 ± 0.03 (n = 8)
	KO	1.32 ± 0.05 (n = 7)
	Tg	1.29 ± 0.04 (n = 9)

[a] Fibers were discriminated by a colorimetric assay that detected SDH (see Materials and Methods). As expected, glycolytic fibers had a significantly larger cross-sectional area than oxidative fibers. However, the sizes of the two populations were similarly maintained in all TAs, irrespective of the PrP^C content. The data are means ± SEM.

The levels of PrP^C do not influence the morphology of adult TA muscles under normal conditions. In the first series of experiments, we examined the actual expression and maturation of PrP^C in the TA muscles of PrP^C-expressing control mice and determined whether the absence of PrP^C influenced normal muscle morphology. As shown in Fig. 1, Western blot analysis of PrP^C showed that, though to a lesser extent than in the brain (lane 1), PrP^C could nonetheless be readily detected in the WT TA muscle (lane 2) and that the PrP transgene present in PrP-Tg mice produced larger amounts of the protein (lane 4) (PrP-Tg/WT PrP^C ratio, 3.7 ± 0.5; n = 8). Significantly, PrP^C was always found mainly in the mature, diglycosylated form in either muscle type, indicating that, even if overexpressed, muscle PrP^C undergoes the cell processing typically found in the brain. As expected, no immunosignal was present in PrP-KO TA muscles (lane 3).

Next, we examined the TA morphology of the three control animals, using H&E-stained cross sections. However, because fibers with heterogeneous dimensions coexist in a single TA muscle due to different metabolic and contractile properties, we also applied a colorimetric assay that detected mitochondrial SDH to distinguish between oxidative and glycolytic fibers (see Materials and Methods). No difference was observed in the gross morphology (see Fig. S1A to C in the supplemental material) or in the cross-sectional areas of glycolytic and oxidative fibers (Table 1 and Fig. 2A to C) of the TA muscles of all murine lines. Likewise, no significant difference was detected in these mice with regard to the ratio of TA weight to total body weight [WT, $(1.55 \pm 0.03) \times 10^{-3}$, n = 14; PrP-KO, $(1.58 \pm 0.02) \times 10^{-3}$, n = 12; PrP-Tg, $(1.58 \pm 0.02) \times 10^{-3}$, n = 12]. Also, given the absence of variation in the fiber area between 3-month- and 6-month-old mice (data not shown) or overt signs of spontaneous degeneration or regeneration (in H&E-stained fibers) (see Fig. S1A to C in the supplemental material), these data demonstrate that the morphology of adult TA muscles (at least from 3 months after birth) was not influenced by the quantity of PrP^C present during development and adulthood.

The absence of PrP^C delays the acquisition of normal morphology by damaged TA muscles. We next used the well-characterized paradigm of CTx muscle damage and regeneration (18, 24) to study the role of PrP^C during muscle repair. During the first days after CTx injection, extensive necrosis occurred in adult TA muscles irrespective of the mouse strain, which was accompanied by an inflammatory response provided by accumulated blood cells (see Fig. S1D to I in the supplemental material). Hence, to seek unambiguous proof of PrP^C involvement in skeletal-muscle recovery, we examined muscle fibers from 9 days p.t. on, i.e., when the fibers were sufficiently regenerated to be tested with specific morphometric parameters, such as the fiber dimensions and the number of central nuclei.

With regard to the first parameter, the value of the cross-sectional area of regenerating fibers was normalized to the mean fiber area of the contralateral TA muscle injected with medium alone. Consistent with our observations in control animals (Table 1), the latter value was identical in the different lines (data not shown). As for the regenerating muscles, Fig. 3 shows that in all muscles, glycolytic (top) and oxidative (bottom) fibers progressively increased in size until they returned to the mature value (at 30 and 60 days p.t.) (Fig. 2G to I). However, Fig. 3 also demonstrates that at both 9 and 16 days p.t., the cross-sectional areas of both fiber types were significantly smaller in PrP-KO TA muscles than in WT and PrP-Tg muscles (Fig. 2D to F).

During the regeneration process, mononucleated myocytes fuse with each other or with preexisting fibers, producing fibers

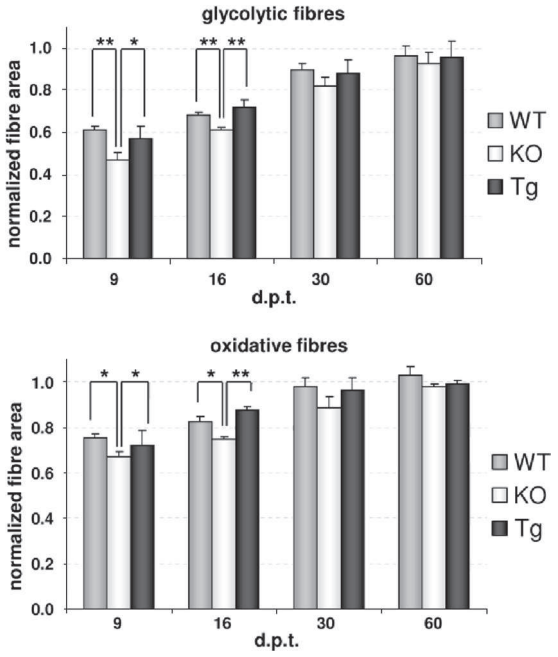

FIG. 3. The fiber size of regenerating TA muscles is significantly reduced in PrP-KO mice. Cryosections of TA muscles at different days p.t. with CTx were processed for SDH content (Fig. 2) to allow the separate calculation of the mean cross-sectional areas of glycolytic and oxidative fibers (see Materials and Methods). The area of CTx-treated fibers was normalized to the respective mean fiber area of the untreated contralateral TA muscle injected with medium alone. During the first phases of regeneration (9 and 16 days p.t.), the dimensions of both glycolytic (top) and oxidative (bottom) fibers were significantly decreased in PrP-KO TA muscles compared to WT and PrP-Tg muscles. This difference, however, disappeared when muscle repair was accomplished (30 and 60 days p.t.), in agreement with the lack of muscle phenotypes in untreated PrP-KO mice (Table 1). The values are means and SEM; n = 4 for each mouse strain at each time point. **, $P < 0.01$; *, $P < 0.05$; Student's t test.

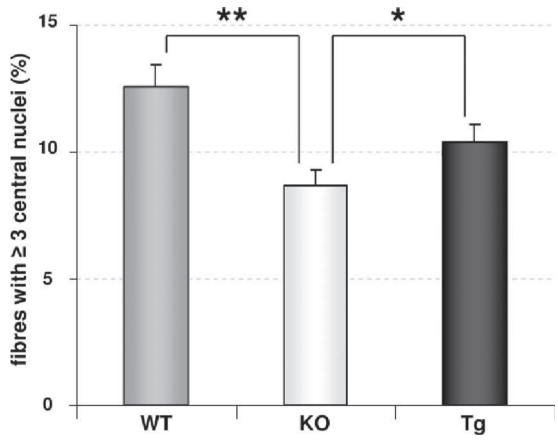

FIG. 4. Regenerating TA muscle fibers from PrP-KO mice have a significantly reduced percentage of fibers with 3 or more central nuclei. Transverse cryosections of CTx-treated TA muscles were stained with hematoxylin and eosin, and the percentage ratio of the number of fibers with 3 or more central nuclei over the total number of regenerating fibers was determined. This parameter was significantly lower in PrP-KO mice than in WT and PrP-Tg mice. The values (means and SEM) are the cumulative values found at 9 and 16 days p.t. with CTx (see Materials and Methods); $n = 8$ for each mouse strain; **, $P < 0.01$; *, $P < 0.05$; Student's t test.

with a progressively increasing number of centrally located nuclei. Consequently, we took the percentage of regenerating fibers with at least three central nuclei as a measure of the fusion events that occurred at a given time point (see Materials and Methods). Importantly, Fig. 4 demonstrates that this parameter was significantly reduced in PrP-KO TA muscles at both 9 and 16 days p.t., in accord with the previously shown dependence of the fiber size on the presence of PrP^C. Data similar to those of Fig. 3 and 4 were obtained using other murine lines, the *ZrchI* line of PrP-KO mice (8) and WT C57BL/6 mice (not shown).

To further validate the relationship between the degree of muscle maturation and PrP^C, we tested the expression of neo-MHC, a late marker of the differentiation process. Once again, neo-MHC showed distinctive behavior in PrP-KO TA muscles compared with PrP^C-expressing muscles (Fig. 5). Initially (at 7 and 9 days p.t.), it was significantly less abundant in the PrP-KO strain. Notably, however, examination of the PrP-KO muscle at 16 days p.t. revealed the presence of considerable levels of neo-MHC, in contrast to the PrP^C-expressing TA muscles, in which the protein was already downregulated. At 30 days p.t., all TA muscles had almost no neo-MHC, further confirming that at that time recovery from damage had been uniformly accomplished, irrespective of the mouse genotype.

Molecular mechanisms of the regenerating process controlled by PrP^C. The above data clearly demonstrate that the deprivation of PrP^C retarded muscle recovery and that this phenotype was completely abolished by rescuing the expression of the protein. To clarify the original cause of the PrP-KO phenotype, we set out to examine the early phases of the regeneration process, in which inflammatory cells play a substantial role. We focused on macrophages, in view of their ability to affect muscle regeneration. Indeed, after presenting a proinflammatory profile, macrophages rapidly acquire features essential for muscle repair by scavenging the necrotic material

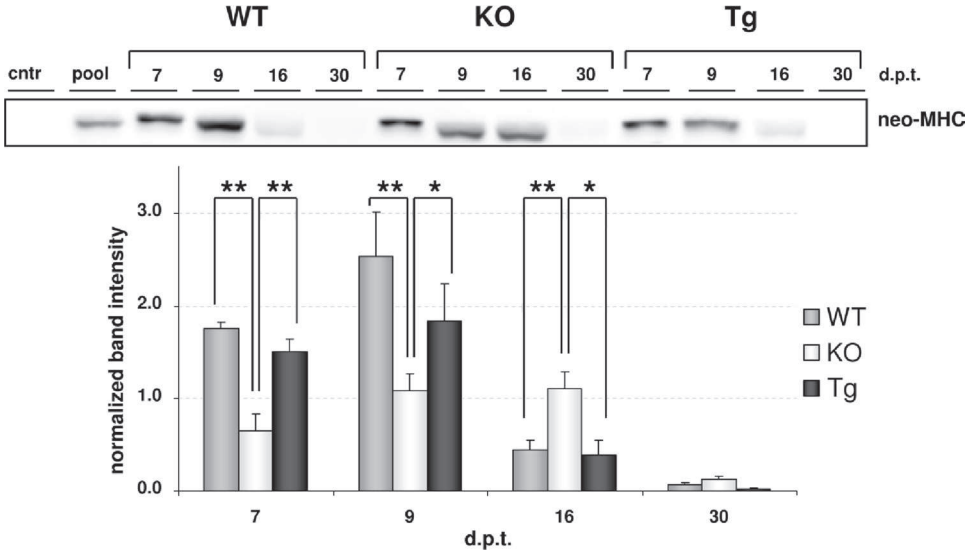

FIG. 5. The expression of neo-MHC is delayed and prolonged in CTx-treated PrP-KO TA muscles. Western blot analysis for the expression of neo-MHC, a marker of skeletal-muscle differentiation, was carried out using the anti-neo-MHC MAb BF-34 on different days p.t. with CTx. At the top, a Western blot, representative of 4 independent experiments, is shown. An untreated TA muscle sample (cntr) and a pool of all CTx-treated samples (see Materials and Methods) were also loaded in the gel. Below is shown the densitometric analysis of the expression levels of neo-MHC in CTx-treated TA muscles with different PrP^C contents. The intensity of each band was normalized to the band intensity of the pooled sample running in the same gel. As expected, neo-MHC was absent in the untreated TA muscle sample (cntr), while it transiently increased in regenerating TA muscles. However, compared with WT and PrP-Tg TA muscles, the expression of neo-MHC in PrP-KO muscles was significantly lower at 7 and 9 days p.t., though it persisted for a longer time (until 16 days p.t.). The values are means and SEM; $n = 4$ for each mouse strain at each time point. **, $P < 0.01$; *, $P < 0.05$; Student's t test. Other experimental details are as in the legend to Fig. 1, except that 5 μg of protein in each lane was separated on 7% SDS-PAGE gels under reducing conditions.

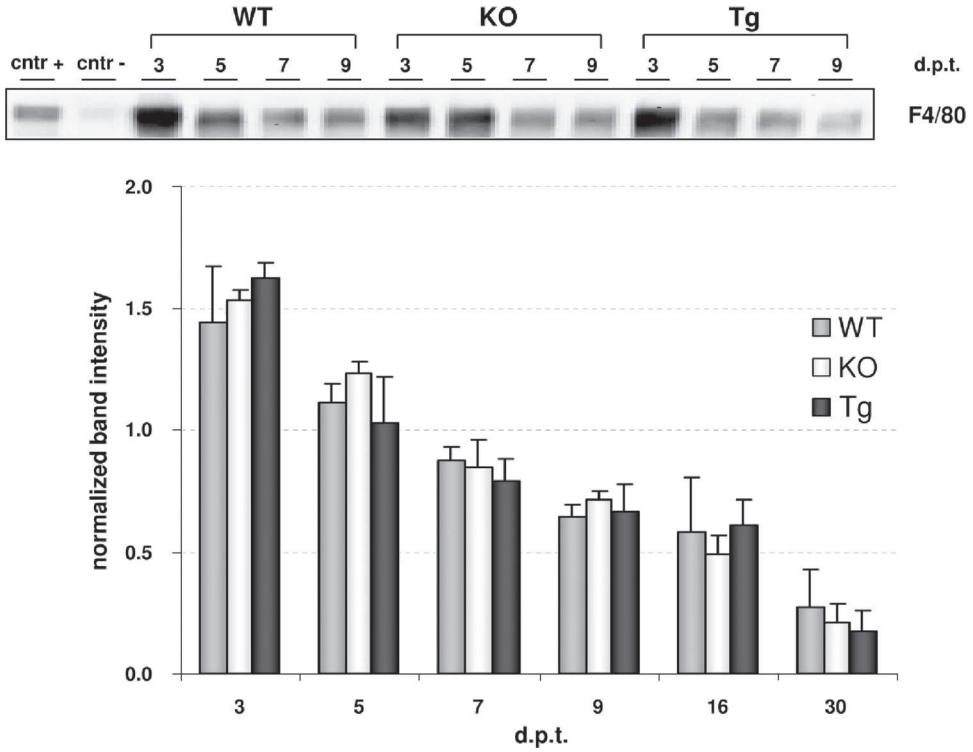

FIG. 6. The quantity of macrophages in regenerating TA muscles does not depend on the presence of PrP^C. The amount of macrophages present in TA homogenates between 3 and 30 days p.t. with CTx was estimated by Western blot analysis using a MAb against the macrophage marker protein F4/80. At the top, a Western blot, representative of 4 independent experiments, is shown. An untreated TA muscle sample (cntr−) and a lysate of macrophages (cntr+) were also loaded in the gel as a negative and positive control, respectively. At the bottom is shown the densitometric analysis of the expression levels of F4/80 in CTx-treated TA muscles with different quantities of PrP^C. The intensity of each band was normalized to the band intensity of the cntr+ sample running in the same gel. The progressive decrease of macrophages during regeneration showed no statistically significant difference between PrP-KO and PrP^C-expressing muscles. The values are means and SEM; $n = 4$ for each mouse strain at each day p.t. Other experimental details are as in the legend to Fig. 1, except that 5 μg of proteins for the cntr+ sample and 30 μg of proteins for the other lanes were separated on 4 to 12% gradient SDS-PAGE gels under reducing conditions.

and by releasing several factors, including cytokines, which regulate the proliferation and differentiation of myogenic cells (10, 12, 45). We first quantified the presence of macrophages in the different regenerating muscles (from 3 to 30 days p.t.) by evaluating the levels of the macrophage marker F4/80 (44), using Western blot analysis. Based on this parameter, no statistically significant difference was observed in the macrophage contents of WT, PrP-KO, and PrP-Tg muscles (Fig. 6). Then, we analyzed, at 3 and 5 days p.t., the levels of the soluble cytokine TNF-α, which, originating from the cleavage of the membrane-bound precursor (pro-TNF-α) via the TNF-α-converting enzyme (TACE) (5), is well known to actively take part in muscle repair (14, 15). It should be noted, however, that not only macrophages, but also myogenic cells, secrete this factor (15, 34, 73). As shown in Fig. 7, we found that, whereas the expression of both pro-TNF-α (left) and soluble TNF-α (right) decreased as expected with the progression of muscle recovery, at 3 days p.t. the level of soluble TNF-α was significantly lower in PrP-KO TA muscles than in WT and PrP-Tg samples. *In vitro* and *in vivo* experiments have documented that TNF-α regulates myogenesis through the activation of the mitogen-activated protein kinase (MAPK) p38 (15, 73). This kinase is crucial for the muscle differentiation process. On one hand, it promotes the expression of transcription factors specific for muscle genes (28, 61, 62, 69, 72); on the other hand, it promotes exit from the cell cycle by inducing the expression of p21, an inhibitor of cyclin-dependent kinases (9, 69). In view of this, we examined whether the lower release of TNF-α in the absence of PrP^C had an impact on the phosphorylation of p38 and, consequently, on the proliferation of myogenic precursors.

To assess p38 activation, both the phosphorylated form (P-p38) and the total amount of the enzyme were analyzed by Western blotting in the time frame 3 to 9 days p.t. (Fig. 8). Although the total quantity of p38 did not vary significantly with respect to the time point or the mouse genotype, the levels of P-p38 sharply increased during the TA muscle regeneration of all mouse strains (Fig. 8, top). Importantly, however, the ratio between P-p38 and total p38 amounts (Fig. 8, bottom) indicated that at 5 and 7 days p.t., P-p38 was significantly less in PrP-KO samples than in those expressing PrP^C. This finding prompted us to investigate the activation of Akt, in view of the fact that during muscle regeneration, Akt cooperates with p38 in the chromatin remodeling at muscle-specific loci that allows the expression of myogenic factors (61, 69). Intriguingly, at 5 days p.t., both total (phosphorylated and nonphosphorylated) Akt and P-Akt were significantly less abundant in PrP-KO myogenic cells than in their PrP^C-expressing counterparts,

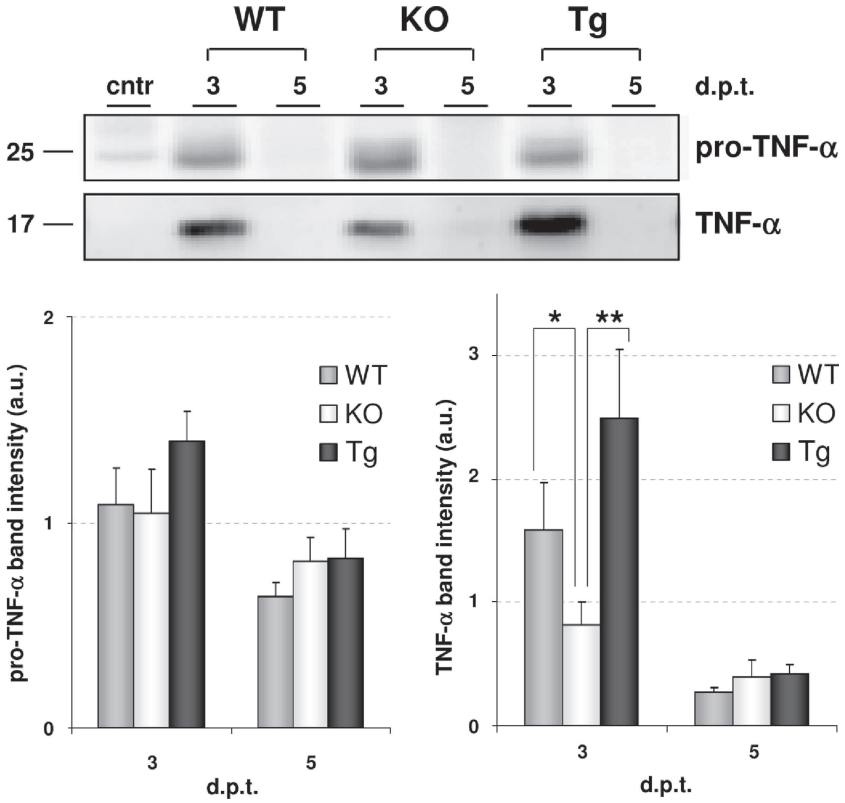

FIG. 7. The release of TNF-α is reduced in the regenerating TA muscles of PrP-KO mice at 3 days p.t. TA muscle homogenates were analyzed by Western blotting using a PAb against TNF-α at 3 and 5 days p.t. with CTx. At the top, a Western blot, representative of 6 independent experiments, is shown. An untreated TA muscle sample (cntr) was also loaded in the gel as a negative control. The antibody recognized two distinct immunoreactive bands at around 25 and 17 kDa, corresponding to the membrane-bound TNF-α precursor (pro-TNF-α) and the soluble TNF-α form, respectively. Molecular mass standards (kDa) are shown on the left. At the bottom is shown the densitometric analysis of the expression levels of pro-TNF-α (left) and TNF-α (right) in CTx-treated TA muscles. Whereas no significant difference was observed in the pro-TNF-α levels in the different mouse strains, at 3 days p.t. PrP-KO TA muscles contained significantly smaller amounts of soluble TNF-α than PrP^C-expressing muscles. The values (arbitrary units [a.u.]) are means and SEM; $n = 6$ for each mouse strain at each day p.t. **, $P < 0.01$; *, $P < 0.05$; Student's *t* test. Other experimental details are as in the legend to Fig. 6.

while at 7 days p.t. the reduction of P-Akt remained significant only with respect to the PrP-Tg cells (Fig. 9).

We then evaluated the extent of proliferation of muscle precursors following the *in vivo* incorporation of intraperitoneally injected BrdU. BrdU was applied in two ways. In the first, animals were given a single pulse of BrdU 18 h before their sacrifice at 5 days p.t. This treatment produced a significantly higher percentage of BrdU-positive myonuclei (i.e., nuclei in myogenic precursors and in muscle cells/fibers) in PrP-KO TA muscles than in their PrP^C-expressing counterparts (Fig. 10A and B), indicating that PrP-KO muscle precursors replicated more extensively between 4 and 5 days p.t. Such a difference was emphasized when BrdU was administered every 48 h, starting from 2 days p.t., until the animals' sacrifice at 9 days p.t. (Fig. 10C). These data provide further evidence that PrP^C-deficient myoblasts are likely to proliferate for a longer period than PrP^C-expressing cells and hence have delayed differentiation.

Proliferation of muscle precursors was also evaluated through the expression of Pax7, a transcription factor present in quiescent and proliferating satellite cells and in cycling myoblasts that becomes downregulated as the myoblasts start to differentiate (7, 12, 19, 31, 33, 70). One important result of this analysis (Fig. 11) was that Pax7 had similar overall behavior in all muscle paradigms. We explicitly refer to the progressive downregulation of the protein in the time interval 5 to 16 days p.t., during which the entire differentiation program of myogenic cells takes place. Notably, however, at both 5 and 7 days p.t., Pax7 was expressed at a significantly higher level in PrP-KO TA muscles than in WT and PrP-Tg regenerating muscles. It is important to note that this event could not be ascribable to a different reservoir of quiescent satellite cells in PrP-KO muscles, because similar amounts of Pax7 were found in all untreated age-matched TA muscles (PrP-KO/WT Pax7 ratio, 1.1 ± 0.2, $n = 6$; PrP-Tg/WT Pax7 ratio, 1.0 ± 0.2, $n = 6$). Hence, the protracted upregulation of Pax7 in PrP-KO muscle precursors appears to be fully in accord with the aforementioned delayed withdrawal from the cell cycle of these cells, both features highlighting that the absence of PrP^C retarded the priming of the differentiation program.

DISCUSSION

Elucidating the physiological function of PrP^C is of prime importance for understanding the mechanisms of prion-induced neurodegeneration and for devising safe therapeutic

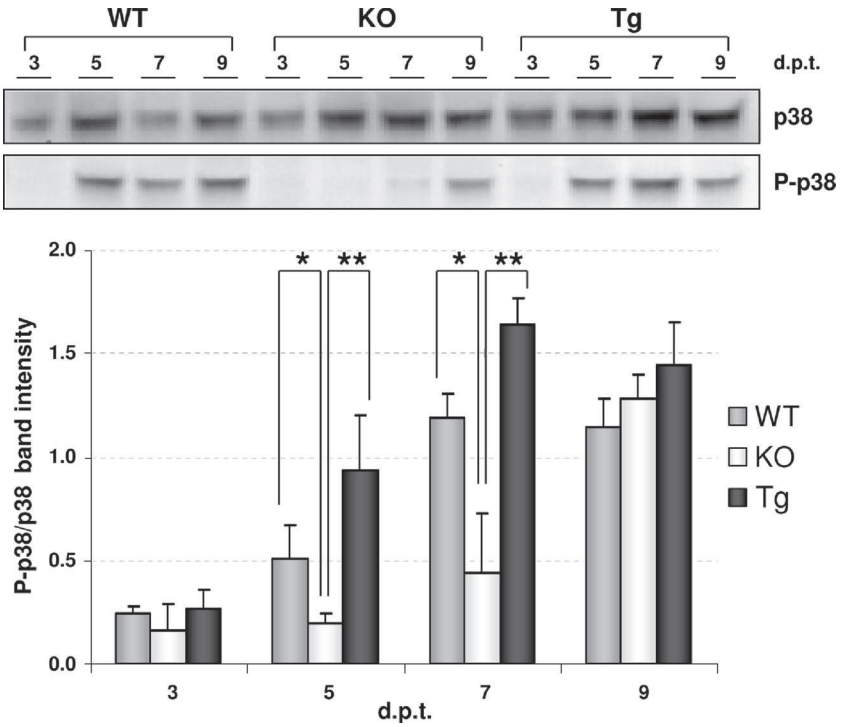

FIG. 8. PrP-KO TA muscles have reduced activation of the MAPK p38 at 5 and 7 days p.t. Homogenates of regenerating TA muscles at different days p.t. with CTx were analyzed by Western blotting with antibodies that recognize either total (phosphorylated or not) MAPK p38 or, specifically, its phosphorylated (P-p38) form (at both Thr180/Tyr182). At the top, Western blots, representative of 4 independent experiments, are shown. At the bottom, the densitometric analysis of the activation of p38 is shown. Given that total p38 levels did not significantly change with time or with respect to the mouse genotype (top), activation of p38 is given as the ratio between P-p38 and total p38 immunoreactive bands. Although p38 phosphorylation increased with time in all mouse strains, at 5 and 7 days p.t. it was significantly reduced in PrP-KO TA muscles compared to their WT and PrP-Tg counterparts. The values are means and SEM; $n = 4$ for each mouse strain at each day p.t. **, $P < 0.01$; *, $P < 0.05$; Student's t test. Other experimental details are as in the legend to Fig. 6.

strategies that target PrP^C directly. The lack of overt phenotypes in PrP-KO mice has so far precluded the precise definition of PrP^C function by simple genetic approaches, thus leaving open the question of whether the protein is dispensable for cell life under all circumstances (e.g., stress conditions) and if the loss of function of PrP^C contributes to prion-associated neurodegeneration. However, several reports have indicated that the protein takes part in important cell functions. In this work, we focused on the role of PrP^C in cell proliferation and differentiation, which has been previously proposed for nerve tissue (13, 22, 27, 36, 55, 59, 64). Experimentally, this was achieved by exploiting a novel strategy in the prion field based on determining the impact of PrP^C in an *in vivo* paradigm of adult skeletal-muscle morphogenesis, i.e., regeneration of the tissue after CTx-induced damage. This aim was pursued by comparing muscles expressing (WT) or not expressing (PrP-KO) PrP^C. Furthermore, the use of PrP-KO animals in which the presence of PrP^C had been reestablished (PrP-Tg) allowed us to ascertain the effective specificity of the PrP^C contribution to muscle regeneration. By demonstrating that PrP^C is part of the machinery for repairing injured adult skeletal muscles and, in particular, that it contributes to the rate of regeneration, our data imply that the role of PrP^C is not restricted to the CNS, but rather, that PrP^C may be broadly involved in the maintenance and repair of tissues during the entire lifetimes of animals.

These conclusions stem from the observation that there was no difference in the TA morphologies of adult (3-month-old) control mice expressing differing amounts of PrP^C (WT, PrP-KO, and PrP-Tg) or 30 days after CTx-induced damage to the muscle. However, while PrP^C is not required for the full accomplishment of skeletal-muscle morphogenesis during both embryonic and adult life, our morphometric and biochemical assays have clearly demonstrated that there is a skeletal phenotype in PrP-KO animals. This presented with the mid-late stages of the recovery from the CTx-caused injury, represented by the delayed acquisition of myofiber size and the delayed expression of muscle-specific proteins (neo-MHC) (Fig. 2 to 5). Defects in the differentiation or fusion process, or a delayed activation or prolonged proliferation, of myogenic precursors (satellite cells and/or myoblasts) could have been the cause of this delay. This prompted us to analyze in sequence the earlier events triggered by the damage, such as the infiltration of macrophages and the proliferation of muscle precursor cells.

In the first days after damage, the most remarkable observation was the discrete reduction of TNF-α attributable to the absence of PrP^C (Fig. 7). It has been shown that this factor is of crucial importance in myogenesis (15, 73) and that mice deficient in TNF-α receptors have impaired regeneration of CTx-injured muscles (soleus) (14). TNF-α-mediated myogenic signaling acts through the activation of p38 (15, 73). In turn, p38 plays a major role in skeletal-muscle development (28, 72),

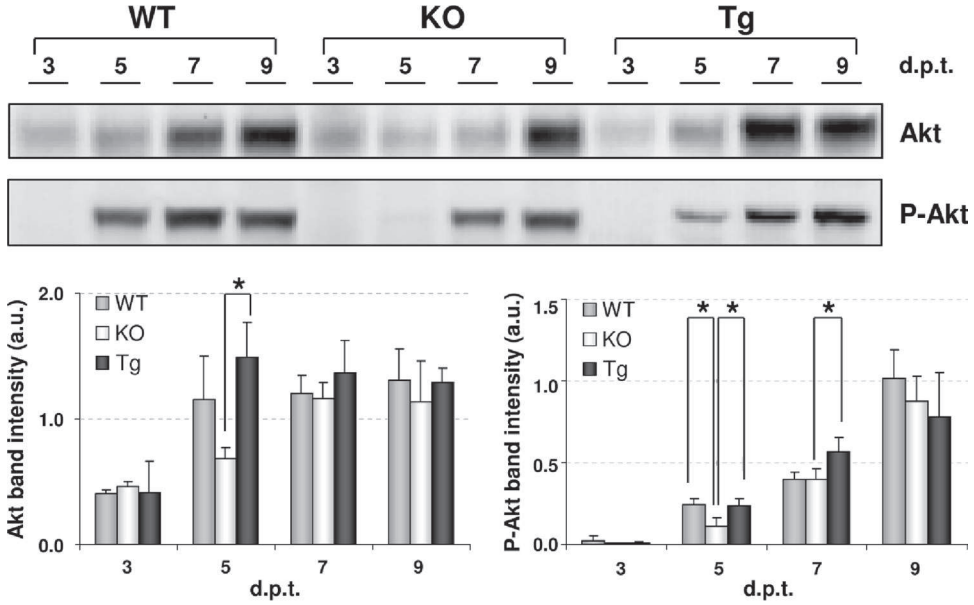

FIG. 9. Active (phosphorylated) Akt is reduced in regenerating PrP-KO TA muscles. Homogenates of regenerating TA muscles at different days p.t. with CTx were analyzed by Western blotting with antibodies that recognize either total (phosphorylated or not) Akt or specifically its phosphorylated (at Ser473) form (P-Akt). At the top, Western blots, representative of 5 independent experiments, show that in the different muscles the levels of both Akt and P-Akt increased with the progression of the regeneration process in a way that was dependent on the mouse genotype. As also shown below, the densitometric analyses of total Akt (left) and P-Akt (right) at 5 days p.t. showed that the amount of P-Akt was significantly reduced in PrP-KO TA muscles with respect to PrP^C-expressing muscles. At 7 days p.t., significant differences persisted only between PrP-KO and PrP-Tg samples. It should also be noted that, compared with PrP-Tg muscles, the total Akt amount was significantly less in PrP-KO TA muscles at 5 days p.t. The values are means and SEM; $n = 5$ for each mouse strain at each day p.t. *, $P < 0.05$; Student's t test. Other experimental details are as in the legend to Fig. 6.

as was also demonstrated by the fact that the pharmacologic inhibition or the constitutive activation of this kinase inhibits or stimulates muscle differentiation (15, 69, 73). It has been proposed that regulation of muscle differentiation by p38 occurs in a bimodal fashion, by activating the transcription of muscle-specific genes (61, 62) and by inducing p21, the action of which eventually accomplishes cell cycle arrest and terminal differentiation (9). It has also been reported that the phosphatidylinositol 3-kinase (PI3K)/Akt pathway acts independently of, and synergistically with, p38 in promoting the differentiation event at the chromatin/transcriptosome level (61, 69). Clearly, our observations during the *in vivo* regeneration of PrP-KO TA muscles are fully consistent with these notions. PrP-KO myoblasts showed not only around 60% and 75% less active p38 (Fig. 8) and around 50% less active P-Akt (Fig. 9) than WT and PrP-Tg cells, but also a retarded exit from the cell cycle. Indeed, both the proliferation index (Fig. 10) and the expression of Pax7 (Fig. 11) strongly suggest that in the absence of PrP^C muscle precursors replicated for a longer time than in the presence of PrP^C. In untreated TA muscles, we found that the levels of Pax7, the gold standard marker of adult satellite cells (mostly quiescent under these conditions), did not change as a function of the mouse genotype. Therefore, the defective regeneration of injured PrP-KO TA muscles cannot be attributed to differing reservoirs of myogenic precursors. This finding also suggests that PrP^C is dispensable for the self-renewal of satellite cells, in contrast to what has been previously suggested for long-term hematopoietic stem cells (74). With respect to the activation of Akt, we did not investigate the molecule responsible for triggering the PI3K/Akt pathway, although IGF-1 is a plausible candidate, in accord with studies that implicate this growth factor in muscle regeneration and growth (4, 32, 47, 48, 58).

In considering the above set of results, together with the delayed acquisition of normal morphology occurring in PrP-KO TA muscles, it seems reasonable to hypothesize that the central event causing the retarded commitment to differentiation of PrP-KO myogenic cells is the smaller quantity of TNF-α these cells were exposed to. This fact raises the question of which cell type is responsible for the diminished TNF-α production, given that macrophages also express PrP^C (26) and that the PrP-KO mouse used in this study lacked PrP^C in all tissues. TNF-α is released by macrophages; hence, the coincidence between the peak of TNF-α production (Fig. 7) and the maximal presence of macrophages (Fig. 6) may lead to the conclusion that the lower TNF-α release is caused by the absence of PrP^C in macrophages. However, although at high levels TNF-α is a pathological factor mediating inflammatory myopathies, cachectic muscle wasting, and other muscle disorders (37, 57), it is now clear that TNF-α is constitutively released by myoblasts, especially during differentiation (15, 34, 73). Therefore, notwithstanding the relevant contribution that, proportionally, macrophages certainly make to the process, it is highly possible that the early stages of muscle regeneration are under the control of PrP^C residing in both myogenic and inflammatory cells.

The mechanism by which PrP^C controls the generation of TNF-α does not appear to be related to the amounts of mac-

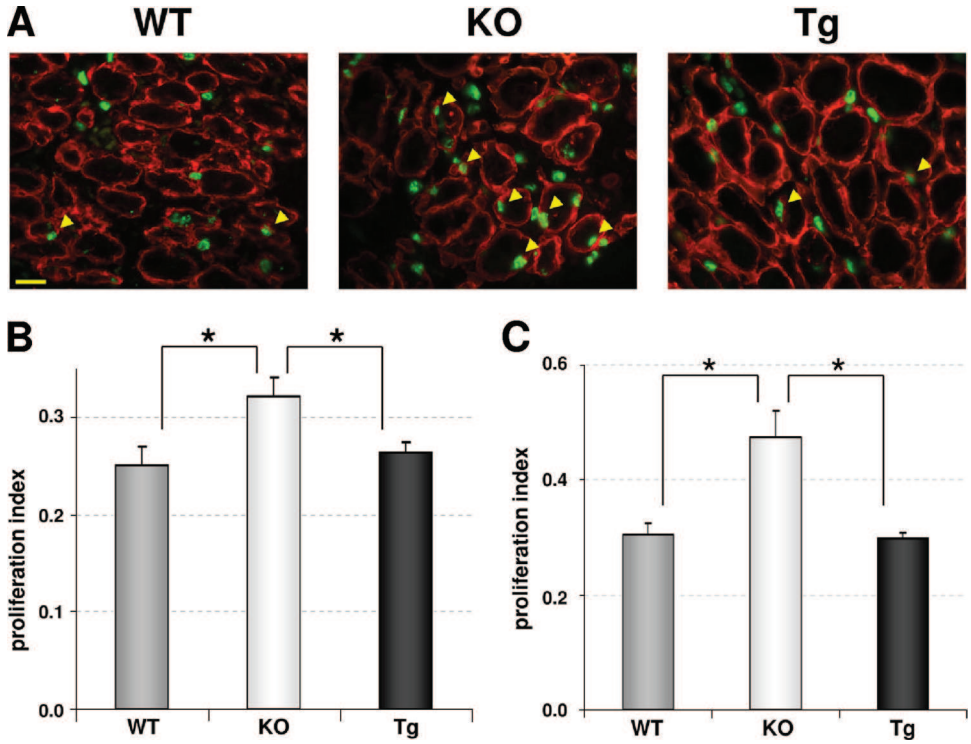

FIG. 10. The proliferation index of myogenic cells is significantly increased in regenerating PrP-KO TA muscles. CTx-treated mice were injected with a single BrdU pulse 18 h before sacrifice at 5 days p.t. (A and B) or with multiple BrdU pulses at 2, 4, 6, and 8 days p.t. before sacrifice at 9 days p.t. (C). (A) TA muscle cryosections were immunolabeled for the presence of BrdU (marking proliferating nuclei; green signal) and laminin (red signal), and photomicrographs were acquired with a CCD camera-equipped fluorescence microscope (see Materials and Methods). BrdU-positive nuclei in laminin-positive cells/fibers (yellow arrowheads) were more frequent in the regenerating TA muscle of PrP-KO mice than in PrP^C-expressing samples. Each photomicrograph is representative of at least 4 independent experiments. Scale bar, 25 μm. (B and C) The proliferation index, calculated as the ratio of the number of BrdU-positive nuclei in laminin-positive cells/fibers over the number of laminin-positive cells/fibers. Following either single (B) or multiple (C) BrdU pulses, this parameter was significantly higher in the regenerating TA muscles of PrP-KO muscles than in their PrP^C-expressing counterparts, especially when determined over a longer time (C). The values are means and SEM; $n = 4$ (B) and $n = 3$ (C) for each mouse strain. *, $P < 0.05$; Student's t test.

rophages, as they were comparable in all the examined muscles during the entire regeneration process (Fig. 6), nor does PrP^C affect the synthesis of pro-TNF-α, the levels of which were also similar in all mouse lines (Fig. 7). Instead, by showing that at 3 days p.t. the levels of TNF-α were directly related to the quantity of PrP^C (Fig. 7), our results strongly suggest that PrP^C is intimately implicated in the release of mature TNF-α from its precursor. This possibility is fully consistent with the findings of Pradines et al. (54) in two neuronal cell lines, demonstrating that PrP^C stimulation (through antibody-mediated cross-linking) resulted in increased TACE activation and TNF-α release.

In interpreting the observed variations in muscle regeneration between PrP-KO mice and WT (FVB) controls, it is fair to consider the possibility that genetic differences linked to the PrP locus were responsible for our results. The PrP-KO mice used in this study were backcrossed 10 times into the FVB background, thus producing a PrP-KO (F10) line with an almost, but not entirely, pure FVB genotype (40). However, the results obtained with PrP-Tg mice, which were generated by reintroducing into PrP-KO FVB mice a murine PrP-coding transgene (in multiple copies) (39), militate against this possibility, given that the muscular phenotype observed in the absence of PrP^C was completely abrogated by rescuing the expression of PrP^C.

Incidentally, the presence of larger amounts of PrP^C in PrP-Tg TA muscles did not generate a TA phenotype distinguishable from the WT, in contrast to the accelerated differentiation that, compared to normally expressed PrP^C, was observed in embryonic neural precursors overexpressing PrP^C (64). Possible explanations for this difference may be the kind of tissue used and the experimental constraints imposed on it—*in vivo*-regenerating adult skeletal-muscle cells instead of *in vitro*-differentiating neuronal precursors—or the quantity of expressed PrP^C, which in the work of Steele et al. (64) might have been higher than the approximately four times the normal level we used. However, in spite of the different approaches, there was good correspondence between our results and the observations by Steele and coworkers (64) showing that the absence of PrP^C delayed the rate of *in vitro* differentiation of embryonic neural precursors without affecting either the *in vivo* net neurogenesis or the gross morphology of the adult CNS. Another convergence on this theme has been provided by Prestori et al. (55). They showed that the protracted mitosis of cerebellar granule cell precursors in the absence of PrP^C delayed the maturation of the granule layer in the first post-

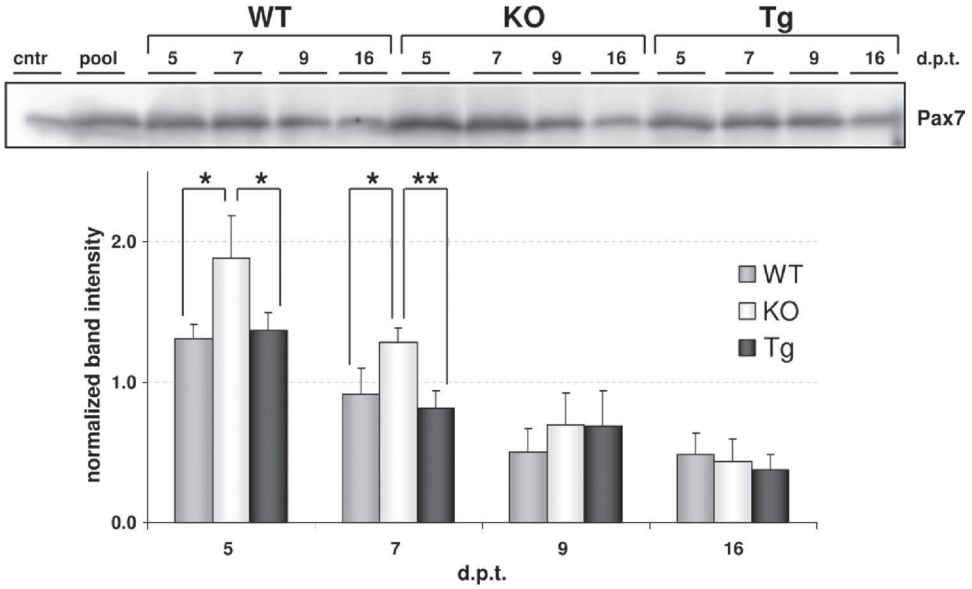

FIG. 11. The differentiation of muscle precursors is significantly delayed in regenerating PrP-KO TA muscles. Western blot analysis for the expression of Pax7, a marker of quiescent and cycling satellite cells/myoblasts, was carried out using an anti-Pax7 MAb on TA muscles on different days p.t. with CTx. At the top, a Western blot, representative of 4 independent experiments, is shown. An untreated adult TA muscle sample (cntr) and a pool of all CTx-treated samples were also loaded in the gel. At the bottom is shown the densitometric analysis for Pax7 expression in CTx-treated TA muscles with different PrP^C quantities. The intensity of each band was normalized as described in the legend to Fig. 5. In accordance with its transient expression, in all regenerating muscles the expression of Pax7 decreased with the progression of the differentiation process of muscle precursors, eventually reaching the same level as in the untreated control sample. In PrP-KO TA muscles, however, at 5 and 7 days p.t. Pax7 levels were significantly higher than in the WT and PrP-Tg counterparts, indicating prolonged maintenance of PrP-KO satellite cells/myoblasts in the proliferative state. The values are means and SEM; $n = 4$ for each mouse strain at each time point. **, $P < 0.01$; *, $P < 0.05$; Student's t test. Other experimental details are as in the legend to Fig. 1, except that 40 μg of protein in each lane was separated on a 10% SDS-PAGE gel.

natal weeks but that the delay did not compromise the final acquisition of normal architecture of the cerebellum. Thus, these works and the present study all support the contention that, by affecting the rate but not the endpoint of tissue morphogenesis, PrP^C is a component that cooperates with other factors in the maturation of neuronal and muscle tissues.

In conclusion, our *in vivo* experiments imply that, in CTx-degenerated skeletal muscles, PrP^C affects the release of TNF-α, a factor involved in muscle differentiation and downstream signaling pathways, thereby influencing the *in vivo* morphogenesis of adult injured extraneural tissue. In particular, our data support the possibility that PrP^C modulates the activity of the enzyme (TACE) that hydrolyzes TNF-α from its precursor. Future *in vitro* studies will help verify this hypothesis rigorously and clarify whether the two proteins (PrP^C and TACE) interact directly or indirectly. In this context, many examples of the interaction of PrP^C with membrane or extracellular proteins have already been proposed, e.g., binding to the NMDA receptor subunit 2D (29), which attenuates glutamate-induced Ca^{2+} influx, and the glycosaminoglycan-mediated interaction with BACE1, which attenuates β-secretase cleavage of the amyloid precursor protein (52). For the first time, to our knowledge, our results also demonstrate that the regulation of (p38 and Akt) signaling pathways by PrP^C has clear physiologic importance in an extraneural tissue *in vivo*.

ACKNOWLEDGMENTS

We thank S. Schiaffino, M. S. Sy, and L. Vitiello for providing antibodies; the MRC Prion Unit, Imperial College, and A. Aguzzi for providing the mouse strains; S. Schiaffino and his laboratory for helpful suggestions on the use of the mouse model system; and A. Hill for precious help in improving the work.

This work was supported by grants from the Italian Ministry of University and Research (Prin 2008, to M.C.S.) and from the University of Padova (Progetto d'Ateneo CPDA089551, to A.B.).

REFERENCES

1. **Aguzzi, A., F. Baumann, and J. Bremer.** 2008. The prion's elusive reason for being. Annu. Rev. Neurosci. **31:**439–477.
2. **Andréoletti, O., S. Simon, C. Lacroux, N. Morel, G. Tabouret, A. Chabert, S. Lugan, F. Corbiere, P. Ferre, G. Foucras, H. Laude, F. Eychenne, J. Grassi, and F. Schelcher.** 2004. PrP^{Sc} accumulation in myocytes from sheep incubating natural scrapie. Nat. Med. **10:**591–593.
3. **Angers, R. C., S. R. Browning, T. S. Seward, C. J. Sigurdson, M. W. Miller, E. A. Hoover, and G. C. Telling.** 2006. Prions in skeletal muscles of deer with chronic wasting disease. Science **311:**1117.
4. **Barton, E. R., L. Morris, A. Musarò, N. Rosenthal, and H. L. Sweeney.** 2002. Muscle-specific expression of insulin-like growth factor I counters muscle decline in mdx mice. J. Cell Biol. **157:**137–148.
5. **Black, R. A.** 2002. Tumor necrosis factor-alpha converting enzyme. Int. J. Biochem. Cell Biol. **34:**1–5.
6. **Bosque, P. J., C. Ryou, G. Telling, D. Peretz, G. Legname, S. J. DeArmond, and S. B. Prusiner.** 2002. Prions in skeletal muscle. Proc. Natl. Acad. Sci. U. S. A. **99:**3812–3817.
7. **Buckingham, M., and D. Montarras.** 2008. Skeletal muscle stem cells. Curr. Opin. Genet. Dev. **18:**330–336.
8. **Büeler, H., M. Fischer, Y. Lang, H. Bluethmann, H. P. Lipp, S. J. DeArmond, S. B. Prusiner, M. Aguet, and C. Weissmann.** 1992. Normal development and behaviour of mice lacking the neuronal cell-surface PrP protein. Nature **356:**577–582.
9. **Cabane, C., W. Englaro, K. Yeow, M. Ragno, and B. Derijard.** 2003. Regulation of C2C12 myogenic terminal differentiation by MKK3/p38α pathway. Am. J. Physiol. Cell Physiol. **284:**C658–C666.
10. **Cantini, M., M. L. Massimino, A. Bruson, C. Catani, L. Dalla Libera, and U. Carraro.** 1994. Macrophages regulate proliferation and differentiation of satellite cells. Biochem. Biophys. Res. Commun. **202:**1688–1696.

11. **Caughey, B., and G. S. Baron.** 2006. Prions and their partners in crime. Nature **443:**803–810.
12. **Chargé, S. B., and M. A. Rudnicki.** 2004. Cellular and molecular regulation of muscle regeneration. Physiol. Rev. **84:**209–238.
13. **Chen, S., A. Mange, L. Dong, S. Lehmann, and M. Schachner.** 2003. Prion protein as trans-interacting partner for neurons is involved in neurite outgrowth and neuronal survival. Mol. Cell Neurosci. **22:**227–233.
14. **Chen, S. E., E. Gerken, Y. Zhang, M. Zhan, R. K Mohan, A. S. Li, M. B. Reid, and Y. P. Li.** 2005. Role of TNF-alpha signaling in regeneration of cardiotoxin-injured muscle. Am. J. Physiol. Cell Physiol. **289:**1179–1187.
15. **Chen, S. E., B. Jin, and Y. P. Li.** 2007. TNF-alpha regulates myogenesis and muscle regeneration by activating p38 MAPK. Am. J. Physiol. Cell Physiol. **292:**1660–1671.
16. **Chiesa, R., A. Pestronk, R. E. Schmidt, W. G. Tourtellotte, B. Ghetti, P. Piccardo, and D. A. Harris.** 2001. Primary myopathy and accumulation of PrP^{Sc}-like molecules in peripheral tissues of transgenic mice expressing a prion protein insertional mutation. Neurobiol. Dis. **8:**279–288.
17. **Criado, J. R., M. Sanchez-Alavez, B. Conti, J. L. Giacchino, D. N. Wills, S. J. Henriksen, R. Race, J. C. Manson, B. Chesebro, and M. B. Oldstone.** 2005. Mice devoid of prion protein have cognitive deficits that are rescued by reconstitution of PrP in neurons. Neurobiol. Dis. **19:**255–265.
18. **d'Albis, A., R. Couteaux, C. Janmot, A. Roulet, and J. C. Mira.** 1988. Regeneration after cardiotoxin injury of innervated and denervated slow and fast muscles of mammals. Myosin isoform analysis. Eur. J. Biochem. **174:** 103–110.
19. **Dhawan, J., and T. A. Rando.** 2005. Stem cells in postnatal myogenesis: molecular mechanisms of satellite cell quiescence, activation and replenishment. Trends Cell Biol. **15:**666–673.
20. **Donselaar, Y., O. Eerbeek, D. Kernell, and B. A. Verhey.** 1987. Fibre sizes and histochemical staining characteristics in normal and chronically stimulated fast muscle of cat. J. Physiol. **382:**237–354.
21. **Glatzel, M., E. Abela, M. Maissen, and A. Aguzzi.** 2003. Extraneural pathologic prion protein in sporadic Creutzfeldt-Jakob disease. N. Engl. J. Med. **349:**1812–1820.
22. **Graner, E., A. F. Mercadante, S. M. Zanata, O. V. Forlenza, A. L. Cabral, S. S. Veiga, M. A. Juliano, R. Roesler, R. Walz, A. Minetti, I. Izquierdo, V. R. Martins, and R. R. Brentani.** 2000. Cellular prion protein binds laminin and mediates neuritogenesis. Brain Res. Mol. Brain Res. **76:**85–92.
23. **Hajj, G. N., M. H. Lopes, A. F. Mercadante, S. S. Veiga, R. B. da Silveira, T. G. Santos, K. C. Ribeiro, M. A. Juliano, S. G. Jacchieri, S. M. Zanata, and V. R. Martins.** 2007. Cellular prion protein interaction with vitronectin supports axonal growth and is compensated by integrins. J. Cell Sci. **120:** 1915–1926.
24. **Harris, J. B.** 2003. Myotoxic phospholipases A2 and the regeneration of skeletal muscles. Toxicon **42:**933–945.
25. **Huang, S., J. Liang, M. Zheng, X. Li, M. Wang, P. Wang, D. Vanegas, D. Wu, B. Chakraborty, A. P. Hays, K. Chen, S. G. Chen, S. Booth, M. Cohen, P. Gambetti, and Q. Kong.** 2007. Inducible overexpression of wild-type prion protein in the muscles leads to a primary myopathy in transgenic mice. Proc. Natl. Acad. Sci. U. S. A. **104:**6800–6805.
26. **Isaacs, J. D., G. S. Jackson, and D. M. Altmann.** 2006. The role of the cellular prion protein in the immune system. Clin. Exp. Immunol. **146:**1–8.
27. **Kanaani, J., S. B. Prusiner, J. Diacovo, S. Baekkeskov, and G. Legname.** 2005. Recombinant prion protein induces rapid polarization and development of synapses in embryonic rat hippocampal neurons in vitro. J. Neurochem. **95:**1373–1386.
28. **Keren, A., Y. Tamir, and E. Bengal.** 2006. The p38 MAPK signaling pathway: a major regulator of skeletal muscle development. Mol. Cell Endocrinol. **252:**224–230.
29. **Khosravani, H., Y. Zhang, S. Tsutsui, S. Hameed, C. Altier, J. Hamid, L. Chen, M. Villemaire, Z. Ali, F. R. Jirik, and G. W. Zamponi.** 2008. Prion protein attenuates excitotoxicity by inhibiting NMDA receptors. J. Cell Biol. **181:**551–565.
30. **Klamt, F., F. Dal-Pizzol, M. J. Conte da Frota, R. Walz, M. E. Andrades, E. G. da Silva, R. R. Brentani, I. Izquierdo, and J. C. Fonseca Moreira.** 2001. Imbalance of antioxidant defense in mice lacking cellular prion protein. Free Radic. Biol. Med. **30:**1137–1144.
31. **Kuang, S., M. A. Gillespie, and M. A. Rudnicki.** 2008. Niche regulation of muscle satellite cell self-renewal and differentiation. Cell Stem Cell **2:**22–31.
32. **Lawlor, M. A., and P. Rotwein.** 2000. Insulin-like growth factor-mediated muscle cell survival: central roles for Akt and cyclin-dependent kinase inhibitor p21. Mol. Cell Biol. **20:**8983–8995.
33. **Le Grand, F., and M. A. Rudnicki.** 2007. Skeletal muscle satellite cells and adult myogenesis. Curr. Opin. Cell Biol. **19:**628–633.
34. **Li, Y. P., and R. J. Schwartz.** 2001. TNF-alpha regulates early differentiation of C2C12 myoblasts in an autocrine fashion. FASEB J. **15:**1413–1415.
35. **Linden, R., V. R. Martins, M. A. Prado, M. Cammarota, I. Izquierdo, and R. R. Brentani.** 2008. Physiology of the prion protein. Physiol. Rev. **88:**673–728.
36. **Lopes, M. H., G. N. Hajj, A. G. Muras, G. L. Mancini, R. M. Castro, K. C. Ribeiro, R. R. Brentani, R. Linden, and V. R. Martins.** 2005. Interaction of cellular prion and stress-inducible protein 1 promotes neuritogenesis and neuroprotection by distinct signaling pathways. J. Neurosci. **25:**11330–11339.
37. **Lundberg, I. E., and M. Dastmalchi.** 2002. Possible pathogenic mechanisms in inflammatory myopathies. Rheum. Dis. Clin. North Am. **28:**799–822.
38. **Malaga-Trillo, E., G. P. Solis, Y. Schrock, C. Geiss, L. Luncz, V. Thomanetz, and C. A. Stuermer.** 2009. Regulation of embryonic cell adhesion by the prion protein. PLoS Biol. **7:**e55.
39. **Mallucci, G., A. Dickinson, J. Linehan, P. C. Klohn, S. Brandner, and J. Collinge.** 2003. Depleting neuronal PrP in prion infection prevents disease and reverses spongiosis. Science **302:**871–874.
40. **Mallucci, G. R., S. Ratte, E. A. Asante, J. Linehan, I. Gowland, J. G. Jefferys, and J. Collinge.** 2002. Post-natal knockout of prion protein alters hippocampal CA1 properties, but does not result in neurodegeneration. EMBO J. **21:**202–210.
41. **Manson, J., J. D. West, V. Thomson, P. McBride, M. H. Kaufman, and J. Hope.** 1992. The prion protein gene: a role in mouse embryogenesis? Development **115:**117–122.
42. **Manson, J. C., A. R. Clarke, M. L. Hooper, L. Aitchison, I. McConnell, and J. Hope.** 1994. 129/Ola mice carrying a null mutation in PrP that abolishes mRNA production are developmentally normal. Mol. Neurobiol. **8:**121–127.
43. **Massimino, M. L., J. Ferrari, M. C. Sorgato, and A. Bertoli.** 2006. Heterogeneous PrP^{C} metabolism in skeletal muscle cells. FEBS Lett. **580:**878–884.
44. **McKnight, A. J., A. J. Macfarlane, P. Dri, L. Turley, A. C. Willis, and S. Gordon.** 1996. Molecular cloning of F4/80, a murine macrophage-restricted cell surface glycoprotein with homology to the G-protein-linked transmembrane 7 hormone receptor family. J. Biol. Chem. **271:**486–489.
45. **Merly, F., L. Lescaudron, T. Rouaud, F. Crossin, and M. F. Gardahaut.** 1999. Macrophages enhance muscle satellite cell proliferation and delay their differentiation. Muscle Nerve **22:**724–732.
46. **Miele, G., A. R. Alejo Blanco, H. Baybutt, S. Horvat, J. Manson, and M. Clinton.** 2003. Embryonic activation and developmental expression of the murine prion protein gene. Gene Expr. **11:**1–12.
47. **Musarò, A., K. J. McCullagh, F. J. Naya, E. N. Olson, and N. Rosenthal.** 1999. IGF-1 induces skeletal myocyte hypertrophy through calcineurin in association with GATA-2 and NF-ATc1. Nature **400:**581–585.
48. **Musarò, A., K. McCullagh, A. Paul, L. Houghton, G. Dobrowolny, M. Molinaro, E. R. Barton, H. L. Sweeney, and N. Rosenthal.** 2001. Localized Igf-1 transgene expression sustains hypertrophy and regeneration in senescent skeletal muscle. Nat. Genet. **27:**195–200.
49. **Nachlas, M. M., K. C. Tsou, E. De Souza, C. S. Cheng, and A. M. Seligman.** 1957. Cytochemical demonstration of succinic dehydrogenase by the use of a new p-nitrophenyl substituted ditetrazole. J. Histochem. Cytochem. **5:**420–436.
50. **Nazor, K. E., T. Seward, and G. C. Telling.** 2007. Motor behavioral and neuropathological deficits in mice deficient for normal prion protein expression. Biochim. Biophys. Acta **1772:**645–653.
51. **Nico, P. B., B. Lobao-Soares, M. C. Landemberger, W. Marques, Jr., C. I. Tasca, C. F. de Mello, R. Walz, C. G. Carlotti, Jr., R. R. Brentani, A. C. Sakamoto, and M. M. Bianchin.** 2005. Impaired exercise capacity, but unaltered mitochondrial respiration in skeletal or cardiac muscle of mice lacking cellular prion protein. Neurosci. Lett. **388:**21–26.
52. **Parkin, E. T., N. T. Watt, I. Hussain, E. A. Eckman, C. B. Eckman, J. C. Manson, H. N. Baybutt, A. J. Turner, and N. M. Hooper.** 2007. Cellular prion protein regulates beta-secretase cleavage of the Alzheimer's amyloid precursor protein. Proc. Natl. Acad. Sci. U. S. A. **104:**11062–11067.
53. **Peden, A. H., D. L. Ritchie, M. W. Head, and J. W. Ironside.** 2006. Detection and localization of PrP^{Sc} in the skeletal muscle of patients with variant, iatrogenic, and sporadic forms of Creutzfeldt-Jakob disease. Am. J. Pathol. **168:**927–935.
54. **Pradines, E., D. Loubet, S. Mouillet-Richard, P. Manivet, J. M. Launay, O. Kellermann, and B. Schneider.** 2009. Cellular prion protein coupling to TACE-dependent TNF-alpha shedding controls neurotransmitter catabolism in neuronal cells. J. Neurochem. **110:**912–923.
55. **Prestori, F., P. Rossi, B. Bearzatto, J. Laine, D. Necchi, S. Diwakar, S. N. Schiffmann, H. Axelrad, and E. D'Angelo.** 2008. Altered neuron excitability and synaptic plasticity in the cerebellar granular layer of juvenile prion protein knock-out mice with impaired motor control. J. Neurosci. **28:**7091–7103.
56. **Prusiner, S. B.** 1998. Prions. Proc. Natl. Acad. Sci. U. S. A. **95:**13363–13383.
57. **Reid, M. B., and Y. P. Li.** 2001. Tumor necrosis factor-alpha and muscle wasting: a cellular perspective. Respir. Res. **2:**269–272.
58. **Rommel, C., S. C. Bodine, B. A. Clarke, R. Rossman, L. Nunez, T. N. Stitt, G. D. Yancopoulos, and D. J. Glass.** 2001. Mediation of IGF-1-induced skeletal myotube hypertrophy by PI(3)K/Akt/mTOR and PI(3)K/Akt/GSK3 pathways. Nat. Cell Biol. **3:**1009–1013.
59. **Santuccione, A., V. Sytnyk, I. Leshchyns'ka, and M. Schachner.** 2005. Prion protein recruits its neuronal receptor NCAM to lipid rafts to activate p59fyn and to enhance neurite outgrowth. J. Cell Biol. **169:**341–354.
60. **Schiaffino, S., M. Sandri, and M. Murgia.** 2007. Activity-dependent signaling pathways controlling muscle diversity and plasticity. Physiology **22:**269–278.
61. **Serra, C., D. Palacios, C. Mozzetta, S. V. Forcales, I. Morantte, M. Ripani, D. R. Jones, K. Du, U. S. Jhala, C. Simone, and P. L. Puri.** 2007. Functional interdependence at the chromatin level between the MKK6/p38 and IGF1/PI3K/AKT pathways during muscle differentiation. Mol. Cell **28:**200–213.

62. **Simone, C., S. V. Forcales, D. A. Hill, A. N. Imbalzano, L. Latella, and P. L. Puri.** 2004. p38 pathway targets SWI-SNF chromatin-remodeling complex to muscle-specific loci. Nat. Genet. **36:**738–743.
63. **Sorgato, M. C., C. Peggion, and A. Bertoli.** 2009. Is, indeed, the prion protein a Harlequin servant of "many" masters? Prion **3:**202–205.
64. **Steele, A. D., J. G. Emsley, P. H. Ozdinler, S. Lindquist, and J. D. Macklis.** 2006. Prion protein (PrP^c) positively regulates neural precursor proliferation during developmental and adult mammalian neurogenesis. Proc. Natl. Acad. Sci. U. S. A. **103:**3416–3421.
65. **Steele, A. D., S. Lindquist, and A. Aguzzi.** 2007. The prion protein knockout mouse: a phenotype under challenge. Prion **1:**83–93.
66. **Telling G. C., T. Haga, M. Torchia, P. Tremblay, S. J. DeArmond, and S. B. Prusiner.** 1996. Interactions between wild-type and mutant prion proteins modulate neurodegeneration in transgenic mice. Genes Dev. **10:**1736–1750.
67. **Thomzig, A., W. Schulz-Schaeffer, C. Kratzel, J. Mai, and M. Beekes.** 2004. Preclinical deposition of pathological prion protein PrP^{Sc} in muscles of hamsters orally exposed to scrapie. J. Clin. Invest. **113:**1465–1472.
68. **Westaway, D., S. J. DeArmond, J. Cayetano-Canlas, D. Groth, D. Foster, S. L. Yang, M. Torchia, G. A. Carlson, and S. B. Prusiner.** 1994. Degeneration of skeletal muscle, peripheral nerves, and the central nervous system in transgenic mice overexpressing wild-type prion proteins. Cell **76:**117–129.
69. **Wu, Z., P. J. Woodring, K. S. Bhakta, K. Tamura, F. Wen, J. R. Feramisco, M. Karin, J. Y. Wang, and P. L. Puri.** 2000. p38 and extracellular signal-regulated kinases regulate the myogenic program at multiple steps. Mol. Cell. Biol. **20:**3951–3964.
70. **Zammit, P. S.** 2008. All muscle satellite cells are equal, but are some more equal than others? J. Cell Sci. **121:**2975–2982.
71. **Zanusso, G., G. Vattemi, S. Ferrari, M. Tabaton, E. Pecini, T. Cavallaro, G. Tomelleri, M. Filosto, P. Tonin, E. Nardelli, N. Rizzuto, and S. Monaco.** 2001. Increased expression of the normal cellular isoform of prion protein in inclusion-body myositis, inflammatory myopathies and denervation atrophy. Brain Pathol. **11:**182–189.
72. **Zetser, A., E. Gredinger, and E. Bengal.** 1999. p38 mitogen-activated protein kinase pathway promotes skeletal muscle differentiation. Participation of the Mef2c transcription factor. J. Biol. Chem. **274:**5193–5200.
73. **Zhan, M., B. Jin, S. E. Chen, J. M. Reecy, and Y. P. Li.** 2007. TACE release of TNF-alpha mediates mechanotransduction-induced activation of p38 MAPK and myogenesis. J. Cell Sci. **120:**692–701.
74. **Zhang, C. C., A. D. Steele, S. Lindquist, and H. F. Lodish.** 2006. Prion protein is expressed on long-term repopulating hematopoietic stem cells and is important for their self-renewal. Proc. Natl. Acad. Sci. U. S. A. **103:**2184–2189.

paper II

Cell Cycle 9:23, 1-6; December 1, 2010; © 2010 Landes Bioscience

This manuscript has been published online, prior to printing. Once the issue is complete and page numbers have been assigned, the citation will change accordingly.

Prion and TNFα

TAC(E)it agreement between the prion protein and cell signaling

Roberto Stella,[1] Maria Lina Massimino,[2] M. Catia Sorgato[1] and Alessandro Bertoli[1,*]

[1]Department of Biological Chemistry; and [2]CNR-Institute of Neuroscience; University of Padova; Padova, Italy

Prion diseases are rare and fatal neurodegenerative disorders that occur when the cellular prion protein (PrP^C) is converted into a conformationally modified isoform that originates the novel infectious agent, called prion. Although much information is now available on the different routes of prion infection, both the mechanisms underlying prion neurotoxicity and the physiologic role of PrP^C remain unclear. By use of a novel paradigm, we have shown in a recent paper that—following a myotoxin-induced degenerative challenge—PrP^C is implicated in the morphogenesis of the skeletal muscle of adult mice. PrP^C accomplished this task by modulating signaling pathways central to the myogenic process, in particular the p38 kinase pathway. The possibility that PrP^C acts in cell signaling has already been suggested after in vitro studies. Using our in vivo approach, we have instead provided proof of the physiologic relevance of PrP^C commitment in signaling events, and that PrP^C likely performed the task by controlling the activity of the enzyme (TACE) secreting the signaling TNFα molecule. After a brief summary of our data, here we will discuss the suggestion, arising from our and other recent findings, implying that regulation of TACE, and of other members of the protease family TACE belongs to, may be exploited by PrP^C in different cell contexts. Notably, this advancement of knowledge on PrP^C physiology could also shed light on the defense mechanisms against the onset of a more common neurodegenerative disorder than prion disease, such as Alzheimer disease.

©2010 Landes Bioscience. Do not distribute

Key words: PrP, prion, TNFα, TACE, ADAM, Alzheimer disease

Abbreviations: ADAM, a disintegrin and metalloprotease; AD, Alzheimer disease; APP, amyloid precursor protein; BACE, β-site APP cleaving enzyme; ECM, extra-cellular matrix; GPI, glycosylphosphatidylinositol; KO, knock-out; PrP, prion protein; RIP, regulated intramembrane proteolysis; ROS, reactive oxygen species; TACE, TNFα converting enzyme; TNFα, tumor necrosis factor; TSE, transmissible spongiform encephalopathies; WT, wild-type

Submitted: 10/29/10

Revised: 11/03/10

Accepted: 11/04/10

Previously published online: www.landesbioscience.com/journals/cc/article/14135

*Correspondence to: Alessandro Bertoli; Email: alessandro.bertoli@unipd.it

The Prion Protein in Pathology and Physiology

It is now established that a kind of rare and fatal neurodegenerative disorders, known as transmissible spongiform encephalopathies (TSE) or prion diseases, is intimately related to a protein called prion protein (PrP). These disorders occur on sporadic, genetic or infectious grounds, and include Creutzfeldt-Jakob disease in humans, scrapie in sheep and bovine spongiform encephalopathy (or mad-cow disease) in cattle.[1] In recent years, another TSE form (chronic wasting disease, CWD) affecting deer and elk, has rapidly spread among wild and captive animals in the USA and Canada.[2] This has raised serious concerns over the route of infection sustaining such epidemics, which may include contaminated environments.[3] In TSE, the sialo-glycosylated native isoform of PrP (PrP^C), which binds to the outer leaflet of the plasma membrane via a glycosylphosphatidylinositol (GPI) anchor, undergoes a conformational switch to a pathogenic isoform (PrP^{Sc}). PrP^{Sc} is characterized by distinct physico-chemical and biological properties that include high propensity to aggregate, resistance to proteolysis, and—possibly—neurotoxic potentials. In fact, PrP^{Sc} is the major component of the etiologic TSE agent, the prion, which has the remarkable capacity to self-replicate and propagate into host organisms, i.e., to be infectious. It is now largely accepted that this process proceeds in an auto-catalytic fashion, whereby pre-formed seeds of PrP^{Sc} continuously promote the structural conversion of native PrP^C molecules.[1,4] It is not yet clear, however, if the resulting

neurodegeneration is due to a gain of toxicity of PrP^{Sc}, a loss of function of PrP^{C} or a combination of both mechanisms. This issue is further complicated by the still enigmatic role played by PrP^{C} in cell physiology, and a definite answer has neither been provided by the generation of mice carrying the pre- or post-natal ablation of the PrP gene (*Prnp*).[5-7] Other than resistance to prion infection,[8] these animals display only marginal, if any, phenotypes in lifespan, development or behavior.[9,10] On the other hand, the possibility exists that a hidden phenotype becomes manifest only under defined stress conditions. However, the conservation of PrP^{C} in the vertebrate *sub-phylum* and its ubiquitous tissue expression, argue against the possibility that PrP^{C} may have been evolutionarily selected to only enable the onset and transmission of these fatal brain disorders.

Knowledge of PrP^{C} function is not just a mere conceptual issue, and indeed it is now increasingly accepted that insight into PrP^{C} physiology be strategic to understand the mechanism of prion-induced neurodegeneration, and to develop safe and effective therapeutic interventions. This notion has triggered multiple studies, the majority of which have agreed that PrP^{C} takes part in multi-component surface platforms activating various signaling pathways, and that the outcomes of these signals are beneficial to the cell. To name a few, protection against a variety of cell insults ranging from oxidative stress to apoptotic stimuli and implication in cell adhesion, proliferation and differentiation.[11,12] This kind of data has been collected using primarily cell model systems, which may explain why the physiologic significance of PrP^{C}-mediated signals still remains largely undefined in whole animals or intact tissues.

In this respect, we have recently provided the first clear evidence that PrP^{C} regulates a specific signaling pathway that is instrumental to adult tissue morphogenesis.[13] To obtain this data, our strategy considered the use of an in vivo paradigm novel to the field of PrP^{C} biology. It consisted in acutely damaging the hind limb *Tibialis anterior* muscle of adult mice expressing or not PrP^{C}, and then in following regeneration from muscle precursors cells. Adult skeletal muscles have the remarkable capacity to recover from injury and express substantial PrP^{C} amounts. Therefore, compared to using cell paradigms, this model had the key advantage of retaining all natural elements necessary to accomplish tissue morphogenesis. This condition allowed us to verify in vivo if and how PrP^{C} served in cell differentiation. Also, by imposing an acute stress to adult PrP-knockout (KO) animals, we could circumvent possible compensatory mechanisms occurring during embryogenesis or normal adult life, which have likely prevented until now the identification of clear PrP-KO phenotypes.

Our results have highlighted a significant delay in the regeneration process of PrP-KO muscles with respect to the wild-type (WT) counterpart. When tracing the origin of this delay, we found that PrP-KO muscles had reduced amounts of the inflammatory cytokine tumor necrosis factor α (TNFα), which acts in the very early stages after muscle injury. In turn, the lower TNFα levels severely downregulated in these animals the signaling pathway involved in the progression of the myogenic program.

After a brief outline of our results and a concise review of recent suggestions inherent to the issue, we will discuss the possible mechanism by which PrP^{C} regulates cell signaling in muscle differentiation, and whether PrP^{C} performs the task by modulating the activity of cell surface enzymes.

PrP^{C} Promotes Regeneration of Adult Skeletal Muscle

Our study comprised two phases. In the first part, WT and PrP-KO muscles were compared at advanced stages of regeneration, using selected macroscopic parameters such as morphometric aspects (i.e., the fibre cross-section area and the percentage of fused fibres), and a biochemical signature of muscle maturation (i.e., expression of neonatal myosin heavy chain). Taken together, these measurements concurred to highlight that PrP-KO muscles regenerated more slowly that the WT counterpart. It is important to underline, however, that regeneration of adult murine muscles, which mimics embryonic myogenesis, reached full and identical accomplishment irrespective of the Prnp genotype. This finding is consistent with the lack of developmental phenotypes of PrP-KO mice repeatedly reported in the past, and re-confirmed in our study.

Next, we examined which could have been the preceding event of the complex myogenic process responsible for the delayed recovery of PrP-KO muscles, including the events that, immediately after injury, critically ensue muscle regeneration, i.e., recruitment of macrophages and production of cytokines. We found that macrophages were similarly present in both damaged muscle types, but that PrP-KO muscles had significantly reduced levels of TNFα, at the first allowed time point of analysis (three days after damage). Given also the similar amounts of the TNFα precursor, pro-TNFα, in WT and PrP-KO samples, these results strongly indicated that PrP^{C} could have played a role in TNFα release by regulating proteolysis of the TNFα precursor.

TNFα is secreted by both inflammatory cells and skeletal muscle precursors, thereby sustaining regeneration by paracrine and autocrine mechanisms. It is also established that TNFα stimulates differentiation of muscle precursor cells[14,15] by activating the mitogen-activated protein kinase p38.[15,16] Expectedly, we found that PrP-KO muscles displayed significantly reduced amounts of active (phosphorylated (P-)) p38 than WT samples. P-p38 regulates muscle differentiation in multiple ways; it directly activates pioneer muscle regulatory factors (MRFs), such as MyoD and Myf5, but it also regulates the ATP-dependent SWI/SNF chromatin remodeling complex that allows access and binding of muscle transcription factors (MEF-2 and MRFs) to their specific loci.[17-20] Finally, P-p38 induces p21, an inhibitor of cyclin-dependent kinases, promoting cell cycle arrest and terminal differentiation of muscle precursors.[18,21] Interestingly, we found that the Akt kinase, which works synergistically with p38 in the SWI/SNF-mediated chromatin remodeling,[20,22] was also downregulated in regenerating PrP-KO muscles. That the absence of PrP^{C} delayed withdrawal of muscle precursors from the cell cycle and, hence, retarded their differentiation, was further confirmed by the prolonged

©2010 Landes Bioscience. Do not distribute

period of time in which PrP-KO progenitors remained in the proliferating stage compared to the WT counterpart. This assay was carried out by both following the in vivo incorporation of a thymidine analog and the expression of Pax7, the gold-standard marker of cycling skeletal muscle stem cells. Pax7 is critical to maintaining proliferation of muscle precursors, and needs therefore to be shut off for differentiation to proceed. Very recently, it has been reported that TNFα-mediated activation of p38 epigenetically controls the differentiation of muscle stem cells also by inducing the repressive silencing of the Pax7 promoter.[23] This finding nicely fits with our observation that in the early phases of regeneration the expression of Pax7 was much higher in PrP-KO muscles than in WT samples.

Importantly, the PrP-KO phenotype observed in our study was completely abrogated in a mouse line in which a *Prnp* transgene had been reintroduced into PrP-KO animals. Taken together, our findings are therefore highly suggestive for the implication of PrP^C in the very early events of muscle regeneration, specifically in the release of TNFα that is essential to the myogenic program (see **Fig. 1**).

There is a strong parallelism between our data and those reported by Steele and co-workers.[24] Using different methodologies and model systems, these authors have shown that the absence of PrP^C delayed the rate of the in vitro differentiation of embryonic neural precursors, without affecting neither the in vivo net neurogenesis, nor the gross morphology of the adult central nervous system. Also in agreement with our results is the demonstration that the absence of PrP^C protracted both mitosis of cerebellar granule cell precursors and maturation of the granule layer in the first post-natal weeks, and that both events did not compromise the final acquisition of a normal architecture of the cerebellum.[25] Thus, all these findings support the contention that, by affecting the rate, but not the end point, of tissue morphogenesis, PrP^C is involved in the maturation of different tissues. As our data have highlighted the importance of using in vivo models to best decipher the physiologic action of PrP^C, this same mean of experimentation could be used to assess whether PrP^C also assists the neurogenic process, by stimulating activity of extracellular proteases (see below), and/or release of signaling molecules.

PrP^C as Regulator of Extra-Cellular Matrix Proteases

A long standing question that has puzzled the prion field regards the way by which PrP^C, a cell surface protein with no intracellular domain, conveys a biologic information to the inside of the cell. One of the most accepted hypotheses entails that PrP^C serves as co-receptor in multicomponent complexes or as scaffold protein to recruit other molecules into these signaling platforms. The many studies on this topic have forwarded a large number of putative interacting partners of PrP^C, among which plasma membrane and extra-cellular matrix (ECM) proteins.[11] Our data intimately relate to this issue, by supporting the proposition that PrP^C participates in transducing signals that eventually regulate the cell phosphorylation cascades.[26] However, having identified TNFα as precocious actor of PrP^C-mediated signals, they also raise the hypothesis that PrP^C could modulate the activity of enzymes that release signaling molecules, as is TNFα.

Specifically, we know that this factor is released from its transmembrane precursor pro-TNFα, thanks to the proteolytic cleavage by the TNFα converting enzyme (TACE, also named ADAM17). TACE is the best known member of the ADAM (*a d*isintegrin *a*nd *m*etalloproteinase) family.[27,28] TACE and other type-I ADAM members span the plasma membrane with the Zn^{2+}-binding catalytic domain invariably facing the ECM. This explains why ADAM members are normally classified as ECM enzymes. To note, however, that some members lack enzymatic activity, and act as cell adhesion molecules. Typically, catalytically active ADAM members release into the ECM the ectodomain of many cell surface proteins. This process is known as "shedding", from which the name sheddases or secretases, for these enzymes. The secretion of protein ectodomains has recently emerged crucial to cell fate determination, cell adhesion, neurite and axon guidance, tissue morphogenesis and other biological processes.[29,30] It is therefore not unexpected the impressive and continuously growing number of identified ADAM substrates, among which growth factors, cytokines, receptors and adhesion molecules. The spectrum of the biological effects of ADAM members is further expanded by the requirement of secretases for the "regulated intramembrane proteolysis" (RIP) of many substrates, which takes place only after ectodomain shedding. Thus, RIP activity on transmembrane proteins generates cytosolic fragments that can translocate to the nucleus and regulate gene transcription, as occurring in Notch signaling, for example.[30]

In addition to the mentioned pro-TNFα, the cohort of TACE substrates includes receptors for TNFα and other cytokines, cell adhesion molecules and the amyloid precursor protein implicated in Alzheimer disease (AD).[27,28] It seems likely, therefore, that the biological consequences of TACE activity depend on both the nature of the shedded substrate and the cellular context in which TACE operates.[27-29] For example, as is the case for TNFα, TACE can generate extracellular soluble messengers that initiate downstream signaling events upon binding to their receptor. Conversely, when the substrate is a cell surface receptor, proteolysis by TACE downregulates, rather than increases, signal transduction. The detailed regulation of TACE is still poorly understood, but it is now believed that also this process (as the regulation of other ADAM members) could be cell-specific. Among the most frequently proposed regulatory means, we can recall:[27,29] (i) direct phosphorylation at sites located in the cytosolic tail of the enzyme; (ii) TACE and substrate co-clustering in response to inducers of shedding; (iii) displacement of an inhibitory molecule; (iv) activation by reactive oxygen species (ROS).[31] Unsurprisingly, the overall multifaceted aspect of ADAM members has often recognized these enzymes as candidate therapeutic targets in several pathological states, such as cancer, autoimmune diseases and neurodegenerative disorders.[28-30]

As for PrP^C-TACE relationship, our suggestion that PrP^C could regulate (directly or indirectly) TACE activity is

©2010 Landes Bioscience. Do not distribute

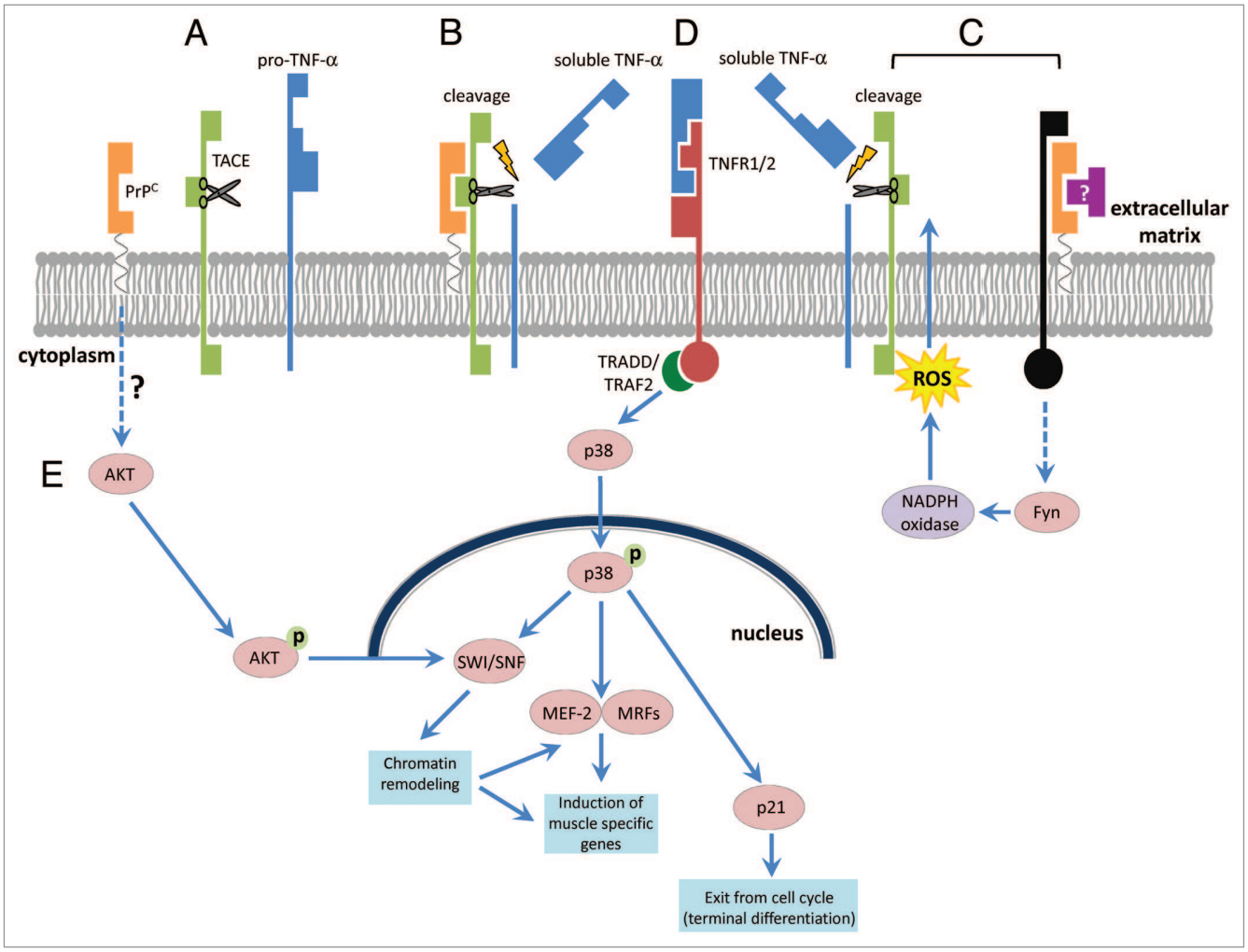

Figure 1. Hypothetical scheme for PrP^C-dependent signaling events in skeletal muscle regeneration. The GPI-anchored PrP^C (yellow) is located to the surface of muscle precursor cells (A), together with the trans-membrane enzyme TACE (green), and the TACE substrate pro-TNFα (blue). Following myogenic cues, PrP^C activates TACE either directly (B) or indirectly (C) (see below). Activated TACE promotes ectodomain shedding of pro-TNFα and release of soluble TNFα. In turn, binding of TNFα to its membrane receptors (TNFR1/2, red) (D) triggers activation of the p38 signaling pathway through the possible involvement of TRADD and TRAF2 adaptor proteins. Activated (phosphorylated, P-) p38 translocates to the nucleus, where it stimulates the myogenic program by different modes of action: (i) activation of the SWI/SNF chromatin remodeling complex; (ii) activation of muscle specific transcription factors (MEF-2 and MRFs); (iii) induction of p21, which promotes exit from the cell cycle of muscle progenitors. By unknown mechanisms, PrP^C can also upregulate Akt (E), which works synergistically with P-p38 in regulating the SWI/SNF complex. As to the mechanism by which PrP^C stimulates TACE, this may occur by direct physical interaction of the two proteins (B), which could also result in the delivery of PrP^C-bound Zn^{2+} to the catalytic site of the enzyme. Alternatively, PrP^C could take part in an as yet unknown signaling platform (black) (C). Binding of a hypothetical ligand (magenta) to the complex could then trigger TACE activity via the Fyn-dependent NADPH oxidase route and subsequent ROS production, as has been shown in neuronal cell lines.[37] See the text for further details.

consistent with other observations on the interplay of PrP^C with ADAM proteins. One example of this functional interaction is the shedding of the far C-end of PrP^C itself by the coordinated action of ADAM9 and ADAM10.[32] In particular, following activation by ADAM9 by an as yet unknown mechanism, ADAM10 cleaves PrP^C three amino acid residues prior to the GPI anchor attachment site. Also the central region of PrP^C undergoes two distinct endo-proteolytic events, termed α- and β-cleavage, of which the α-cleavage implicates ADAM9, ADAM10 and ADAM17 (TACE).[33-35] Although the latter report has recently been questioned,[32] the patho-physiologic relevance of PrP^C shedding and of the endo-proteolytic processes remains unclear.

If ADAM23, which lacks the catalytic domain typical of metalloproteases and acts as a cell adhesion molecule, has been claimed to function as PrP^C partner,[36] much more important information on PrP^C-TACE relationship has come from the work by Kellermann and coworkers. These authors have provided compelling in vitro evidence for a role of PrP^C in the activation of TACE. This was achieved by stimulating serotonergic and noradrenergic neurons with antibody-mediated PrP^C cross-linking that, by triggering Fyn-dependent NADPH oxidase

activation and the subsequent production of ROS, ultimately resulted in ROS-mediated upregulation of TACE activity.[37] This result opens the possibility that the NADPH oxidase route be the mechanism by which PrP^C commonly regulates TACE, and consequently, that it could also occur in the differentiation of muscle precursors. However, because regulation of ADAM enzymes could be cell context-dependent, at this stage a direct PrP^C-TACE interaction cannot be excluded. In support of this possibility stands the above mentioned enzyme-substrate interaction allowing PrP^C shedding by ADAM10,[32] and the notion that—among all ADAM family members—ADAM10 shares with TACE the highest degree of sequence homology.[29] Finally, given that N-terminal octapeptide repeats of PrP^C bind metal ions (primarily Cu^{2+} but also Zn^{2+} and other ions),[38,39] one may tentatively suggest that the interaction serves for PrP^C to deliver Zn^{2+} to TACE catalytic site (**Fig. 1**).

PrP^C, ECM Proteases and Alzheimer Disease

An exciting outcome arising from the suggested capacity of PrP^C to stimulate TACE is that this interaction may be relevant in another devastating neurodegenerative disorder, such as AD. AD affects more than 30 million individuals worldwide, but no effective drug is currently available to cure or counteract the disease. AD is characterized by the brain deposition of senile plaques, predominantly composed of 40 or 42, amino acid-long fragments (Aβ) of the amyloid precursor protein (APP). However, it is Aβ oligomers, particularly if made of 1–42 peptides, those believed to cause a series of synaptic dysfunctions that eventually lead to neurodegeneration.[40,41] Aβ derives from the proteolytic processing of APP, an integral type-I protein of the plasma membrane, which is firstly cleaved in its ectodomain by the membrane-bound aspartyl protease β-site APP cleaving enzyme (BACE1 or β-secretase), and then subjected to RIP by means of an intra-membrane complex known as γ-secretase. The combined action of the two enzymes thus generates extra-cellular Aβ (1-40/1-42) peptides and an intra-cellular fragment that regulates gene transcription.[40,42-44] Recently, it has been suggested that PrP^C protects against AD onset because, by markedly downregulating BACE1-mediated cleavage of APP, it reduces Aβ production both in vitro and in vivo.[45,46] Analyses on model cells have proposed that the glycosamminoglycan-mediated interaction between PrP^C and BACE1 can either inhibit BACE1 activity or recruit BACE1 into raft regions, thereby displacing the enzyme from its substrate.[45,47] Alternative to the action of BACE1 that governs the above described "amyloidogenic pathway", APP can enter the "non-amyloidogenic pathway".[48-50] In this case, APP processing is catalyzed by an enzyme historically known as α-secretase, which sheds APP ectodomain at a site distinct from that of BACE1. The consequence of this action is the breaking down of toxic Aβ fragments and the prevention of their neurotoxic effects.[50,51] At least three members of the ADAM family, including TACE, have been shown to possess α-secretase activity.[28-30,48,49]

Hence, were indeed PrP^C able to stimulate TACE activity as our work suggests, and were this valid also with respect to APP shedding, PrP^C would then strongly favor the non-amyloidogenic pathway by downregulating the β-cleavage and by simultaneously stimulating the α-cleavage of APP. An important corollary of this possibility is that the proposed depletion of PrP^C to prevent or treat prion diseases could dangerously reduce the physiological defenses against AD.

Concluding Remarks

In many neurodegenerative disorders characterized by protein misfolding and aggregation, elucidation of the pathogenic mechanism has often been hampered by the uncertain physiologic function of the proteins implicated in the disease. In this respect, PrP^C is no exception. Considerable efforts have long been focused on the disease-associated PrP^{Sc} isoform, and on the mechanisms of prion transmission and replication, with less emphasis being devoted to the role of PrP^C in cell physiology. A plethora of putative functions has however been ascribed to PrP^C, but it did not result in a proposition recapitulating the multiple, sometime contrasting, observations collected in cell (mainly neuronal) models. With few exceptions, also animal models have only provided phenomenological data on this issue. Conversely, our in vivo paradigms of WT and PrP-KO mice have forwarded strong evidence that PrP^C is involved in adult skeletal muscle morphogenesis. Remarkably, while confirming that PrP^C controls signaling pathways, these same models have underscored that the signal has an undoubted physiologic significance, and that it likely triggers the release of signaling molecules mediated by TACE. To the best of our knowledge, this is the first clear PrP-KO phenotype detected in mammals.

The possibility that PrP^C regulates ADAM members other than TACE, and that this process takes place also in neurons or other tissues, is attractive and worthy of further investigation. In this way, we could improve our understanding on the regulatory mechanisms of ADAM enzymes. At the same time, given the wide spectrum of roles attributed to ADAM members, we could perhaps also find a rationale for the heterogeneous phenomenological dataset so far reported for the biology of PrP^C.

©2010 Landes Bioscience. Do not distribute.

Acknowledgements

This work was supported by grants of the Italian Ministry of University and Research (Prin 2008, to M.C.S.), and by the University of Padova (Progetto d'Ateneo CPDA089551, to A.B.).

References

1. Aguzzi A, Calella AM. Prions: protein aggregation and infectious diseases. Physiol Rev 2009; 89:1105-52.
2. Sigurdson CJ, Aguzzi A. Chronic wasting disease. Biochim Biophys Acta 2007; 1772:610-8.
3. Genovesi S, Leita L, Sequi P, Andrighetto I, Sorgato MC, Bertoli A. Direct detection of soil-bound prions. PLoS One 2007; 2:1069.
4. Prusiner SB. Prions. Proc Natl Acad Sci USA 1998; 95:13363-83.
5. Büeler H, Fischer M, Lang Y, Bluethmann H, Lipp HP, DeArmond SJ, et al. Normal development and behaviour of mice lacking the neuronal cell-surface PrP protein. Nature 1992; 356:577-82.
6. Manson JC, Clarke AR, Hooper ML, Aitchison L, McConnell I, Hope J. 129/Ola mice carrying a null mutation in PrP that abolishes mRNA production are developmentally normal. Mol Neurobiol 1994; 8:121-7.
7. Mallucci GR, Ratté S, Asante EA, Linehan J, Gowland I, Jefferys JG. Post-natal knockout of prion protein alters hippocampal CA1 properties, but does not result in neurodegeneration. EMBO J 2002; 21:202-10.

8. Büeler H, Aguzzi A, Sailer A, Greiner RA, Autenried P, Aguet M, et al. Mice devoid of PrP are resistant to scrapie. Cell 1993; 73:1339-47.
9. Criado JR, Sanchez-Alavez M, Conti B, Giacchino JL, Wills DN, Henriksen SJ, et al. Mice devoid of prion protein have cognitive deficits that are rescued by reconstitution of PrP in neurons. Neurobiol Dis 2005; 19:255-65.
10. Nazor KE, Seward T, Telling GC. Motor behavioral and neuropathological deficits in mice deficient for normal prion protein expression. Biochim Biophys Acta 2007; 1772:645-53.
11. Aguzzi A, Baumann F, Bremer J. The prion's elusive reason for being. Annu Rev Neurosci 2008; 31:439-77.
12. Linden R, Martins VR, Prado MA, Cammarota M, Izquierdo I, Brentani RR. Physiology of the prion protein. Physiol Rev 2008; 88:673-728.
13. Stella R, Massimino ML, Sandri M, Sorgato MC, Bertoli A. Cellular prion protein promotes regeneration of adult muscle tissue. Mol Cell Biol 2010; 30:4864-76.
14. Chen SE, Gerken E, Zhang Y, Zhan M, Mohan RK, Li A, et al. Role of TNFalpha signaling in regeneration of cardiotoxin-injured muscle. Am J Physiol Cell Physiol 2005; 289:1179-87.
15. Chen SE, Jin B, Li YP. TNFalpha regulates myogenesis and muscle regeneration by activating p38 MAPK. Am J Physiol Cell Physiol 2007; 292:1660-71.
16. Zhan M, Jin B, Chen SE, Reecy JM, Li YP. TACE release of TNFalpha mediates mechanotransduction-induced activation of p38 MAPK and myogenesis. J Cell Sci 2007; 120:692-701.
17. Zetser A, Gredinger E, Bengal E. p38 mitogen-activated protein kinase pathway promotes skeletal muscle differentiation. Participation of the Mef2c transcription factor. J Biol Chem 1999; 274:5193-200.
18. Wu Z, Woodring PJ, Bhakta KS, Tamura K, Wen F, Feramisco JR, et al. p38 and extracellular signal-regulated kinases regulate the myogenic program at multiple steps. Mol Cell Biol 2000; 20:3951-64.
19. Simone C, Forcales SV, Hill DA, Imbalzano AN, Latella L, Puri PL. p38 pathway targets SWI-SNF chromatin-remodeling complex to muscle-specific loci. Nat Genet 2004; 36:738-43.
20. Albini S, Puri PL. SWI/SNF complexes, chromatin remodeling and skeletal myogenesis: it's time to exchange! Exp Cell Res 2010; 316:3073-80.
21. Cabane C, Englaro W, Yeow K, Ragno M, Dérijard B. Regulation of C2C12 myogenic terminal differentiation by MKK3/p38alpha pathway. Am J Physiol Cell Physiol 2003; 284:658-66.
22. Serra C, Palacios D, Mozzetta C, Forcales SV, Morantte I, Ripani M, et al. Functional interdependence at the chromatin level between the MKK6/p38 and IGF1/PI3K/AKT pathways during muscle differentiation. Mol Cell 2007; 28:200-13.
23. Palacios D, Mozzetta C, Consalvi S, Caretti G, Saccone V, Proserpio V, et al. TNF/p38α/polycomb signaling to Pax7 locus in satellite cells links inflammation to the epigenetic control of muscle regeneration. Cell Stem Cell 2010; 7:455-69.
24. Steele AD, Emsley JG, Ozdinler PH, Lindquist S, Macklis JD. Prion protein (PrP^{c}) positively regulates neural precursor proliferation during developmental and adult mammalian neurogenesis. Proc Natl Acad Sci USA 2006; 103:3416-21.
25. Prestori F, Rossi P, Bearzatto B, Lainé J, Necchi D, Diwakar S, et al. Altered neuron excitability and synaptic plasticity in the cerebellar granular layer of juvenile prion protein knock-out mice with impaired motor control. J Neurosci 2008; 28:7091-103.
26. Sorgato MC, Peggion C, Bertoli A. Is, indeed the prion protein a Harlequin servant of "many" masters? Prion 2009; 3:202-5.
27. Black RA. Tumor necrosis factoralpha converting enzyme. Int J Biochem Cell Biol 2002; 34:1-5.
28. Gooz M. ADAM-17: the enzyme that does it all. Crit Rev Biochem Mol Biol 2010; 45:146-69.
29. Edwards DR, Handsley MM, Pennington CJ. The ADAM metalloproteinases. Mol Aspects Med 2008; 29:258-89.
30. Reiss K, Saftig P. The "a disintegrin and metalloprotease" (ADAM) family of sheddases: physiological and cellular functions. Semin Cell Dev Biol 2009; 20:126-37.
31. Zhang Z, Oliver P, Lancaster JR Jr, Schwarzenberger PO, Joshi MS, Cork J, et al. Reactive oxygen species mediate tumor necrosis factoralpha-converting, enzyme-dependent ectodomain shedding induced by phorbol myristate acetate. FASEB J 2001; 15:303-5.
32. Taylor DR, Parkin ET, Cocklin SL, Ault JR, Ashcroft AE, Turner AJ, et al. Role of ADAMs in the ectodomain shedding and conformational conversion of the prion protein. J Biol Chem 2009; 284:22590-600.
33. Vincent B, Paitel E, Saftig P, Frobert Y, Hartmann D, De Strooper B, et al. The disintegrins ADAM10 and TACE contribute to the constitutive and phorbol ester-regulated normal cleavage of the cellular prion protein. J Biol Chem 2001; 276:37743-6.
34. Cissé MA, Sunyach C, Lefranc-Jullien S, Postina R, Vincent B, Checler F. The disintegrin ADAM9 indirectly contributes to the physiological processing of cellular prion by modulating ADAM10 activity. J Biol Chem 2005; 280:40624-31.
35. Alfa Cissé M, Sunyach C, Slack BE, Fisher A, Vincent B, Checler F. M1 and M3 muscarinic receptors control physiological processing of cellular prion by modulating ADAM17 phosphorylation and activity. J Neurosci 2007; 27:4083-92.
36. Costa MD, Paludo KS, Klassen G, Lopes MH, Mercadante AF, Martins VR, et al. Characterization of a specific interaction between ADAM23 and cellular prion protein. Neurosci Lett 2009; 46:16-20.
37. Pradines E, Loubet D, Mouillet-Richard S, Manivet P, Launay JM, Kellermann O, et al. Cellular prion protein coupling to TACE-dependent TNFalpha shedding controls neurotransmitter catabolism in neuronal cells. J Neurochem 2009; 110:912-23.
38. Brown DR, Qin K, Herms JW, Madlung A, Manson J, Strome R, et al. The cellular prion protein binds copper in vivo. Nature 1997; 390:684-7.
39. Watt NT, Hooper NM. The prion protein and neuronal zinc homeostasis. Trends Biochem Sci 2003; 28:406-10.
40. Haass C, Selkoe DJ. Soluble protein oligomers in neurodegeneration: lessons from the Alzheimer's amyloid beta-peptide. Nat Rev Mol Cell Biol 2007; 8:101-12.
41. Nimmrich V, Ebert U. Is Alzheimer's disease a result of presynaptic failure? Synaptic dysfunctions induced by oligomeric beta-amyloid. Rev Neurosci 2009; 20:1-12.
42. Walter J, Kaether C, Steiner H, Haass C. The cell biology of Alzheimer's disease: uncovering the secrets of secretases. Curr Opin Neurobiol 2001; 11:585-90.
43. Haass C. Take five—BACE and the gamma-secretase quartet conduct Alzheimer's amyloid beta-peptide generation. EMBO J 2004; 23:483-8.
44. Müller T, Meyer HE, Egensperger R, Marcus K. The amyloid precursor protein intracellular domain (AICD) as modulator of gene expression, apoptosis and cytoskeletal dynamics-relevance for Alzheimer's disease. Prog Neurobiol 2008; 85:393-406.
45. Parkin ET, Watt NT, Hussain I, Eckman EA, Eckman CB, Manson JC, et al. Cellular prion protein regulates beta-secretase cleavage of the Alzheimer's amyloid precursor protein. Proc Natl Acad Sci USA 2007; 104:11062-7.
46. Kellett KA, Hooper NM. Prion protein and Alzheimer disease. Prion 2009; 3:190-4.
47. Hooper NM, Turner AJ. A new take on prions: preventing Alzheimer's disease. Trends Biochem Sci 2008; 33:151-5.
48. Allinson TM, Parkin ET, Turner AJ, Hooper NM. ADAMs family members as amyloid precursor protein alpha-secretases. J Neurosci Res 2003; 74:342-52.
49. Hooper NM. Roles of proteolysis and lipid rafts in the processing of the amyloid precursor protein and prion protein. Biochem Soc Trans 2005; 33:335-8.
50. Vardy ER, Catto AJ, Hooper NM. Proteolytic mechanisms in amyloid-beta metabolism: therapeutic implications for Alzheimer's disease. Trends Mol Med 2005; 11:464-72.
51. Fahrenholz F. Alpha-secretase as a therapeutic target. Curr Alzheimer Res 2007; 4:412-7.

©2010 Landes Bioscience. Do not distribute.

CONCLUSIONS AND PERSPECTIVES

Elucidating the physiologic function of PrP^C is of major importance to understand the mechanisms of prion-induced neurodegeneration, and to devise safe and effective therapeutic strategies against prion diseases. In the papers reported in this Chapter, we focused on the role of PrP^C in cell proliferation and differentiation, which has been previously proposed for the nervous tissue (Prestori *et al*., 2008; Santuccione *et al*., 2005; Steele *et al*., 2006). Experimentally, this was achieved by exploiting a novel strategy in the prion field, based on determining if PrP^C influenced regeneration of injured hindlimb *tibialis anterior* (TA) muscles from adult mice expressing (WT), or not (PrP-KO), PrP^C. PrP-KO mice reconstituted with transgenic PrP^C served as further control. Our findings demonstrated that PrP^C takes part in the repair of injured skeletal muscles, thus implying that the role of PrP^C in cell differentiation is not restricted to the CNS, but that it may be broadly involved in the maintenance and repair of tissues during the entire lifetime of animals.

In particular we observed that PrP-KO TAs regenerated more slowly than the PrP-expressing counterparts, and that they were exposed to lower amount of TNF-α. TNF-α is known to be a crucial actor in myogenesis, in light of its capacity to trigger the MAPK p38 pathway leading to differentiation of muscle precursor cells (Chen *et al*., 2005; Chen *et al*., 2007; Zhan *et al*., 2007). Accordingly we found that PrP-KO muscles displayed significantly reduced amounts of active (phosphorylated) p38 than WT samples. Active p38 is known to regulate the: (i), activation of pioneer muscle regulatory factors (MRFs), such as MyoD and Myf5 (Simone *et al*., 2004; Serra *et al*., 2007); (ii), chromatin remodeling complex that allows access and binding of muscle transcription factors (MEF-2 and MRFs) to their specific loci (Albini and Puri, 2010); (iii), induction of p21, an inhibitor of cyclin-dependent kinases, promoting cell cycle arrest and terminal differentiation of muscle precursors (Cabane *et al*., 2003); (iv), silencing of the Pax7 promoter (Palacios *et al*., 2010). Thus, our observations that PrP-KO muscles had both a higher Pax7 expression level, and a lower active Akt (which acts to promote muscle differentiation

synergistically with p38) (Serra *et al*., 2007; Albini and Puri, 2010), were fully consistent with the possibility that the prime cause of the delayed acquisition of normal morphology of PrP-KO TA muscles was to be ascribed to the diminished TNF-α production by both macrophages and myoblasts themselves. Our data therefore, strongly suggest that the early stages of muscle regeneration are under the control of PrP^C and that PrP^C modulates the activity of the TNF-α converting enzyme (TACE, a member of the *a disintegrin an metalloproteases* (ADAM) protein family) that hydrolyzes and releases mature TNF-α from pro-TNF-α.

In conclusion, our study has provided evidence, for the first time *in vivo*, that PrP^C controls intracellular signaling pathways, and that this property has a remarkable importance in a physiologic process, such as skeletal muscle regeneration. Our data also suggest that PrP^C could impinge on signaling events by modulating the activity of extracellular enzymes (e.g., TACE) that promote the release of soluble signaling molecules. Given the wide spectrum of roles attributed to TACE and other ADAM family members, this observation could provide a rationale for multiple, sometime contrasting observations so far provided for PrP^C physiologic function. At the same time this work opens a number of possible investigations on:

(1) the cell type that contributes mostly to the release of TNF-α during muscle regeneration. This issue could be clarified by using, for example, primary cultures of WT myoblasts, and, likewise, PrP-KO myoblasts, co-cultured in presence of PrP-KO or PrP-expressing macrophages, and following in the different cell mixtures the activation of the p38 pathway, or myoblast differentiation process;

(2) the mechanism by which TACE, and other ADAM proteins, are regulated. Indeed, a detailed comprehension of the modulation of TACE activity is still lacking, and it is now believed that this process could be cell context-specific. Therefore, the possibility that PrP^C regulates TACE in different cell types is of great interest and worthy of further investigation;

(3) the relation of PrP^C with Alzheimer's disease (AD) another devastating neurodegenerative disorder. AD-associated neurodegeneration is caused by the brain accumulation of the amyloid β peptide (Aβ), which is generated by two sequential proteolytic cleavages of the amyloid precursor protein (APP) through the action of β- and γ-secretases (Haass and Selkoe, 2007). Conversely, by governing the so-called non-amyloidogenic pathway, the cleavage of APP by α-secretase avoids the production and accumulation of the neurotoxic Aβ (Allison *et al*., 2003; Hooper, 2005; Vardy *et al*., 2005). Importantly, at least three members of the ADAM family, including TACE, have been shown to possess α-secretase activity. Of consequence, were indeed PrP^C able to stimulate TACE activity also with respect to APP cleavage, PrP^C would then strongly favor the non-amyloidogenic pathway, thus preventing AD pathogenesis.

CHAPTER II

PROTEOMICS PROFILING FOR BIOMARKERS DISCOVERY IN BULLS TREATED WITH GROWTH PROMOTING AGENTS

INTRODUCTION

Growth promoting agents (GPA)

In recent years, food safety problems have become a frequently recurring phenomenon. To reach the required level of protection, reliable data have to be made available, to enable adequate risk evaluation and subsequent action. In other words, sophisticated and robust analytical methods have to be developed for a wide variety of micro-contaminants, which are primarily organic compounds.

In modern agricultural practice, veterinary drugs are being used on a large scale and administered as feed additives, or via the drinking water, for several purposes. For example, they are used in the case or, to prevent the outbreak, of diseases, and to prevent losses during animal transportation. In addition, growth-promoting agents (GPA), such as hormones, are often applied to stimulate the growth by various mechanisms. The prohibition of the use of growth-promoting agents such as hormones, corticosteroids and β-agonists is laid down in Council Directive 96/22/EC. Council Directive 96/23/EC regulates the residue control (monitoring) of pharmacologically active compounds (i.e. environmental contaminants, dyes, chemical elements, etc.) in products of animal origin, and, for this purpose, also establishes National Surveillance Programs for the monitoring of residues. Control for forbidden compound has a higher priority because of public-health concern: relatively large numbers of samples have to be analyzed and more stringent criteria have to be used in view of the serious implications of positive results for public health.

Corticosteroids are anti-inflammatory drugs whose use as growth-promoters is banned in the EU. Corticosteroids are frequently used in veterinary medicine,

often in combination with other drugs, such as antimicrobial drugs or β-agonists. They can be divided in two main groups: mineralocorticoids and glucocorticoids. Together with anti-inflammatory activities, the latter have important effects on gluconeogenesis, glycogen deposition and protein metabolism. The glucocorticoid dexamethasone is widely used because, thanks to its anti-inflammatory properties, it suppresses the clinical manifestations of disease in a wide range of disorders (Reynolds, 1996). Although it has long been recognized that large doses of synthetic glucocorticoids reduce growth rates and lead to muscle atrophy, dexamethasone and other corticosteroids are frequently used as illegal growth promoters in livestock production. Very low doses of glucocorticoids, indeed, result in improved feed intake, increased live weight gain, reduced feed conversion ratio, reduced nitrogen retention and increased water retention and fat content (Istasse *et al*., 1984).

Sexual steroids, such as estrogens, are believed to act *via* receptors in the muscular tissue, as well as indirectly through the stimulation of growth hormone release from the hypophysis, and other growth factors from liver. Steroid hormones are nowadays seldom used alone, but rather in combination with other compounds in order to improve the anabolic effects, and to reduce the administered dosages so that it becomes easier to escape the analytical controls performed by the official laboratories (Cantiello *et al*., 2008).

Corticosteroids are often combined with β-agonists and/or other anabolic steroids. Cocktails with β-agonists appear to be in use to prevent receptor down-regulation and tolerance in the animals. In muscle tissue, β-agonists promote lipolysis. This may result in reduced carcass fat, and increased carcass proteins up to 40% (Courtheyn *et al*., 2002). While the therapeutic treatment with β-agonists in cattle affected by respiratory diseases is permitted, the use of these compounds as growth promoters in cattle is forbidden in the EU. In several countries clenbuterol, a β_2-agonist, is authorized for therapeutic use as a bronchospasmolytic agent in veterinary medicine. High dosages of clenbuterol has marked anabolic effects leading to a remarkable increase of growth rate and an improvement of carcass composition because of a reduced fat content (Mitchell *et al*., 1994). The β-agonists enhance growth efficiency by stimulation

of β-adrenergic receptors on cell surfaces. In muscle tissue, this stimulation promotes protein synthesis and cell hypertrophy by inhibition of proteolysis. In adipose tissue, β-agonists promote lipolysis. This redirecting of cellular energy metabolism has prompted the referencing of some β-agonists as “re-partitioning agents”. For this reason, they have been frequently used in meat-producing animals. The illegal use of these active substances resulted in several cases of food poisoning with symptoms, such as tremor, tachycardia and nervousness (Mazzanti *et al*., 2003). In addition, a series of clenbuterol-like compounds that have occurred in black market preparations possesed stronger lipophilicity and a predominant β_1-activity, which could be more effective for anabolic purposes but also increases the toxicological risk on consumer’s health.

Conventional analytical techniques

The most employed techniques for the detection of pharmacological treatments in livestock animals for growth promoting purpose are based on the direct detection of pharmacologically active compounds or their metabolites in target organs or urines. Generally, the matrix of interest for corticosteroids analysis is animal urine, liver or meat. Most analytical methods are based on solid phase extraction (SPE) as sample extraction and clean-up method. Prior to this step, the release of analytes from glucuronide and/or sulphate conjugates is performed, when they have to be determined in liver or urine (Stolker *et al*., 2005). A recent study has compared different techniques employed during the last years for the determination of corticosteroid residues in biological matrices. This investigation concluded that liquid chromatography, coupled to tandem mass spectrometry (LC-MS/MS), is the ideal tool for monitoring corticosteroids (Antignac *et al*., 2004). By applying the multiple reaction monitoring (MRM) mode, this system achieves the best sensitivity and selectivity. This type of analysis is typically performed using triple-quadrupole mass spectrometers and achieved as follows: after ionization, the specific m/z of the compound under investigation is selected in the first quadrupole (Q1), this ion is then fragmented in the second quadrupole (Q2) using collision induced dissociation (CID), and,

finally, only ions of interest are monitored in the third quadrupole (Q3). Then, measured intensities are converted into drug concentrations.

As for the detection of β-agonists, several reports demonstrated that the accumulation of such compounds occur in the retinal tissue of food-producing animals (Gowik *et al*., 2000). Specifically, the study showed that the concentration of clenbuterol in the retina exceeds that found in liver, suggesting this matrix as the best candidate for the residue control of β-agonists. However, the limited amount of retinal tissue obtainable from a single animal may pose an analytical hurdle (Elliott *et al*., 1993). Also for these compounds, non-selective SPE resulted the best choice for multi-residue β-agonists extraction (dos Ramos, 2000). As for separation and detection, the most used technique is LC-MS/MS operation mode, based on two specific transitions for each compound.

Finally, the use of natural sex steroid hormones and their esters is still a remarkable problem in the control of residues of growth promoters, given that exogenous administration of these compounds leads to the same hormones and metabolites as the endogenous molecules. Therefore, an illegal treatment must be determined by means of quantitative measurements. In this regard, methods have been proposed that are based on the by liquid-liquid extraction of gestagens from kidney, fat, or meat, and their determination, after derivatization, by gas chromatography coupled to mass spectrometry (GC-MS), or, more recently, by LC-MS/MS (Stolker *et al*., 2005).

Although in dept examinations have provided evidence for the continued illegal use of a large variety of growth promoters, their detection in matrices of biological origin is still elusive because of the low dosages used, and because the concentration of the corresponding endogenous hormones can widely vary according to animal physiology (species, sex, age physio-pathological states, etc.). Hence, quantitative measurement of other indirect parameters is highly warranted. Furthermore, new substances and modified molecules introduced in the meat industry can elude screening and confirmatory tests. In this respect the use of structure-targetted methodologies, such as tandem MS, which are increasingly applied for screening purposes, is not suitable in detecting molecules with unknown structure.

In conclusion, the improvement of screening approaches is strongly needed. To this purpose, the application of screening methods based on the measurement of indirect parameters, such as histological and/or physiological modifications in specific tissues, should be encouraged.

Proteome complexity

The term proteome, coined by Wilkins in 1994 (Wilkins *et al*., 1996), describe the complete set of proteins that are expressed by a cell at any given condition. In contrast to the genome, the proteome is highly dynamic with both instantaneous and long-term variations throughout the life cycle of an organism. Proteomics today refers to a scientific discipline that, using a number of different approaches, analyzes the protein content in a given cell or tissue. Since proteins are the key players in the physiology of an organism, and interact with each other in complex networks of signaling cascades, studying proteins at a global level allows to better understand the whole biological system. The set of all different proteins in a biological system has proven to be extremely complex, in part because of mRNA splicing that lead to different proteins from a single gene. In addition, proteins are post-translationally modified (e.g., glycosylation, phosphorylation), whereby different protein molecules display a wide range of physicochemical properties that further complicate the analysis of whole proteomes (Hanash, 2003).

It soon became evident that the information arising from genome sequencing was insufficient to decipher how gene products actually function in their biological context, and that it was not possible to use only nucleotide sequence data to elucidate complex biological processes. For this reason, the focus has turned to investigate (qualitatively and quantitatively) the components of a biological system, mainly mRNA (transcriptomics), proteins (proteomics) and metabolites (metabolomics). Protein functions are regulated by their abundance and post-translational modifications, such as phosphorylation, glycosylation and cleavage (Moritz and Meyer, 2003). Accordingly, changes in protein concentrations and the extent of post-translational modifications greatly influences biological processes. Any defects in these processes can result in

pathogenic effects. For this reason, proteins are an important target for therapeutic designs, while assessment of changes between normal and altered states can be used for prognosis and diagnosis.

Tools for global and systematic analysis of the genome have been developed (e.g. mRNA microarrays), which, however, are not sufficient for the characterization of whole biological systems, mainly because mRNA abundances are not reliable indicators of the corresponding protein abundances. Indeed, protein abundance depends not only on the mRNA level, but also on translational and protein degradation systems (Gygi, 1999; Cox and Mann, 2007). Proteomics, on the other hand, is inherently more complex than DNA-based technologies. So far, no complete protein expression map of any organism has been presented because currently available techniques cannot cope with such a level of complexity. Yet, because sufficiently comprehensive information about a biological system can be obtained by proteomic approaches, proteomics is an attractive tool to study a complex biological system.

Proteomics originally aimed only at identifying protein expression patterns and the differences in protein expression between pairs of samples derived from different tissues or conditions. Subsequently, however, it has extended to define structural and functional features of proteins on a large scale. The analysis of proteomes is significantly more challenging than that of genomes. In particular, there is greater diversity in proteins at the amino acid composition level, the proteome is dynamic (both spatially and temporally), and a wide range of variation of proteins concentrations exists within, and between, cells. Unfortunately, proteomic analysis is substrate limited, because methods for protein amplification are not available. Two main areas of this field are ‘profiling’ and ‘functional’ proteomics. Profiling proteomics encompasses the description of the whole proteome of an organism (by analogy with the genome) and includes organelle mapping and differential measurement of expression levels between cells or conditions. Functional proteomics characterizes protein activity, interactions and the presence of post-translational modifications (Patterson and Aebersold, 2003).

Biomarkers discovery

Biomarkers are indicators of relevant biological conditions. In medical and pharmacogenomic applications, they are intended to provide answers to a variety of essential questions in human health. Biomarkers have a role in risk assessment, disease prediction, early detection, diagnosis, prognosis, disease monitoring, and evaluation of therapeutic response. As such, improved biomarkers are urgently needed to facilitate both clinical care and biomedical research. Biomarker discovery has historically been dominated by targeted approaches, in which candidates derived from biological knowledge were evaluated for their correlations with biological conditions. What gives a protein the status of a biomarker is its consistent variation in some fundamental characteristic, such as abundance, between physiologic and pathologic states, or between two different physiologic states. Such abundance variation can occur *via* many mechanisms, including differential expression, sequestration, secretion, leakage, cleavage, etc. (Gillette *et al*., 2005). Ideally a biomarker exists at a high expression level in one state, and is completely absent in the other. Unfortunately, this is most often not the case and a certain threshold in a protein's expression level has to be established to distinguish two different biological conditions. In addition, a single marker protein is not sufficient to distinguish between two different physiologic states, and the recognition of large-scale expression patterns could be fundamental in medical diagnostics. If different biomarkers behave independently as predictor of a certain physiologic state, then the combination of many of them remarkably improves both sensitivity and specificity of analytical procedures. The major reason for putting such high hopes to proteomics in the context of biomarkers discovery is the ability to test many potential candidate biomarkers simultaneously.

PROTEOMICS APPROACHES

Separation techniques

Because of protein diversity, a range of proteomic technologies has emerged, which rely on integration of biological, chemical and analytical methods. The principal technologies that currently underlie most proteomic platforms can be classified as mass spectrometry (MS) coupled with protein separation (Aebersold and Mann, 2003). MS is a highly sensitive and versatile technique for studying proteins. It can be used to derive *de novo* sequences as well as to quantify relative and absolute amounts of proteins. In proteomics, the most common approaches used are peptide mass fingerprinting and tandem mass MS sequencing. Technical improvements and the availability of genome sequences have established the use of these MS methods as a powerful tool for rapidly identifying proteins from very complex biological samples. The combination of MS protein identification with two-dimensional gel electrophoresis (2DE) remains a standard tool in proteomics since its introduction over 30 years ago (Klose, 1975; O'Farrell, 1975).

The potential of 2DE has been greatly advanced with the development of the method itself (Gorg *et al*., 2004), as well as the development of MS technologies for identification of proteins. 2DE separates the proteins and provide also a relative quantity of the proteins when comparing different samples. However, 2DE remains subject to technical and analytical limitations, the most significant of these being that certain key classes of proteins, such as membrane proteins, are not efficiently represented on 2DE. Alternative protein separation techniques complementary to 2DE have emerged. A common approach involves tryptic digestion of protein mixtures followed by multi-dimensional high performance liquid chromatography (HPLC) coupled with MS. This separation mode fits very well as the last step before introduction of analytes to the mass spectrometer. The most commonly used separation technique is the reversed phase (RP)-HPLC that separate molecules based on their reversible interaction with the hydrophobic matrix of the stationary phase.

In this way samples are eluted according to their degree of hydrophobicity, with earlier delivery of more hydrophilic analytes (Dong, 1992).

When handling complex samples, a common practice is to combine RP-HPLC with a preceding chromatography separation, a strategy named two-dimensional liquid chromatography (2D-LC). In this way, two different physical properties of peptides can be utilized for a more extensive separation. For this arrangement, strong cation exchange (SCX) has found the most widespread use, because it separates molecules based on their positive charge and bound entities are displaced by increasing amount of salts in the mobile phase. These two modes of separation are very compatible since the eluate from SCX columns can be directly applied to the RP column where samples are cleaned from salts (Wagner *et al*., 2002; Dwivedi *et al*., 2008). The combination of multidimensional chromatography with MS provides a gel-free approach to analyzing very complex protein samples. Among different possible approaches to study proteins, MS-based proteomics is increasingly used to acquire the data important for understanding complex biological processes.

Mass analyzer

Mass spectrometry has increasingly become the method of choice for analysis of complex protein samples. MS-based proteomics is a discipline made possible by the availability of gene and genome sequence databases and technical and conceptual advances in many areas, most notably the discovery and development of protein ionization methods (Aebersold, 2003). In general, mass spectrometers are forming, separating and detecting molecular ions based on their mass-to-charge ratio (m/z). Simply described, a mass spectrometer consist of three main components: the ionization source, where analyte molecules are transferred into gas-phase ions, the mass analyzer where the ions are separated, and the detector where these ions are recorded.

Electrospray ionization (ESI) (Fenn *et al*., 1989) and matrix-assisted laser desorption ionization (MALDI) (Karas *et al*., 1987) are the two techniques most commonly used to ionize peptides for mass spectrometric analysis offering an extended mass range and higher sensitivity. ESI ionizes the analytes out of a

solution and is therefore suitable to be coupled to liquid-based separation tools. MALDI sublimates and ionizes the samples out of a dry, crystalline matrix applying laser pulses.

There are four main types of mass analyzer that are widely used: ion trap, time-of-flight (TOF), quadrupole, and Fourier transform ion cyclotron resonance (FT-ICR and Orbitrap). Each type of analyzer has its advantages and weakness in term of accuracy, sensitivity and resolution. These analyzers can stand alone or combined to take advantage of the strengths of each. When two or more mass analyzers are applied in series to separate ions, MS is known as tandem MS (MS/MS). Specific ions from a mixture are isolated in the first mass analyzer on the basis of their m/z ratio and fragmented within the instrument. Peptide ions are fragmented along their backbone, usually by collision with an inert gas such as helium or nitrogen at low pressure (CID). The resulting spectrum, called an MS/MS spectrum, is basically a list of m/z ratios for different fragments with some of the differences corresponding to the specific mass of one amino acid, therefore, in principle, in the spectrum is represented the peptide amino acid sequence (Aebersold and Mann, 2003). In ion-trap analyzers, the ions are first captured or 'trapped' for a certain time interval and are then subjected to MS or MS/MS analysis. Ion traps are robust, sensitive, but a disadvantage of ion traps is their relatively low mass accuracy. The introduction of linear ion traps has overcome this problem allowing increased sensitivity, resolution and mass accuracy (Schwartz *et al*., 2002). The FT-MS instrument is also a trapping mass spectrometer, its strengths are high sensitivity, mass accuracy, resolution and dynamic range. All these analyzers are mostly been coupled to ESI ion sources.

MALDI is usually coupled to TOF analyzers that measure the mass of intact peptides, but more recently, new configurations of mass analyzers have found wide application for protein analysis. To allow the fragmentation of MALDI-generated precursor ions, two TOF sections can be separated by a collision cell (TOF-TOF instrument) (Medzihradszky *et al*., 2000), alternatively, the collision cell can be placed between a quadrupole mass filter and a TOF analyzer (Q-TOF instrument) (Loboda *et al*., 2000). Ions of a particular m/z are selected in a first mass analyzer, fragmented in the collision cell and the resulting fragments

are sorted by a TOF analyzer. These instruments have high sensitivity, resolution and mass accuracy. The resulting fragment ion spectra are often more extensive and informative than those generated in trapping instruments.

Another possible configuration is the combination of a linear ion trap with an Orbitrap instrument (that is a Fourier transform type analyzer), most commonly coupled to ESI ion sources. In this hybrid mass spectrometer ions circulate around a central, spindle-shaped electrode (Makarov, 2000; Scigelova and Makarov, 2006), and the axial frequency of oscillations of the ions on this trajectory is proportional to the square root of m/z. Because this frequency can be determined with high precision, the m/z is measured very accurately. As a result of its excellent mass accuracy, high resolution and sensitivity, this instrument has recently become one of the most widespread in proteomics field.

Quantification techniques

Relative abundance of proteins between two cellular states, for example between control and specific perturbation, is a crucial variable in cell biology experiments. In order to obtain a relative quantification of peptides contained in different samples, from HPLC-based proteomics analyses, there are two main approaches: the use of isotopic tags or label-free quantification. The alternative to metabolic labelling is chemical modification of peptides by stable isotope-containing tags. The best known strategy to this end is called isobaric Tagging for Relative and Absolute Quantification (iTRAQ). It uses up to eight isobaric tags that react with primary amine groups of peptides. During MS analysis, the tags are fragmented into reporter groups of different mass for each tag. The intensity of the different reporter groups is then used to derive the relative abundance of the corresponding peptides and proteins in the starting mixture (Ross *et al*., 2004). Similar to this technique are the Isotope Coded Affinity Tags (ICAT) that allow double-plexing (Gygi *et al*., 1999), and Tandem Mass Tags (TMT) that can be used with up to six samples to be compared (Thompson *et al*., 2003; Dayon *et al*., 2008).

Another approach is the use of non-radioactive isotope-containing amino acids to label proteins in cell cultures. This technique is called metabolic labelling or

Stable Isotope Labelling with Amino acids in Cell culture (SILAC) (Ong *et al*., 2002). To this end, cell are grown in a medium containing "heavy" arginine and/or lysine labelled with ^{13}C and/or ^{15}N, which are integrated into all proteins in the course of several cell doublings. Potentially all proteins can be labelled and the absence of any chemical steps make the method easy to apply as well as compatible with multistage purification procedures. Digestion of these proteins with an enzyme that specifically cuts after arginine or lysine (i.e. trypsin), leads to peptides with a heavy amino acid at their C-terminus. The heavy labelled proteome remains distinguishable from the non labelled control proteome and the two can be combined together immediately after cell lysis, highly reducing technical variability during samples processing. The resulting mixture contains SILAC peptide pairs that have the exact mass difference between the heavy and normal amino acids. The relative intensity of the peaks reflects the relative abundance of the peptides, and, indirectly, of the proteins in the mixture.

Besides stable isotope labelling, the “label-free” quantification is increasingly used. The basic idea of this technique is to align separate LC-MS/MS runs of peptide mixtures and to calculate differences in intensities of the same peptides detected in each run. This quantification is simpler than isotope-based methods, although less accurate, and is suitable for primary cell cultures that are impossible to be labelled with amino acids (Old *et al*., 2005).

Though all these relatively new techniques have emerged, the classical and most widely used method to separate and analyze complex mixtures of proteins is the 2DE.

METHODS USED IN THE STUDY

2D gel based proteomics

One of the most employed method for quantitative proteome analysis combines protein separation by high resolution two-dimensional gel electrophoresis with tandem mass spectrometric (MS/MS) identification of selected protein spots. In this technique, proteins are separated according to two independent parameters, isolelectric point (pI) in the first dimension, and molecular mass in the second, by coupling isoelectric focusing (IEF) and sodium dodecyl sulfate polyacrylamide gel electrophoresis (SDS-PAGE). Following separation the proteins are visualized and the protein expression profiles can be compared between samples and analyzed qualitatively and quantitatively using any of numerous computers software commercially available (Rogers *et al*., 2003). The proteins can then be subsequently excised from the gel and identified, most commonly, by mass spectrometry. Although many have predicted 2DE to be played out by other novel proteomics techniques it still remains one of the major approach for large proteomics studies especially thanks to the development of the technology leading to increasing resolution and reproducibility (Gorg *et al*., 2009).

2DE can routinely be applied for analyzing many samples in parallel and it also allow for quantitative expression profiling. Depending on gel size and pH gradient used, 2DE resolve more than 2000 proteins simultaneously, it can be highly reproducible and since the proteins are separated in a gel they can be saved for long time for further analysis. The separation occurs at protein level, which is advantageous both for further protein identification and since post-translational modified proteins are separated. Modifications such as phosphorylation or glycosylation are important for several biological processes and their dysregulation have been implicated in different type of pathological and altered physiological conditions. These are the reasons for choosing this technology for the bovine skeletal muscle analysis (paper III).

Despite the improvements of the 2DE technique, the main inherent limitation still remains the fact that many proteins are expressed at such low levels that

they will escape detection. For some applications, this problem can be partly overcome by subcellular fractionation or immuno- or affinity-depletion of the most abundant proteins (Huber *et al*., 2003; Kim and Kim 2007), although these methods can lead to reproducibility problems. Moreover membrane proteins, highly hydrophobic, are difficult to be solubilized, and they tend to precipitate at the interface between the IPG strip and the polyacrylamide gel (Santoni *et al*., 2000; Rabilloud, 2009). Finally 2DE is a very labour-intensive technique with several time-consuming steps to optimize to get satisfactory results.

Sample preparation for 2DE

Sample preparation is one of the most critical steps in proteomics. Almost any kind of tissue can be analyzed by 2DE and although a protocol has always to be optimized for the sample under study, there are some general principles. Sample preparation begins with the disruption of the tissue which should be done rapidly and keeping the sample cold in order to avoid proteolysis and protein degradation. Preferably samples are disrupted directly in a buffer containing strongly denaturing agents (detergents and chaotropic agents) and proteases inhibitor cocktail. Insoluble material is removed by centrifugation.
After homogenization, proteins have to be placed in a suitable buffer for the IEF. To achieve this, a sample for 2DE must contain a chaotropic agent such as urea or thiourea, neutral or zwitterionic detergents such as Triton-X or CHAPS to solubilize protein and minimize aggregation, and a reducing agent, such as dithiotreitol (DTT), to disrupt disulfide bonds. In addition, carrier ampholytes are often used in order to ensure conductivity and buffering capacity during IEF.

First dimension - isoelectric focusing

Proteins are amphoteric molecules that carry a positive, negative or zero net charge depending on the pH of their surroudings. The isoelectric point (pI) of a protein is the pH value at which the protein has a zero net charge. The IEF is achieved by using an immobilized pH gradient and applying an electrical field through it, in this way the proteins migrate to the pH where they have zero net charge (their pI). The slope of the pH gradient and the strength of the electrical

field determine the resolution. The introduction of commercially available immobilized pH gradient strips (IPG strips) improved reproducibility and allowed to save time when running large sample sets.

Second dimension - SDS PAGE

The second dimension is based on SDS-PAGE that allow to separate proteins on the basis of their molecular weight. This is achieved using polyacrylamide gel containing SDS. SDS is an anionic strongly denaturing detergent that disrupts hydrogen bonds, blocks hydrophobic interactions, partially unfolds proteins, and gives proteins a net negative charge proportional to their mass. Prior to SDS-PAGE, reduced disulfide bonds are carboxymethylated using an alkylating agent such as iodoacetamide. After first dimension separation and denaturation in presence of SDS, proteins are separated by applying the IPG strip to the polyacrylamide gel. Depending on the percentage and the ratio of acrylamide : bisacrylamide, the gel posses a specific distribution of pore sizes. When an electric field is applied through the gel, negatively charged proteins are forced to migrate across the gel towards the cathode. Depending on their size, the electrophoretic mobility of each protein is different through the gel. In particular, proteins with low molecular weight move easier in the gel matrix, while high molecular weight proteins are slowed down by the gel matrix (Laemmli, 1970).

Protein detection

A large number of methods have been developed to detect proteins separated in a 2D-gel. The most common ones involve the binding of a dye or precipitated silver salts to the proteins. The most important requirements are high sensitivity, high linear dynamic range, high reproducibility, and compatibility with mass spectrometry (Westermeier and Marouga, 2005). Common staining methods include coomassie blue (Neuhoff *et al*., 1988), which is easy to use, and is compatible with mass spectrometry, and silver staining that is more sensitive (around 2 ng), but is laborious, difficult to be standardized and modification to

the protocols have to be introduced to ensure compatibility with mass spectrometry.

More recently a number of fluorescent dyes have been developed that are sensitive, compatible with mass spectrometry and provide easy protocols. One such example is Sypro Ruby that provides excellent sensitivity (Rabilloud *et al*., 2001).

Differential in gel electrophoresis (DIGE)

2DE is an important proteomics tool, where thousands of protein spots can be visualized in order to give a global view of the proteome. By comparing the 2D spot patterns from different samples, changes in individual proteins can be detected and quantified. This allows identification of protein markers (called biomarkers) that are characteristic of a specific physiological or pathological state of a cell or tissue (Friso *et al*., 2001). A limitation of comparative 2DE analysis is the high degree of gel-to-gel variation in spot patterns, indeed conventional 2DE separates one sample per gel and thus the biological differences between the samples cannot readily be separated from technical variation between gels and several technical replicates has to be run in order to mean these technical variations. In 2D differential in gel electrophoresis (DIGE), samples are labelled prior to electrophoresis with spectrally resolvable fluorescent dyes (Cy2, Cy3 and Cy5) known as CyDyes (Figure 5). The linearity, sensitivity, and wide dynamic range of these dyes have made 2D DIGE into a quantitative technique.

These CyDyes are used to differentially label proteins prior to electrophoresis for comparative analysis of up to three different samples on the same gel. Two types of CyDyes are available: one for "minimal labelling", and the other for "saturation labelling". Lysine labeling is referred to as minimal because the ratio of dye to protein is kept very low so that the only protein visualized on the gel are those that are labeled with a single dye molecule. The relatively high lysine content of most proteins makes this amino acid suitable for this strategy, in which single CyDye covalently attaches to the epsilon amino group of lysine residues thanks to an N-hydroxysuccinimide-ester reactive group. The

fluorophores are very similar in molecular masses and are positively charged to match the charge that is replaced on the lysine residue.

By contrast, the saturation dyes label all available cysteine groups on each protein. To achieve optimum labeling of cysteine residues, a high dye to protein ratio is required. The relatively low prevalence of cysteine residues in proteins, in addition to the fact that its chemistry is amenable to chemical modification, makes this amino acid suitable for this labelling strategy, where very high amounts of dye are used (Shaw *et al*., 2003). These dyes have a neutral charge and possess a maleimide reactive group which is designed to form a covalent bond with the thiol group of cysteine residues via a thioether linkage. They are recommended for applications in which a very small amount of sample is available.

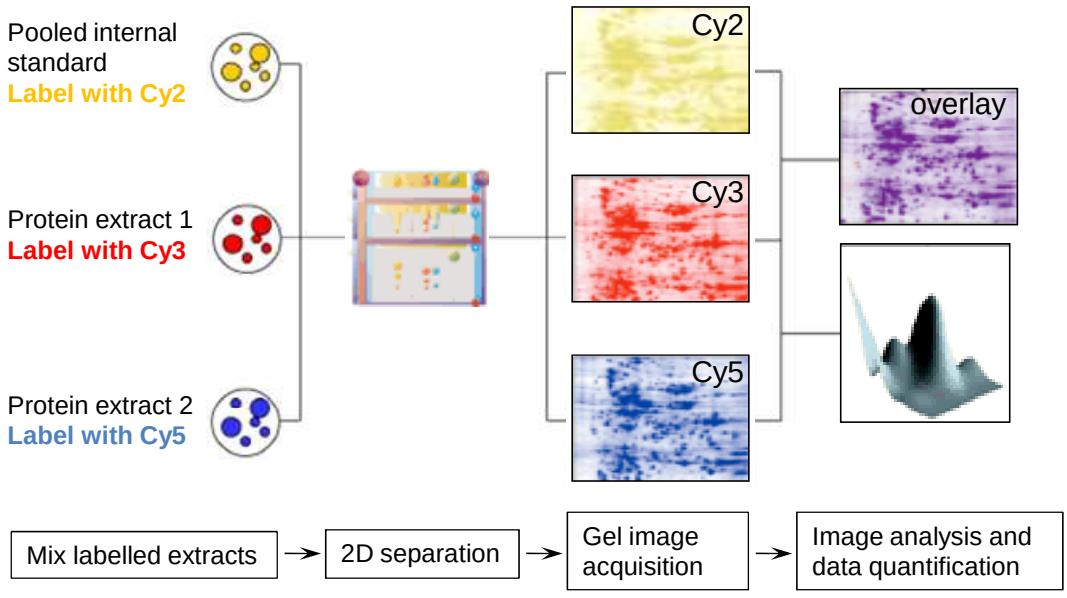

Figure 5. Schematic representation showing the DIGE workflow. Image adapted from Ettan DIGE System User Manual.

After labelling, samples are mixed prior to IEF and resolved on the same 2D gel (Unlü *et al*., 1997; Minden *et al*., 2009). The charge and mass matching is crucial and ensures that all the samples essentially comigrate to the same point during electrophoresis. Then the gel is scanned at different wavelengths and

three images, corresponding to the three different samples, are generated. Running multiple samples on the same 2D gel means reduction in spot pattern variation in addition to a reduction in the number of gels required in an experiment. In addition, using one of the three CyDyes (usually Cy2) to label an internal pooled standard that is prepared by mixing equal amounts of protein from each biological sample in the experiment, every protein from all samples will be represented in each analytical gel. In this way, each sample within a gel can be normalized to the internal standard present on that gel, thus the abundance of each protein spot in a biological sample can be measured as a ratio (not a volume) to its corresponding spot present in the internal standard. This enables accurate quantification, more accurate statistics between gels and, most importantly, separation of experimental variation from inherent biological variation (Alban *et al*., 2003).

This methodology significantly improved sample throughput by halving the number of gels required since two analytical samples are run per gel. Labelled proteins are visualized using a Typhoon variable mode scanner. The Cy2, Cy3, and Cy5 dye images are scanned sequentially with 488, 532, and 633 nm lasers, respectively giving the optimum results with minimal crosstalk between fluorescent channels. Unfortunately, image analysis is a user-variable process and is often a major bottleneck in proteomics. For this reason, DeCyder differential analysis software has been developed as part of the DIGE system. This analysis software allows automatic spot detection, normalization and matching between gels. A number of (100-200) manual matched spots (called landmarks) are set for each gel in order to assist the automatic match algorithm. The spot detection is achieved by a cumulative image derived from the merged individual images of each gel. Spots are then quantified using their sum pixel intensity and values are expressed as ratios relative to the internal standard sample. Afterword, these ratios are normalized so that the modal peak of volume ratios is zero (assuming that the majority of proteins are not changed in expression). DeCyder software contains tools for statistical analyses, but other software specific for statistical analyses are freely available (e.g. the statistical platform R).

Database searching using MS and MS/MS spectra

A key advance in biological mass spectrometer was the development of algorithms for the identification of proteins by mass spectrometric data matched to a database, originally using a set of peptide masses (peptide mass fingerprint), and now using the fragmentation spectra of the individual peptide (MS/MS database searching).

In the first method, a "mass fingerprint" is obtained from a protein cleaved using a sequence-specific protease, such as trypsin. This set of masses is then compared to the theoretically expected tryptic peptide masses for each entry in the database. Generally, peptide fingerprint is used for the rapid identification of a single protein component. Protein sequences need to be in the database in substantially full length. Isoforms can be discriminated from each other only if in the peptide map appear peptides covering the sequence differences (Mann *et al*., 2001).

Tandem mass spectrometric data obtained from proteins of interest are generally more specific and discriminating because the spectra contain structural information, related to the sequence of the peptide, rather than only its mass. The peptide sequence method (Mann and Wilm, 1994) makes use of the fact that nearly every tandem mass spectra contains at least a short run of fragment ions that unambiguously specifies a short amino acid sequence. As few as two amino acids can be combined with the start mass and the end mass of the series, which specify the exact location of the sequence in the petide and the known cleavage specificity of the enzyme. Such a peptide sequence tag will then retrieve from the database one of the few sequences whose theoretical fragmentation pattern is matched against the experimental one.

Other methods do not attempt to extract any sequence information from the MS/MS spectrum (Eng *et al*., 1994). Instead, the experimental spectrum is matched against a calculated spectrum for all peptides in the database. A score is given to determine how much the tandem mass spectrum agrees with the calculated sequence. Another score indicates how differently the next most similar sequence in the database fits the spectrum. Although this method can

be highly automated, the sequences need to be verified by manual inspection (Mann *et al*., 2001).

AIM OF THE STUDY

The study described in the second part of this thesis (and in paper III) was aimed at evaluating if a correlation exists between the treatment with growth promoting agents (GPA) and alterations in the two-dimensional electrophoresis protein pattern of skeletal muscle of beef cattle. The strong pharmacological activity of synthetic GPA (in particular corticosteroids and β-agonists) makes the residues of these molecules potentially dangerous for meat consumers. As a consequence, the administration of such drugs for growth promoting purposes has never been allowed in the EU, and their use in livestock is restricted to therapeutic indications. The misuse of GPA in bovine meat industry, however, appears to be quite a common practice. Unfortunately, classical assays, are not suited to detect compounds either of unknown chemical structure, or present at levels well below the limits of quantification. Histological analyses on animals treated with such compounds have underscored the advantages of the detection of the biological effects of the molecules under consideration, rather than the analysis of drug residues by classical analytical methods. These biological effects can be represented by naturally occurring molecules like proteins, which are partially or totally modified in structures or in concentrations following the treatment with GPA. Proteomics could thus represent a powerful tool to detect changes in protein expression mediated by GPA. In an attempt to identify possible biological markers of the treatment with GPA, 48 bulls were divided in treatment and control groups, and a 2D-DIGE-based proteomic approach was exploited using protein extracts from the *biceps brachii* skeletal muscle. Proteins differentially expressed between treated and control animals were identified by MALDI MS/MS analysis.

paper III

Proteomic Profiling of Skeletal Muscle for Discovering Biomarkers for Growth Promoters Abuse in Beef Cattle

Roberto Stella[1,2], Giancarlo Biancotto[1], Morten Krogh[3], Roberto Angeletti[1], Giandomenico Pozza[1], Maria Catia Sorgato[2], Peter James[3,*] and Igino Andrighetto[1]

[1]Istituto Zooprofilattico Sperimentale delle Venezie, Viale dell'Università 10. 35020 Legnaro, Italy; [2]Department of Biological Chemistry, University of Padova, Via G. Colombo 3. 35131 Padova, Italy; [3]Department of Immunotechnology, BMC D13, Lund University. 221 84 Lund, Sweden

*Corresponding author at: Department of Immunotechnology, BMC D13, Lund University. Tel: ++46 46 222 1496; Fax: ++46 46 222 4200; e-mail: peter.james@immun.lth.se

ABSTRACT

The fraudulent treatment of cattle with growth promoting agents (GPAs) is a matter of great concern for the European Union (EU) authorities and consumers. It has been estimated that 10% of animals are being illegally treated in the EU, though only a much lower percentage of sampled animals (< 0.5%) are actually found as being non-compliant by conventional analytical methods (Stephany, 2010). For this reason, it is believed that the application of indirect methods, based on the detection of biological effects of these substances on target organs, such as the alteration of protein expression profiles, should be tested.

Here we present a preliminary study aimed at evaluating if a correlation exists between the treatment with GPAs and alterations in the two-dimensional electrophoresis (2DE) protein pattern of skeletal muscle. To this aim 24 mixed-bred bulls (Charolaise x Limousine) and 24 Charolaise bulls, 18-21 months old, were divided into different groups: 32 bulls were treated with dexamethasone alone, or in combination with clenbuterol, or 17β-oestradiol, and 16 bulls were used as a control group. The efficiency of the treatment was evaluated measuring the drug residue in target organs such as liver and skeletal muscle sampled at the slaughterhouse, and in urine collected at different time points during the treatment.

A 2D-DIGE approach was carried out using protein extracts from the *biceps brachii* skeletal muscle. After statistical evaluation, the protein spots that were differentially expressed between treated and control groups, were isolated, digested and identified by MALDI-MS\MS analysis. These proteins can be taken in consideration as potential indirect biomarkers of the use of glucocorticoids and β_2-agonists as growth promoters.

INTRODUCTION

Despite the ban by the European Union (EU), the misuse of growth promoting agents (GPAs) such as sexual steroids, β_2-agonists and corticosteroids in raising beef cattle appears to be a common practice in the EU. The strong pharmacological activity of synthetic corticosteroids makes the residues of these molecules potentially dangerous for meat consumers. As a consequence, the administration of such drugs for growth promoting purposes has never been allowed in the EU, and their use in livestock is restricted to some limited therapeutic indications. On the other hand, it is well-known that synthetic corticosteroids, especially at low dosages and mostly through oral administration, are illicitly used as growth-promoters either alone or within protocols involving other active principles. Although the effects of dexamethasone (DXM), the most illegally employed glucocorticoid, on cattle weight gain are controversial (Gottardo *et al*., 2008), there is evidence indicating that its effects on improving the overall carcass quality traits, with an increase in subcutaneous fat deposition, are partly explained by the significant increase of serum insulin in treated animals, which is likely responsible for reduced protein catabolism and enhanced lipogenesis (Corah *et al*., 1995). In this respect, the relationship between DXM and insulin level has been underlined by *in vitro* studies, demonstrating that the glucocorticoid drug is able to enhance the proliferation of skeletal muscle cells, induced by both insulin and insulin growth factor-1 (Dodson *et al*., 1985; Giorgino and Smith, 1995). Moreover synthetic glucocorticoids are also administered in combination with other active principles in order to take advantage of their synergistic effects with different illegal growth-promoting agents, so that they may be employed at lowered dosages (Courtheyn *et al*., 2002). In particular, DXM can reverse the β_2-agonist-mediated down-regulation of β_2-adrenoreceptors, thereby enhancing the repartitioning effects of such β_2-adrenergic mimetics (Odore *et al*., 2006).

Therefore it is becoming more and more interesting to investigate the possibility of developing screening methods based on the detection of the biological effects of the molecules under consideration, rather than the analysis of drug residues by classical analytical methods (Nebbia *et al*., 2006). The classical assays, are not suited to detect compounds either of unknown chemical structure, which are frequently found in seized black market preparations (Courtheyn *et al*., 2002) or present at levels well below the limits of quantification. Histological analyses of tissues of target organs -indirectly influenced and modified by these treatments- has indicated the potential of this approach (Castagnaro and Poppi, 2006): the advantage of this methodology is given by the fact that cellular or tissue modifications could be evident even long time after the end of the treatment when chemical residues may be no more detectable. On contrast this approach is significantly limited by the subjective experience and evaluation skill of technicians. Among the new strategic approaches that are under investigation throughout the European Union the most promising ones are based on the detection of indirect biomarkers, in fluids or tissues, represented by naturally occurring molecules like proteins partially or totally modified in structures or in concentrations as an effect of variation of the normal condition status of the animals. Since steroids and β_2-agonists are believed to exert at least part of their biological effects by increasing gene transcription in target tissues (Sillence *et a*l.,

2004), proteomics could ideally represent a powerful tool (Abbott, 1999) to detect changes in protein expression mediated by such GPAs.

In classical proteomic experiments, samples from cellular crude homogenates are resolved by high-resolution two dimensional electrophoresis (2DE) to display the most highly expressed proteins within the system under study given a specific cellular condition (O'Farrell *et al*., 1975). 2DE is the method that is most applicable to high-throughput analysis of highly expressed proteins in tissue, since samples can be run in parallel and multiplexed (Corah *et al*., 1995). Differential in-Gel Electrophoresis, DIGE, greatly improves reproducibility (Bengtsson *et al*., 2007). This approach has been widely adopted also in differential experiments on complex organisms focussed on highlighting variations in proteomic repertoire as result of cellular response to different physiological conditions or disease (Page *et al*., 1999; Alayia *et al*., 2003).

To this aim, cattle destined for meat production were experimentally treated with DXM alone, or in combination with 17β-oestradiol (bE) or clenbuterol (CBT), as part of a larger project aimed at developing complementary biological assays for detecting bovine exposure to GPAs. Since experimental evidence demonstrates that DXM in combination with CBT increase the rate of glycogenolysis and lipolysis in skeletal muscle so that more energy is available for protein synthesis as well as appearing to reduce the activity of proteolytic enzymes. Proteins that are differentially expressed between treated and control samples could potentially be used as biomarkers for detecting the administration of illegal GPAs.

MATERIALS AND METHODS

Chemicals

The Micro-Lowry protein assay kit, dimethylformamide (DMF), trifluoroacetic acid (TFA), and α-cyano-4-hydroxy-cinnamic acid were purchased from Sigma Aldrich (Stockholm, Sweden). Sequence-grade-modified trypsin from porcine pancreas was purchased from Promega (Madison, WI, USA). Sodium dodecyl sulphate (SDS), tri-hydroxymethyl-aminomethane (Tris), acrylamide, bis-acrylamide, IPG strips (pH 3-10 NL, 24 cm), IPG buffer (pH range 3-10 NL), NNN'N' tetramethylethylendiamine (TEMED), ammonium persulphate and CyDyes DIGE fluors for DIGE (Cy2, Cy3, Cy5) were from GE Healthcare (Uppsala, Sweden). Ammonium bicarbonate, magnesium acetate (MgAc), urea, 3-[(3-Cholamidopropyl)-dimethylammonio]-1-propane sulfonate (CHAPS), iodoacetamide (IAA), dithiotreitol (DTT), glycerol, and formic acid (FA) were from Fluka (Buchs, Switzerland). Protease inhibitor cocktail EDTA-free was from Roche (Roche Diagnostics GmbH, Mannheim, Germany). Acetonitrile (ACN), ethanol solution 96% (EtOH), glacial acetic acid (HAc), and water for HPLC were from Merck AG (Darmstadt, Germany). Protein desalting spin columns were obtained from ThermoFischer (VWR, Stockholm, Sweden).

Animal Treatment

Two sets of 24 animals each were taken into consideration for the proteomic profiling study described here. The first set of animals was composed of 24 clinically healthy 18-20 months old mixed-bred (Charolaise x Limousine) bulls, while the second set of animals was composed of 24 clinically healthy 19-21 months old Charolaise bulls. In both cases animals were weighed, housed in ventilated stables and all the experimental procedures were carried out

according to the European Union animal welfare legislation. The experiment began after 3 weeks of acclimatization.

The mixed-bred animals in the first set were randomly allotted to three groups of 8 animals each. The first was used as control ($CNTR_1$), the second group was treated with dexamethasone (DXM) administered *via* feed 0.75 mg *per capita* for 43 days (group DXM_1), and the third one was treated with a combination of 17β-oestradiol (bE) intramuscularly (i.m.) 20 mg *per capita*, after 7, 21, and 35 days from the beginning of the experiment and DXM administered as described above (group DXM+bE) (Figure 1A).

The second set of pure-bred animals was also divided into three groups of 8 animals each. The first was used as control ($CNTR_2$), the second was treated with DXM administered *via* feed 0.75 mg *per capita* for 42 days (group DXM_2), and the third one was treated with an increasing dose of clenbuterol (CBT) *via* feed 2 mg *per capita* during the first week, 4 mg *per capita* during the second week, and 6 mg *per capita* during the third and the fourth weeks (28 days in total), in combination with DXM 0.66 mg *per capita* for 21 days (group DXM+CBT) (Figure 1B).

Tissue Sampling and Storage

In as far as possible, identical small biopsies of the *biceps brachii* muscle was sampled from all the animals in the study. The muscle samples were immediately frozen in vessels containing liquid nitrogen (within 1 minute of removal) and stored at -80°C prior to subsequent analyses.

Drug Residue Studies on Target Organs and Urines

The efficacy of drug administration was evaluated using the urine collected once a week, from the second group of animals (24 Charolaise bulls), for the entire duration of the treatment protocol. The levels of DXM and CBT residue in liver and skeletal muscle at slaughter were also determined. Liver and skeletal muscle samples were subjected to solid phase extraction (SPE) prior to LC-MS/MS analysis. Urinary samples were first treated with β-glucuronidase in order to release the conjugated drug residue. All DXM residue analyses were performed on a reverse phase liquid chromatograph (RP-HPLC) (Waters, Alliance 2695) interfaced to a triple-quadrupole mass spectrometer (Waters Micromass, Quattro Ultima) operating in negative ionization mode. CBT residue analyses were carried out using an ultra performance liquid chromatograph (UPLC, Waters) coupled to a triple-quadrupole mass spectrometer (Waters Micromass, Quattro Premier XE). During analyses the ion acquisition was operated in multiple reaction mode using the transitions from the molecular ion of formiate DXM to the two most abundant fragments: m/z 437 → 361; m/z 437 → 307. For CBT the following transitions were selected: m/z 277 → 203; m/z 277 → 168. The decision limits for DXM and CBT in various biological matrices in the ppb range (ng/ml or μg/kg), depend on the specific matrix studied. In particular, for DXM, CCα values of 0.31 ng/ml and 0.24 μg/kg, were estimated in bovine urine and liver/muscle, respectively. For CBT, the CCα estimated values were of 0.073 ng/ml for urine, and 0.14 μg/kg for liver/muscle.

Sample Preparation for 2D-DIGE analysis

From each muscle sample, about 100-150 mg of tissue were collected using a surgical blade and put in a ceramic mortar containing liquid nitrogen. The muscle was powdered using a ceramic pestle and transferred into an Axygen tube where it was re-suspended using 1.5 ml of

lysis buffer (8 M urea, 4% CHAPS, 5 mM MgAc, 30 mM Tris buffered at pH 8.5, and Protease inhibitor cocktail EDTA-free). Each sample was then vortexed 1 minute and put on ice for 15 minutes. Protein extracts were vortexed again and centrifuged at 12000 g, 10 minutes, 4°C. Supernatants were collected and finally desalted in lysis buffer by centrifugation through desalting spin columns. All the operations described above were performed in a cold room at 4°C in order to minimize protein degradation. The protein concentration of each sample was estimated by using a Micro-Lowry assay kit and aliquots of solutions from each sample were diluted, using lysis buffer, at the same final concentration (2.5 µg/µl) and stocked at –80°C. Protein extracts were thawed and labelled, according to manufacturer's instructions. All 48 samples were labelled with both Cy3 and Cy5, independently, using a total of 250 pmol of dye for 50 µg of protein and stored separately at –80°C. At the same time a reference sample (the pool) was prepared by mixing equal amounts of each non-labelled sample. The pool was labelled with Cy2 as above. Sample duplicates were run on different gels, in presence of the pool, in order to reduce possible systematic errors of single gel preparations.

2D DIGE Gel Experiments

All DIGE gels were run by loading three samples labelled with Cy2, Cy3, and Cy5, respectively. Samples were thawed, and 50 µg of labelled protein from each dye were combined and mixed with rehydration buffer (8 M urea, 2% CHAPS, 0.002% bromophenol blue, 18.2 mM DTT, 2% IPG buffer (pH 3-10 NL)), left at room temperature for 30 minutes, and centrifuged at room temperature for 10 minutes at 12000 g. Then the solution was applied to a 24 cm immobilized pH gradient strip (pH 3-10 NL) for overnight rehydration (12 h). A total of 48 DIGE gels were used. One of the three samples was the pooled reference sample and two others were biological samples (1 control sample and 1 treated sample where possible).

First-dimension isoelectric focusing was carried out on a GE Healthcare IPGphor unit for a total of 70000 Vh. The separation was achieved according to the following gradient potential: 0-12 h (passive rehydration); 12-13 h 500 V step-and-hold; 13-15 h 4000 V gradient; 15-16 h 8000 V gradient; 16-24 h 8000 V step-and-hold. Afterward, the strips were equilibrated in 20 ml of equilibration solution (6 M urea, 75 mM Tris (pH 8.8), 30% (w/v) glycerol, 2% (w/v) SDS, and 0.002% bromophenol blue) and incubated with 65 mM DTT for 20 minutes, followed by 20 minutes in equilibration solution with 135 mM IAA added. The second dimension was run using the Ettan DALT II system (GE Healthcare) on 12.5% SDS-PAGE gels overnight (25°C) at 1 W/gel until the bromophenol blue dye front had run off the base of the gel. Gels were fixed for 30 minutes in a solution containing 30% EtOH and 10% HAc and washed twice with water before being scanned using an Amersham Biosciences Typhoon 9400 variable imager (GE Healthcare) operating at three different wavelengths: 488 nm, 532 nm, 633 nm. Image analysis was performed using DeCyder 6.5 (GE Healthcare).

Spot detection was carried out using DeCyder DIA for each gel. The estimated number of spots was set to 10000 and an area filter approximately < 250-300 was applied together with a volume filter between 15000 and 25000 for different gels to get a final number of included spots around 2900. Matching was done in DeCyder BVA using 150-200 manual landmarks.

Statistical Analysis

All expression values in this study are base 2 logarithms of the standardized abundance (SA). SA is defined as the ratio between the spot volume of the sample and the volume of the corresponding reference spot on the same gel. A set of matched spots across all gel images, from here on called a matched spot set, would typically represent an isoform of a protein, but in rarer cases it may represent two or more unseparated proteins. Expression values of matched spots were compared, pairwise, between treatment group and control group; the fold change and the Mann-Whitney U-test p-value were calculated. All spots that satisfied the following criteria in any pairwise comparison between a treatment group and the control group were selected for mass spectrometry analysis: fold change between treated and control groups < 0.80 and > 1.20, and Mann-Whitney U-test p-value below 0.05. The software used for the statistical tests was written in the statistical language R.

Mass Spectrometry Analysis of Proteins

Proteins were identified by MS/MS after digestion of spots cut from preparative gels run with 800 µg of total protein loaded and stained with SyPro Ruby according to manufacturer's instructions. The protein spot picking, destaining, tryptic digestion, peptides extraction, sample preparation and spotting on MALDI target plates were carried out using a spot handling workstation (Ettan Spot handling workstation, GE Healthcare) and a standard protocol provided by GE Healthcare. An aliquot of 0.5 µl of digest was applied to a clean MALDI target slide surface and allowed to dry. This was followed by 0.5 µl of matrix solution (5 mg/ml of α-cyano-4-hydroxy-cinnamic acid in 50:50 ACN:H_2O containing 0.05% TFA). The dried samples were analysed on a MALDI-LTQ XL (Thermo Scientific) mass spectrometer. A survey scan (MS) was followed by MS/MS scans up to the 50 most abundant ions. This string of scan events was repeated 5 times for each sample spot. A time limit of 4 min/sample was selected, whether or not enough MS/MS spectra could be acquired. The MS spectra were collected in the 600-2000 m/z mass range while the mass range for the MS/MS spectra was automatically selected by the system. A standard collision energy of 35eV was set for all analyses. Database searches were performed using MASCOT (version 2.3 with a parent mass tolerance of 1.4 Da and an MS/MS tolerance of 0.6 Da) search engine against a *Bos Taurus* restricted UniProtKB/SwissProt database version 2010_08.Up to one missed cleavage was allowed, and searches were performed with fixed carbamidomethylation of cysteines and variable oxidation of methionine residues. Expectation values of below 0.05 and a minimum of three peptides were required for a hit.

Western Blotting

To perform one-dimensional Western blots, the protein extracts were resuspended in Laemmli Sample Buffer containing 62.5 mM Tris-HCl (pH 6.8), 10% glycerol, 2% SDS and 50 mM DTT. Equal amounts of proteins (5 µg per lane) were separated on 4-12% SDS-PAGE gels (BioRad) and transferred to nitrocellulose membranes (BioRad). The membranes were blocked with 5% (v/v) non-fat dry milk dissolved in Phosphate Buffered Saline (PBS) and 0.1% Tween 20 (PBS-T) for 1 h at room temperature. Subsequently, the membranes were incubated with the primary antibodies anti-Troponin T fast skeletal isoform, rabbit polyclonal antibody (1:1000), anti-Alpha Actin rabbit polyclonal antibody (1:2000), anti-

Myosin Regulatory Chain 20kDa mouse monoclonal antibody (Sigma Aldrich, 1:1000), overnight at 4°C. Membranes were then rinsed in PBS-T and incubated with the corresponding horseradish peroxidase-conjugated secondary antibody (diluted 1:3000, Santa Cruz Biotechnology) for 1 h at RT. Immunoreactivity was detected after immersion of the membranes into enhanced chemiluminescence (ECL) solution (Millipore) and images were acquired using a digital Kodak Image Station. Densitometric values for each sample were obtained using the Kodak 1D analysis software, after correcting for the background and normalising immunoreactive bands to the total protein loaded estimated by red Ponceau staining (Ponceau-S, Sigma Aldrich).

RESULTS

Drug Excretion Following Treatment Protocol

The urinary excretion of DXM, during and after two different growth-promoting treatments (i.e. DXM_2 and DXM+CBT), is illustrated in Figure 2A (left and right panels respectively). DXM excretion, during the 2 therapeutic schedules, revealed drug concentrations that were similar and maintained from the first to the last day of treatment, showing mean values ranging between 0.8 and 2.2 ng/ml regardless the dose of DXM administered (i.e. 0.75 or 0.66 mg/day). Afterward, the DXM elimination proceeded very rapidly; in fact, both therapeutic schedules showed a mean drug concentration that halved day by day after the end of the treatment. After 3 days of withdrawal, urine samples proved to be virtually free from DXM displaying a concentration below the decision limit of the analytical method. The analysis of liver samples collected at slaughterhouse after 3 days of suspension showed a mean residue level of DXM of 3.66 ± 0.65 µg/kg, but in skeletal muscle the residue was virtually absent. The same was observed in skeletal muscle after 7 days of withdrawal, by contrast, the mean DXM concentration in liver was 0.15 ± 0.04 µg/kg, demonstrating the efficacy of drug elimination using a prolonged suspension period.

The CBT excretion profile in urine, using an increasing dose from 2 to 6 mg/day, is reported in Figure 2B. The estimated drug concentration showed mean values ranging between 10 and 20 ng/ml except for the first week of treatment during which a mean value around 5 ng/ml was found. At the end of the treatment, the β_2-agonist urinary concentration tended to decrease progressively. Its rapid excretion was confirmed by the finding of drug concentrations of 2.48 ± 1.35 ng/ml in samples collected 2 days after treatment withdrawal, and 0.46 ± 0.22 ng/ml after 3 days of withdrawal. After 7 days of suspension the CBT mean concentration in urine (approximate mean value: 0.03 ± 0.01 ng/ml), dropped below the decision limit, but in liver and skeletal muscle samples, it was still appreciable showing mean values of 1.67 ± 0.19 µg/kg and 0.07 ± 0.01 µg/kg respectively. All values are reported as mean ± SE (SE is defined as ratio between standard deviation and the square root of number of animals -1).

Gel Images

48 muscle portions were analyzed using 2D-DIGE to identify potential biomarkers for the detection of fraudulent GPAs treatment. The advantage of this technique is related to the possibility to run on the same gel a protein extract derived from a treated animal, one from a control animal and the pool. All samples were run in duplicate on separate gels using dye swapping (Cy3 and Cy5), and a pool constructed from all samples labelled with Cy2 was included

on every gel. Equal amounts of protein (50 µg) were loaded for each dye, and an average of about 2500 spots were detected. The intra-gel matching was against the pool sample, and then, the inter-gel matching occurred using the pool sample in each gel, dramatically improving match quality, normalization, and relative quantification. For each of the 48 samples, a merged set of expression values was constructed by averaging the two duplicate values. When one of the two values was missing, the available measurement was used. When both values were missing, the sample was assigned a missing value for that spot. The resulting data set comprised 2310 spots measured in 48 samples.

Statistical Analysis of the Gel Images

A Mann-Whitney U-test was performed for the 4 following pairwise comparisons: $CNTR_1$ vs DXM_1; $CNTR_1$ vs DXM+bE; $CNTR_2$ vs DXM_2; $CNTR_2$ vs DXM+CBT. The two comparisons $CNTR_1$ vs DXM_1 and $CNTR_2$ vs DXM_2 were good enough to be taken in consideration to identify possible fraudulent GPA treatment biomarkers, but the comparison that gave best result was the $CNTR_2$ vs DXM+CBT groups, meaning that the combination of DXM and CBT lead to a more significant alteration of the 2D protein pattern. On the other hand no statistical significant difference between the $CNTR_1$ and DXM+bE groups was observed, suggesting that estrogens exert, in skeletal muscle, an effect that is antagonistic to corticosteroids. In fact the combination of these molecules does not change significantly the 2D protein expression pattern. The p-value distributions of the 4 comparisons mentioned above are reported in Figure 3.

In order to increase the number of samples, animals that were subjected to the same treatment were combined in a single group regardless the different animal strain. In this way we obtained a control group ($CNTR_{1-2}$) composed by 16 animals and a dexamethasone-treated group of 16 animals (DXM_{1-2}). To reduce the difference due to animals strain, a correction was applied when statistical tests were performed. Many spots gained a higher statistical significance when Mann-Whitney U-test was performed considering $CNTR_{1-2}$ vs DXM_{1-2} and $CNTR_{1-2}$ vs DXM+CBT comparisons (Figure 4). All spots that were significantly changed between the last 2 comparisons (i.e. $CNTR_{1-2}$ vs DXM_{1-2} and $CNTR_{1-2}$ vs DXM+CBT) were selected for mass spectrometry. The selection resulted in a list of 381 spots to be picked: 115 spots from the $CNTR_{1-2}$ vs DXM_{1-2} comparison that were picked and analysed from a gel where 800 µg of total protein coming from a pool of DXM_{1-2} treated samples were loaded, 97 spots from the comparison $CNTR_{1-2}$ vs DXM+CBT were picked and identified from a gel loaded with 800 µg of protein of DXM+CBT treated pooled samples, and 169 spots that were picked from a gel where 800 µg of protein of control pooled samples were loaded in order to confirm and implement the protein identifications previously obtained avoiding erroneous assignments.

Differentially Expressed Proteins

Of the differentially expressed proteins that serve to distinguish between treated and control samples, a total of 104 spots were identified. Out of this set of identified spots, 29 unique proteins were found. Figure 5 shows all the identified proteins, annotated on the master gel. Identified proteins that are differentially expressed between treated and control samples are given in Table 1. The proteins are grouped by function and are mainly enzymes or contractile proteins. Spots differently identified in treated pool with respect to control pool, were discarded. A majority of the proteins reported

are changed in expression in both considered treatments, but some of them are peculiar of the combination of DXM and CBT. These proteins can be taken into consideration as potential biomarkers of treatments with molecules characterised by steroidal structures, such as corticosteroids, in combination with β_2-agonists.

Biomarker Confirmation

Based on the availability of some specific antibodies, western blot validations of Alpha-Actin (ACT), Myosin Regulatory Light Chain 2 (MLRS), and fast isoform of Troponin T (TNNT3) on 8 different $CNTR_2$, DXM_2 and DXM+CBT samples were carried out , in order to confirm the 2D-DIGE-based quantitative measurements. The western blot revealed the following changes (considered significant when p-value < 0.05, from Mann-Whitney non-parametric test) of their expression level compared to $CNTR_2$ samples (Figure 6). The ratios, expressed as $DXM_2/CNTR_2$ and DXM+CBT/$CNTR_2$, were found to be 1.94 and 3.37 for ACT, 0.65 and 0.83 for MLRS, and 0.55 and 0.51 for TNNT3, respectively. These values correlated with those obtained by 2D-DIGE which were, respectively, 1.28 and 3.54 for ACT, 0.54 and 0.57 for MLRS, and 0.59 and 0.65 for TNNT3, further confirming the accuracy of the quantification method.

DISCUSSION

In this study we investigated the treatment of beef cattle with different combination of GPAs: our aim was to detect differentially expressed proteins as a result of these treatments using a 2D-DIGE approach and to identify specific biomarkers for each treatment protocol.

The first treatment protocol examined was oral administration of DXM alone for 42 days. Glucocorticoids are natural corticosteroids with important functions upon gluconeogenesis, glycogen deposition, protein and calcium metabolism, together with anti-inflammatory and immunosuppressive activities. Low doses of glucocorticoids result in improved feed intake, increased live weight gain, reduced feed conversion ratio, reduced nitrogen retention and increased water retention. The effects of glucocorticoids are often attributed to their potent anti-inflammatory activity, but recent studies indicated that glucocorticoids reduced muscle proteolysis, while increasing myogenic repair and myoblast proliferation (Angelini, 2007). Previous studies of glucocorticoid effects *in vitro* on C_2C_{12} myoblasts showed that high doses of the glucocorticoids, dexamethasone or prednisolone, induced cell death and MyoD degradation via the ubiquitin-proteasome pathway (te Pas *et al*., 2000). On the other hand, treatment with lower doses of dexamethasone or prednisolone led to an increased mRNA levels of myogenic factors such as MyoD, Myf-5, and MRF4, and to an enhancement of myogenic fusion efficiency of C_2C_{12} cells (Belanto *et al*., 2010). At these levels it was found that glucocorticoids had two effects on C_2C_{12} differentiation: acceleration and augmentation of myotube fusion and of the terminal differentiation program. Moreover DXM treatment accelerated and increaseded the levels of the transcription factors (i.e., MyoD and myogenin), and the muscle structural and sarcolemmal proteins. Indeed, it was demonstrated by Giorgino and colleagues that skeletal muscle cell lines treated with low doses of DXM can specifically upregulate the activity of the Src-homology-2-containing protein (Shc) signaling pathway by increasing the expression and tyrosine phosphorylation of the Shc proteins that lead to the Ras-mitogen-activated protein kinase (MAPK) pathway, which is responsible

for the control of cell growth and differentiation (Taniguchi *et al*., 2006).

In this regard, our study shows that DXM treatment influences the expression of key enzymes linked to muscle metabolism, such as mitochondrial ATP synthase and Carbonic Anhydrase-3, and increases the expression of sarcolemmal proteins among which are Actin, Desmin, Myosin Light Chain 6B and Troponin T, slow contracting isoform 1. These findings are fully consistent with the above mentioned studies showing that glucocorticoids can promote myogenesis. By contrast, DXM probably inhibited a second distinct signaling pathway that involves tyrosine phosphorylation of insulin receptor substrate proteins (IRS-1) and activation of phosphatidylinositol 3-kinase (PI3K)-Akt/protein kinase B (PKB) pathway, which regulates most of the metabolic actions of insulin (Avruch, 1998). In our study, animals treated with DXM showed modification in the expression of enzymes of the glycolytic pathway such as Enolases, Glyceraldehyde-3-phosphate dehydrogenase, Triosephosphate isomerase, Pyruvate Kinase, Fructose bisphospate-aldolase and Muscle Creatine Kinase that were found to be downregulated with respect to control animals. On the other hand, it was observed also a decreased expression of Myosin Light Chain 1, Myosin Light Regulatory Chain 2, and isoform 3 of Troponin T, that are fast skeletal isoforms, suggesting that the administration of DXM favors slow-fibre phenotype. These data are supported by a study performed in rats, however, in that case, it was used a high dose of DXM that led to muscle atrophy, mostly affecting fast-twitching fibres (Livingstone *et al*., 1981).

The second treatment taken in consideration was the combined administration of DXM and bE. When estrogens were combined with DXM, it was observed a marked reduction of the effects at the protein expression level. In fact, it was not possible to distinguish between treated and control animals. This result, however, is not surprising because crosstalk between glucocorticoids and estrogens appears to occur at different levels displaying opposite effects (Tsai *et al*., 2007). In addition, there is evidence that estrogens induce degradation of the glucocorticoid receptors through ubiquitin-proteasome pathway (Kinyamu *et al*., 2003), confirming the antagonist action of bE and DXM on skeletal muscle. Similar results were obtained with this same group of animals considered for this study (i.e. $CNTR_1$ and DXM+bE), by Carraro and colleagues at the transcriptional level (Carraro *et al*., 2009).

The last treatment protocol studied was the combination of the glucocorticoid DXM and the β_2-agonist CBT. The β-agonists enhance growth efficiency by increasing the rate of gain, decreasing feed consumption, increasing the amount of skeletal muscle tissue stimulating protein synthesis and cell hypertrophy by inhibition of proteolysis. In adipose tissue they promote lipolysis leading to a reduction of carcass fat and an increase of carcass protein (Mersmann, 1995). For this redirecting of cellular energy metabolism in favor of protein synthesis some β-agonists are called "repartitioning agents" (Courtheyn *et al*., 2002). Muscle growth induced by CBT is associated with a substantial change in the properties of muscle fibres. These changes, toward a fast-contracting phenotype, involve whole muscle architecture as evidenced by the reported alterations in myosin heavy and light chains (Pellegrino *et al*., 2004; Bozzo *et al*., 2003), myosin ATPase activity (Zeman *et al*., 1988), energy metabolism (Rajab *et al*., 2000), and muscle contractile characteristics (Dodd *et al*., 1996; Burniston *et al*., 2007). Corticosteroids are frequently used in veterinary medicine, often

in combination with β-agonists to prevent receptor down-regulation and tolerance in the animal or to affect meat quality by increasing water content (Bridge *et al*., 1998).

In our study, CBT was administered together with DXM, and to some extent, our findings oppose the alterations usually observed in skeletal muscle after CBT administration, alone. In fact we found a protein expression pattern that is very close to the one obtained by treating animals with DXM alone, but, in addition, some proteins displayed a higher fold-change compared to controls (i.e. Actin, Carbonic Anhydrase-3, slow contracting isoform 1 of Troponin T), and other proteins, specific of these drugs combination, were identified: Myosin Heavy Chain (MYH), mitochondrial NADH-ubiquinone oxidoreductase, Serum albumin, Peroxiredoxin-6, and Cofilin-2. Various MYHs were found to be up-regulated after this specific treatment and this finding may let us conclude that the combination of DXM and CBT leads to an enhanced contractile proteins synthesis, if compared to DXM alone, as also underlined by the higher fold-change observed for Actin. The mitochondrial NADH-ubiquinone oxidoreductase enzyme is the core of the respiratory chain (Lowther *et al*., 2000), and, in line with the previous results obtained for the treatment with DXM alone, is up-regulated in treated animals. Peroxiredoxin-6 is an enzyme usually found up-regulated in response to oxidative stress, but recently, it was proposed to be associated to meat tenderness (Jia *et al*., 2009). By contrast the muscle-specific form of Cofilin (CFL-2), that is positively associated with regeneration of skeletal muscle (Thirion *et al*., 2001; Boengler *et al*., 2003), was found to be decreased in DXM+CBT treated samples, making difficult the interpretation of such observation. However the study was not aimed to explain biochemical processes that drive to the alteration of protein expression pattern, but rather to evaluate the effectiveness of proteomics as method for the identification of biomarkers for illicit treatment with GPAs.

Results obtained indicate that two-dimensional gel electrophoresis is useful to evaluate a variety of proteins that can be tested as potential protein markers and as a basis to develop large-scale screening methods. The proteins must be chosen carefully to ensure that they are truly dependent on pharmacological treatments and not on other experimental conditions. Moreover these potential biomarkers must be validated using other approaches. At the moment, this study represents a first step toward the development of screening tests based on the detection of the biological effects at protein level and might be taken in consideration as an additional tool to complement the existing analytical tools against the misuse of GPAs in raising beef cattle.

Acknowledgements

The authors thank the Italian Ministry of Health and Regione Veneto for financial support and Liselotte Andersson, Ulrika Brynnel and Dr. Giorgio Arrigoni for their excellent technical assistance.

REFERENCES

Abbott A., Nature 1999, 402: 715–720.

Alaiya A.A., Roblick U.J., Franzen B., Bruch H.P., Auer G., J. Chromatogr. B 2003, 787: 207.

Angelini C., Muscle Nerve 2007, 36: 424–35.

Avruch, J., Mol. Cell. Biochem. 1998, 182: 31–48, Review.

Belanto J.J., Diaz-Perez S.V., Magyar C.E., Maxwell M.M., Yilmaz Y., Topp K., Boso G., Jamieson C.H., Cacalano N.A., Jamieson C.A., Neuromuscul. Disord. 2010, 20(2): 111-21.

Bengtsson S., Krogh M., Al-Khalili Szigyarto C., Uhlen M., Schedvins K., Silfversward C., Linder S., Auer G., Alaiya A., and James P., J. Prot. Res. 2007, 6: 1440-1450.

Boengler K., Pipp F., Broich K., Fernandez B., Schaper W., Deindl E., Biochem. Biophys. Res. Commun. 2003, 17;300(3): 751-6.

Bozzo C., Stevens L., Toniolo L., Mounier Y., Reggiani C. Am. J. Physiol. 2003, 285: C575–C583.

Bridge K.Y., Smith C.K. 2nd, Young R.B., J. Anim. Sci. 1998, 76(9): 2382-91.

Burniston J.G., McLean L., Beynon R.J., Goldspink D.F., Muscle Nerve. 2007, 35(2): 217-23.

Castagnaro M., and Poppi L., Vet. Res. Communications. 2006, 30(1): 105-108.

Carraro L., Ferraresso S., Cardazzo B., Romualdi C., Montesissa C., Gottardo F., Patarnello T., Castagnaro M., Bargelloni L., Physiol. Genomics. 2009, 38(2): 138-48.

Corah T. J., Tatum J. D., Morgan J. B., Mortimer R. G., Smith G. C., J. Anim. Sci. 1995, 73: 3310–3316.

Courtheyn D., Le Bizec B., Brambilla G., De Brabander H. F., Anal. Chim. Acta 2002, 473: 71–82.

Dodd S.L., Powers S.K., Vrabas I.S., Criswell D., Stetson S., Hussain R. Med. Sci. Sport Exerc. 1996, 28: 669–676.

Dodson M. V., Allen R. E., Hossner K. L., Endocrinology 1985, 117: 2357–2363.

Giorgino F., Smith R. J., J. Clin. InVest. 1995, 96: 1473–1483.

Gottardo F., Brscic M., Pozza G., Ossensi C., Contiero B., Marin A., Cozzi G. Animal 2008, 2: 1073–1079.

Jia X., Veiseth-Kent E., Grove H., Kuziora P., Aass L., Hildrum K.I., Hollung K., J. Anim. Sci. 2009, 87(7): 2391-9.

Kinyamu H.K., and Archer T.K. Mol Cell Biol. 2003, 23(16): 5867–5881.

Livingstone I., Johnson M.A., Mastaglia F.L., Neuropathol. Appl. Neurobiol. 1981, 7(5): 381-98.

Thirion C., Stucka R., Mendel B., Gruhler A., Jaksch M., Nowak K.J., Binz N., Laing N.G., Lochmüller H. Eur. J. Biochem. 2001, 268: 3473-3482.

Lowther W.T., Brot N., Weissbach H., Matthews B.W., Biochemistry. 2000, 39: 13307-13312.

Mersmann H.J., J. Nutr. 1995, 125(6 Suppl): 1777S-1782S, Review.

Nebbia C., Gardini G., Urbani A., Vet. Res. Communications. 2006, 30(1): 121-125

Odore R., Badino P., Pagliasso S., Nebbia C., Cuniberti B., Barbero R., Re G. J. Vet. Pharmacol. Ther. 2006, 29: 91–97.

O'Farrell P., J. Biol. Chem. 1975, 250: 4007.

Page M.J., Amess B., Townsend R.R., Parekh R., Herath A., Brusten L., Zvelebil M., Stein R.C., Waterfield M.D., Davies S.C., O'Hare M.J., Proc. Natl. Acad. Sci. U.S.A. 1999, 96: 12589.

Pellegrino M.A., D'Antona G., Bortolotto S., Boschi F., Pastoris O., Bottinelli R., Exp. Physiol. 2004, 89: 89 –100.

Rajab P., Fox J., Riaz S., Tomlinson D., Ball D., Greenhaff P.L., Am. J. Physiol. 2000, 279: R1076–R1081.

Sillence M. N., Vet. J. 2004, 167: 242–257, Review.

Stephany R.W., Handb. Exp. Pharmacol. 2010, (195): 355-67, Review.

Taniguchi C.M., Emanuelli B., Kahn C.R., Nat. Rev. Mol. Cell. Biol. 2006, 7(2): 85-96, Review.

te Pas M.F., de Jong P.R., Verburg F.J., Mol. Biol. Rep. 2000, 27(2): 87-98.

Tsai W.J., McCormick K.M., Brazeau D.A., Brazeau G.A., Exp. Biol. Med. (Maywood). 2007, 232(10): 1314-25.

Zeman R.J., Ludemann R., Easton T.G., Etlinger J.D., Am. J. Physiol. 1988, 254: E726–E732.

LEGENDS TO FIGURES AND TABLE

Figure 1. Treatment schedule for Charolaise x Limousine (A), and for Charolaise animals (B).

Figure 2. Time-dependent excretion profile of DXM in urines from Charolaise bulls treated with 2 different growth promoting protocols (A): the excretion profile reported on the left panel is relative to DXM_2 group, and the right one is referred to DXM+CBT group (for details see Materials and Methods). The excretion profile of CBT in urines is reported only for DXM+CBT group (B). Values are reported as mean ± SE.

Figure 3. p-value distribution. For every protein matched, we calculated a p-value that its expression changes with treatment. Shown are histograms of p-value distribution generated by the Mann-Whitney U-test, comparing muscles of mixed-bred bulls (Charolaise x Limousine) from $CNTR_1$ with those from DXM_1 (A), and from $CNTR_1$ with those from DXM+bE (B). Histogram of p-values by the Mann-Whitney U-test, comparing muscles of pure Charolaise bulls from $CNTR_2$ with those from DXM_2 (C), and from $CNTR_2$ with muscles from DXM+CBT (D), see Results for details. X-axis shows the p-value and the Y-axis shows the number of proteins with that p-value.

Figure 4. For every protein matched, we calculated a p-value that its expression changes with treatment. The reported histograms show p-value distribution generated by the Mann-Whitney U-test after combining the 2 different animal groups (Charolaise x Limousine and Charolaise). The comparison between $CNTR_{1-2}$ with those from DXM_{1-2} displays a better p-value distribution leading to an increased number of spots that allow the separation between control and treated animals and (A). Moreover the improvement obtained combining the 2 animal sets is appreciable even in the comparison between $CNTR_{1-2}$ and DXM+CBT protein spots (B). Other details are in legend to Figure 3.

Figure 5. 2D-DIGE master gel image. The Sypro Ruby stained pool from control samples run on a pH 3-11 NL strip in the first dimension and a 12.5% polyacrylamide gel in the second. The differentially expressed spots that were identified are annotated and described in Table 1.

Figure 6. Representative immunoblotting experiments (A) and normalized densitometric analysis (B) of MLRS, TNNT3 and ACT levels in control (n = 8), DXM treated (n = 8), and DXM+CBT treated animals (n = 8). A total amount (5 µg) of protein extracts was loaded for each lane. Protein expression normalization between the different samples was pursued by red Ponceau staining as control for the total protein loaded (data not shown). Reported value are mean ± SE. *Mann-Whitney U-test p-value < 0.05.

Table 1. Summary of differentially expressed proteins between the treated and control groups. The protein accession number for each spot is given together with the Mann-Whitney p-value indicating the degree of confidence to distinguish between treated and control groups in the given comparisons ($CNTR_{1-2}$ vs DXM_{1-2} and $CNTR_{1-2}$ vs DXM+CBT). The fold change indicated the direction and magnitude of the change in protein expression level between the two conditions as well as a description of the function of the protein, if known. Protein spots with multiple hits were not included in the table.
* protein picked and identified from the gel loaded with the pool of control samples; ** fold-change values that differs from the overall trend of a given protein.

FIGURE 1.

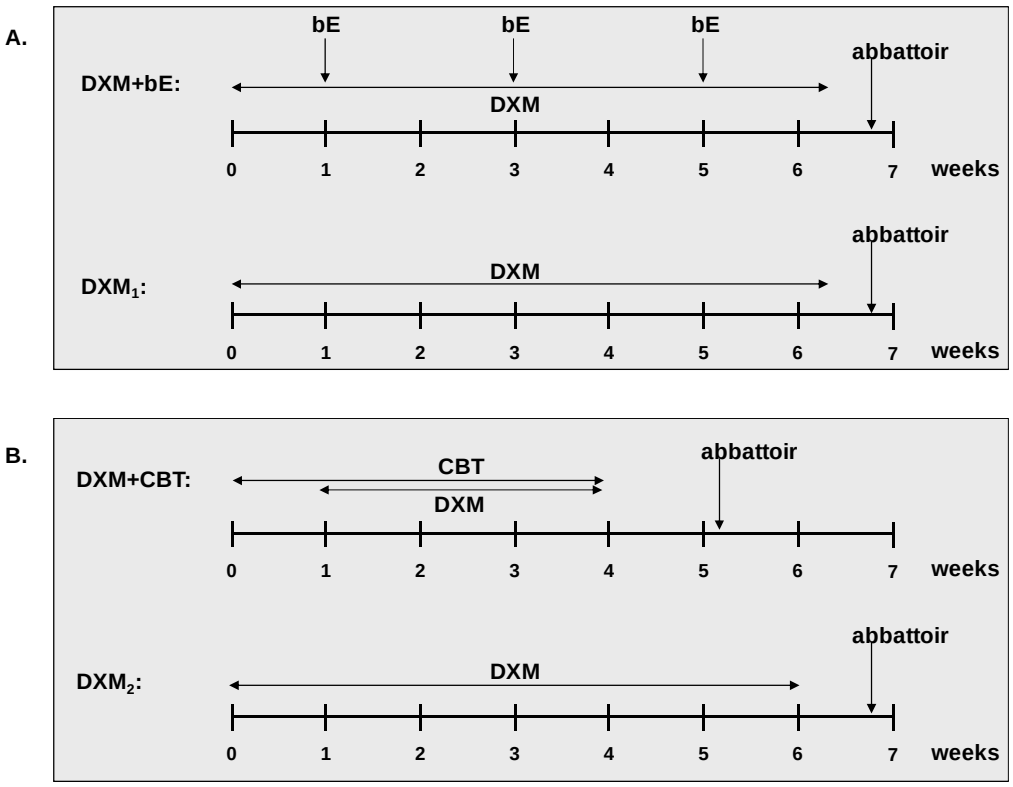

FIGURE 2.

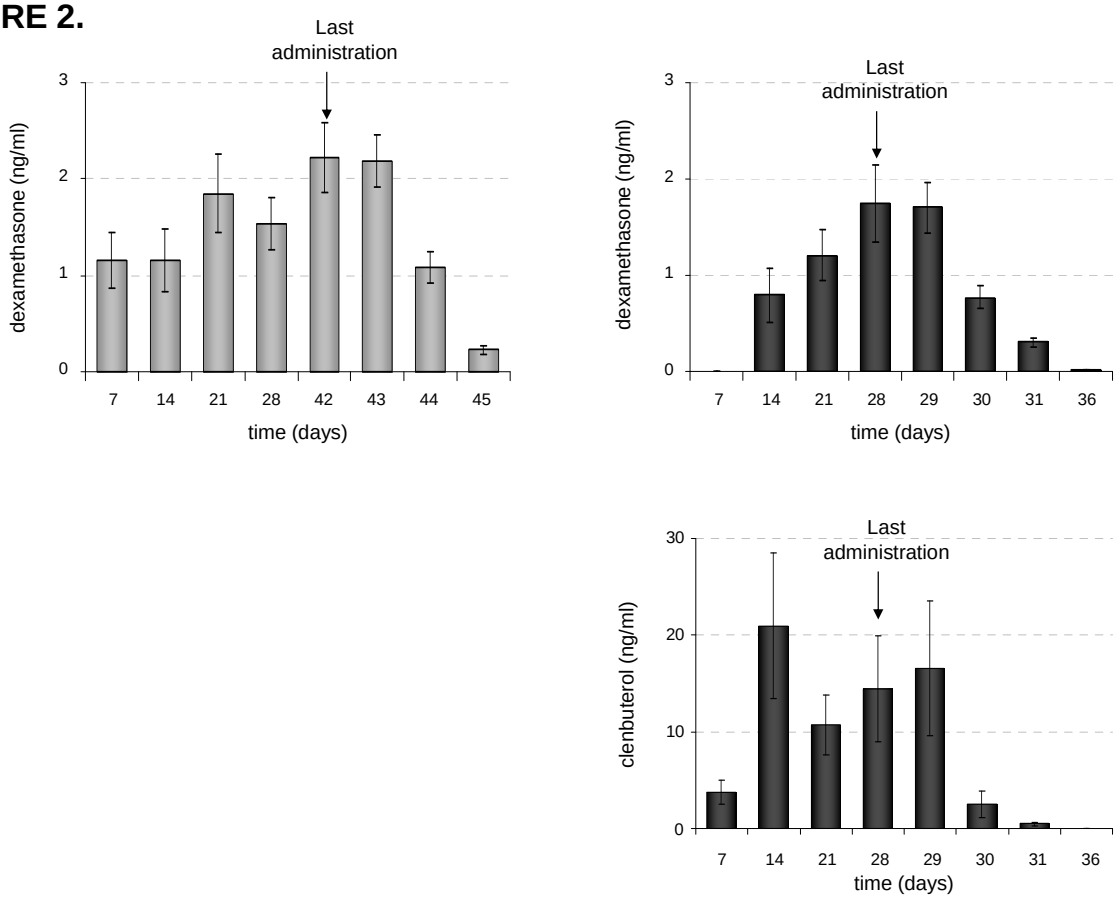

FIGURE 3.

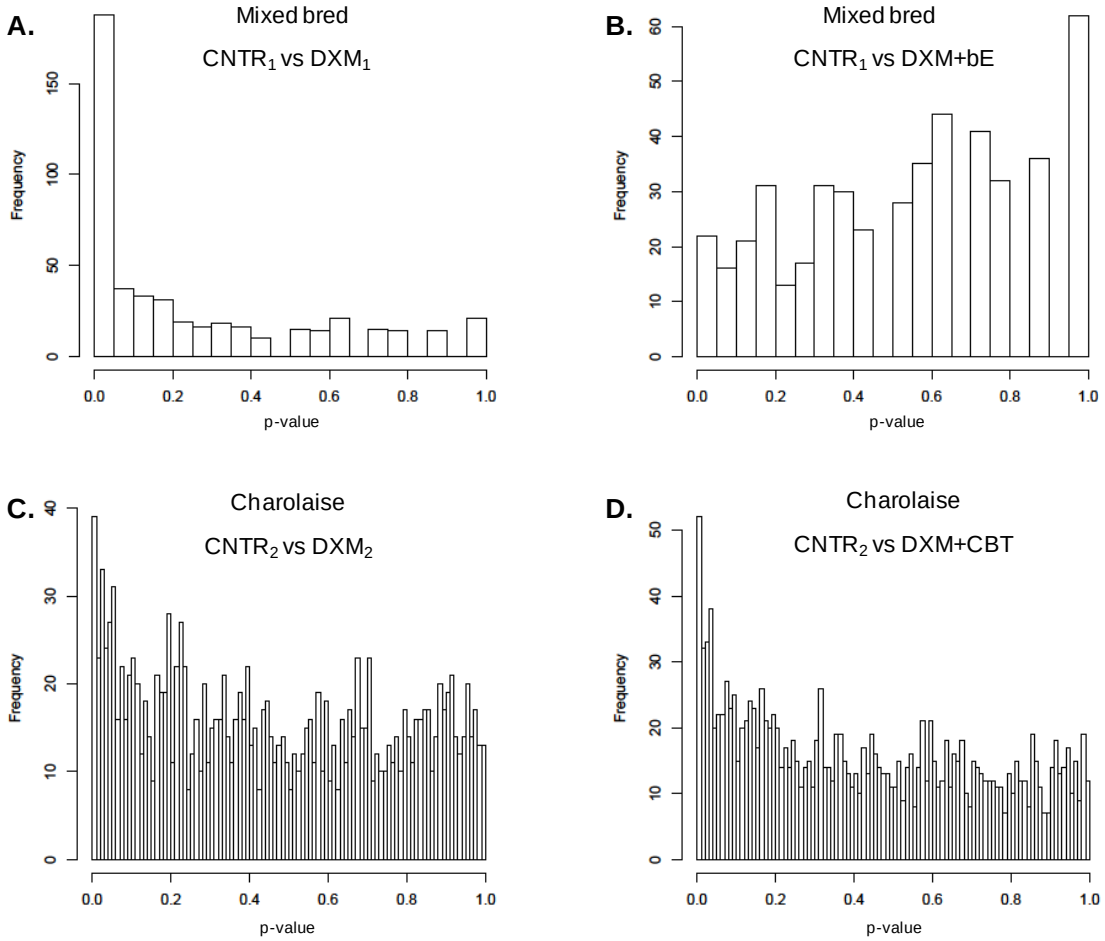

FIGURE 4.

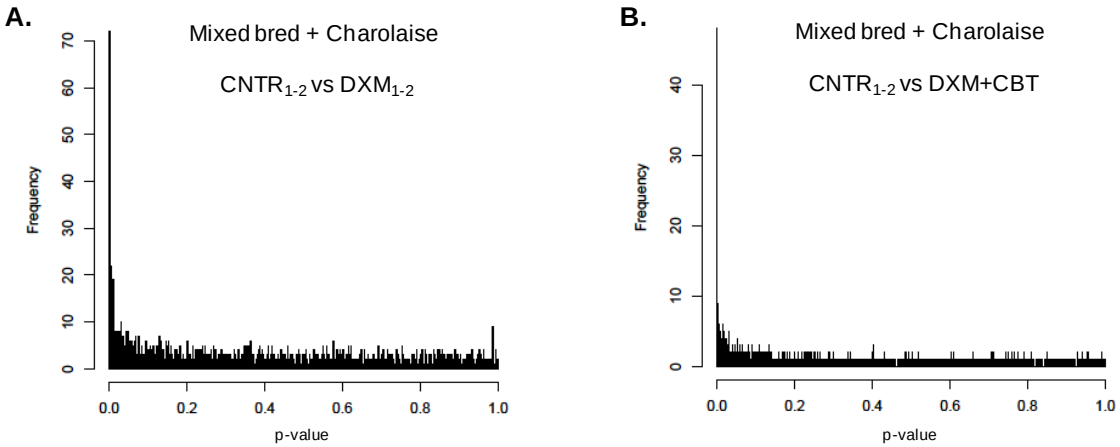

FIGURE 5.

FIGURE 6.

A.

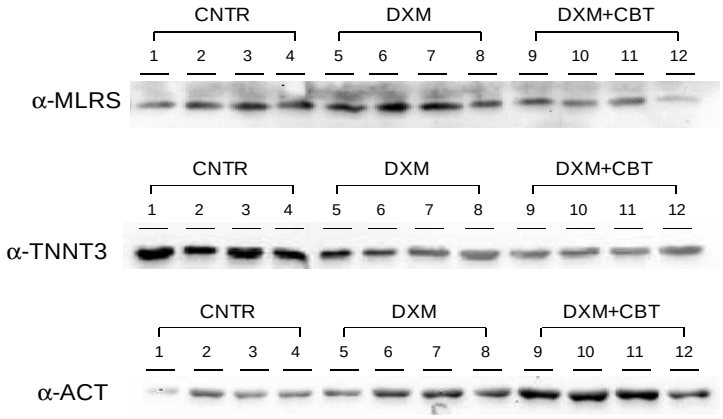

B.

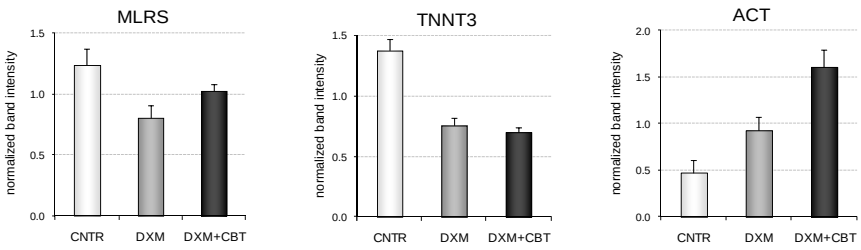

TABLE 1.

Treatment using DXM alone

Protein Name	Spot N°	Short Name	Mascot Score	Swiss Prot	Description	p-value	Fold-Change
Muscle Contraction							
Actin	701	ACT	78	various hits	Highly conserved proteins that are involved in various types of cell motility	8.8E-03	1.28
Desmin	797	DESM	330	O62654	Class-III intermediate filaments that connect myofibrils to each other	2.3E-02	1.21
Myosin, light chain 6B, alkali, smooth muscle	1807	MYL6B	98	Q148H2	Calcium ion binding	5.9E-03	3.23
and non-muscle	1838		116			1.4E-02	3.69
Myosin light chain 1, skeletal muscle isoform	1880	MLE1	86	A0JNJ5	Regulatory light chain of myosin	3.7E-02	0.74
	1881		93			4.6E-02	0.76
	2183		185			9.9E-05	0.55
Myosin regulatory light chain 2, skeletal muscle isoform	2077	MLRS	81	Q0P571	This chain binds calcium and forms Myosin together with heavy chains	2.2E-03	0.61
	2078*		134			3.4E-03	0.47
Troponin C type 2	2070	TNNC2	71	Q148C2	Calcium ion binding	1.2E-02	1.25
Troponin T, fast skeletal muscle	1175	TNNT3	85	Q8MKI3	Troponin T is the thin filament regulatory complex which confers calcium-sensitivity	3.1E-04	0.46
	1181		99		to striated muscle	1.1E-02	0.71
	1204		74			2.0E-03	0.68
	1225		103			4.7E-03	0.54
	1232		72			4.5E-03	0.58
	1248		72			1.5E-03	0.59
Troponin T, slow skeletal muscle	1277	TNNT1	124	Q8MKH6	Troponin T is the thin filament regulatory complex which confers calcium-sensitivity	9.6E-03	1.50
	1281		99		to striated muscle	1.6E-02	1.63
	1282		161			1.2E-02	1.48
	1390		65			1.5E-02	1.22
	1406		107			3.7E-02	1.71
TNNI2 protein (Fragment)	1900*	TNNI2	102	A5PJM2	The inhibitory subunit of troponin that binds to actin and tropomyosin	8.1E-03	0.65
Metabolic Process							
Alpha-crystallin B chain	1996	CRYAB	102	P02510	Interacts with HSPBAP1 and TTN/titin	5.9E-03	1.46
Alpha/Beta-enolase	896	ENOA/ENOB	109	Q9XSJ4/Q3ZC09	Catalyzes the conversion of 2-phospho-D-glycerate to phosphoenolpyruvate	2.0E-03	0.70
	952		101		(Glycolysis)	8.6E-04	0.61
	954		149			2.9E-04	0.65
	955		190			7.9E-05	0.63
	960		122			1.3E-04	0.67
	972		199			1.3E-04	0.64
	1260		94			2.3E-03	0.73
	1268		90			4.3E-04	0.69
ATP synthase subunit alpha, mitochondrial	805	ATPA	205	P19483	Produces ATP from ADP in the presence of a proton gradient across the	2.5E-02	1.20
ATP synthase subunit beta, mitochondrial	844	ATPB	357	P00829	mitochondrial membrane (Energy metabolism)	1.7E-02	1.24
	846		450			4.8E-03	1.28
Carbonic anhydrase 3	1563	CAH3	102	Q3SZX4	Catalyzes Reversible hydration of carbon dioxide	5.4E-03	1.60
	1637		68			4.4E-02	1.58
Creatine kinase M-type	1101	KCRM	103	Q9XSC6	Catalyzes the transfer of phosphate between ATP and creatine (Energy transduction)	4.3E-02	0.66
Fructose-bisphosphate aldolase	1158	ALDOA	69	A6QLL8	Catalyzes the conversion of D-fructose 1,6-bisphosphate to glycerone phosphate	3.4E-03	0.59
	1165		129		and D-glyceraldehyde 3-phosphate (Glycolysis)	5.0E-03	0.61
	1170		115			1.6E-03	0.60
	1184		182			8.3E-04	0.61
	1185		78			3.0E-04	0.63
Glyceraldehyde-3-phosphate dehydrogenase	1319	G3P	68	P10096	Catalyzes the conversion of D-glyceraldehyde 3-phosphate to 3-phospho-	1.9E-05	0.50
	1326		66		D-glyceroyl phosphate (Glycolysis)	5.1E-05	0.55
	1335		143			4.4E-04	0.62
	1340		131			1.9E-04	0.65
	1346		113			6.2E-06	0.65
	1347		60			1.8E-05	0.67
Phosphoglycerate mutase 2	1671	PGAM2	64	Q32KV0	Interconversion of 3- and 2-phosphoglycerate with 2,3-bisphosphoglycerate	5.0E-03	0.68
Pyruvate kinase	690	PKM2	91	A5D984	Catalyzes the conversion of pyruvate to phosphoenolpyruvate (Glycolysis)	3.4E-04	0.66
	704		145			1.3E-05	0.61
Triosephosphate isomerase	1703	TPIS	80	Q5E956	Catalyzes the conversion of D-glyceraldehyde 3-phosphate to glycerone phosphate	2.4E-02	0.76
	1736		99		(Carbohydrate metabolism)	3.1E-02	0.78
Chaperone							
Heat shock protein beta-1	1743	HSPB1	103	Q3T149	Involved in stress resistance and actin organization	2.3E-03	2.07
	1746		95			2.4E-03	1.61
	1749		184			1.0E-03	1.77
	1759		90			7.6E-02	0.71**
	1765		195			5.0E-02	1.54
Heat shock protein beta-6	2022	HSPB6	134	Q148F8	Involved in stress response	2.9E-02	1.42
Transport Protein							
Hemoglobin subunit beta	2248	HBB	95	P02070	Involved in oxygen transport from the lung to the various peripheral tissues	9.0E-02	1.52
Protein Degradation							
Proteasome subunit alpha type-6	1699	PSA6	79	Q2YDE4	Cleavage of peptide bonds with very broad specificity	2.0E-03	0.78

Treatment combining DXM and CBT

Protein Name	Spot N°	Short Name	Mascot Score	Swiss Prot	Description	p-value	Fold-Change
Muscle Contraction							
Actin	1032	ACT	67	various hits	Highly conserved proteins that are involved in various types of cell motility	4.0E-03	1.36
	1693		94			1.3E-05	3.65
	2143		88			5.7E-05	5.60
Cofilin-2	2097	CFL2	63	Q148F1	Controls reversibly actin polymerization and depolymerization	7.2E-03	0.50
Myosin	118	MYH	269	various hits	Hexameric protein that consists of 2 heavy chain subunits and 4 light chain subunits	8.2E-04	1.43
	310		196			1.2E-02	1.54
	713		63			6.3E-03	1.48
Myosin regulatory light chain 2, skeletal muscle isoform	2077	MLRS	81	Q0P571	This chain binds calcium and forms Myosin together with heavy chains	1.4E-02	0.57
Troponin T, fast skeletal muscle	1181	TNNT3	95	Q8MKI3	Troponin T is the thin filament regulatory complex which confers calcium-sensitivity	1.1E-02	0.61
	1194		104		to striated muscle	3.6E-02	0.72
	1204		100			3.4E-02	0.70
Troponin T, slow skeletal muscle	1277	TNNT1	74	Q8MKH6	Troponin T is the thin filament regulatory complex which confers calcium-sensitivity	9.9E-03	1.78
	1281		123		to striated muscle	1.6E-02	2.02
	1282		81			9.6E-03	1.78
	1290		96			7.5E-03	1.71
Metabolic Process							
Alpha/Beta-enolase	959	ENOA/ENOB	120	Q9XSJ4/Q3ZC09	Catalyzes the conversion of 2-phospho-D-glycerate to phosphoenolpyruvate	3.5E-02	0.71
	964		129		(Glycolysis)	4.0E-02	0.75
	1246		66			4.1E-02	0.71
	1430		101			1.5E-02	1.71**
Carbonic anhydrase 3	1627	CAH3	119	Q3SZX4	Catalyzes Reversible hydration of carbon dioxide	2.4E-02	1.95
	1633		93			2.9E-02	1.92
	1637		163			3.2E-02	2.01
Creatine kinase M-type	1092	KCRM	103	Q9XSC6	Catalyzes the transfer of phosphate between ATP and creatine	1.5E-03	0.71
	1095		63		(Energy transduction)	3.5E-03	0.74
	1105*		86			1.1E-02	0.74
	1138		79			1.7E-02	0.79
Fructose-bisphosphate aldolase	1158	ALDOA	73	A6QLL8	Catalyzes the conversion of D-fructose 1,6-bisphosphate to glycerone phosphate and	8.1E-03	0.51
	1165		82		D-glyceraldehyde 3-phosphate (Glycolysis)	7.2E-03	0.52
	1170		72			2.6E-02	0.61
Glyceraldehyde 3-phosphate dehydrogenase	1326	G3P	175	P10096	Catalyzes the conversion of D-glyceraldehyde 3-phosphate to 3-phospho-D-glyceroyl	3.2E-04	0.48
	1335		81		phosphate (Glycolysis)	7.1E-03	0.61
	1340		90			5.9E-03	0.65
	1346		68			2.0E-02	0.75
	1391		63			1.7E-03	0.68
NADH-ubiquinone oxidoreductase 75 kDa subunit	433	NDUS1	89	P15690	Core subunit of the mitochondrial membrane respiratory chain	2.4E-03	1.38
Peroxiredoxin-6	1685	PRDX6	225	O77834	Involved in redox regulation of the cell	2.7E-04	0.69
Pyruvate kinase	680	PKM2	69	Q3ZC87	Catalyzes the conversion of pyruvate to phosphoenolpyruvate (Glycolysis)	6.4E-03	0.76
	683		87			2.2E-02	0.74
	687		93			1.0E-02	0.78
	690		91			9.4E-03	0.66
	704		65			4.0E-03	0.65
Triosephosphate isomerase	1725	TPIS	97	Q5E956	Catalyzes the conversion of D-glyceraldehyde 3-phosphate to glycerone phosphate	2.0E-02	0.65
					(Carbohydrate metabolism)		
Chaperone							
Heat shock protein beta-1	1751	HSPB1	86	Q3T149	Involved in stress resistance and actin organization	1.2E-02	0.57
	1766		155			2.9E-05	0.27
Transport Protein							
Serum albumin	480	ALBU	63	P02769	Regulates the colloidal osmotic pressure of blood	1.4E-02	1.23
Protein Degradation							
Proteasome subunit alpha type-6	1699	PSA6	79	Q2YDE4	Cleavage of peptide bonds with very broad specificity	1.7E-04	0.65

CONCLUSIONS AND PERSPECTIVES

Despite the EU ban, the GPA misuse appears to be a common prcatice, and the lack of efficient analytical tools for detecting illicit pahrmacological treatments at very low dosages increases the toxicological risk for meat consumer's health. For this reason, we applied a 2D-DIGE-based proteomic approach to identify differentially expressed proteins between pharmacologically treated and untreated bulls. Among 169 proteins we found to be differentially expressed between treated and control animals, 29 unique proteins were identified by MALDI-MS/MS analysis. After necessary confirmation studies, these proteins, or a subset of them, can be therefore taken in consideration as potential indirect biomarkers of GPA treatment.

It was reported that low doses of dexamethasone lead to an increased mRNA levels of the myogenic factors MyoD, Myf-5, and MRF4, enhancing the myogenic fusion efficiency of C_2C_{12} cells (Belanto *et al*., 2010). At these levels, glucocorticoids have two main effects on myogenesis: acceleration of differentiation, and increased myotube fusion and accumulation of sarcolemmal proteins. With this respect, our study is consistent with the above findings. We found that dexamethasone treatment influenced the expression of key enzymes linked to muscle metabolism, and increased the expression of sarcolemmal proteins. In addition, our data indicate that the administration of low doses of dexamethasone favors the switch from fast- to slow-muscle contracting phenotype, as underlined by the decreased expression of enzymes involved in glycolysis and of fast-isoforms of contractile proteins.

When dexamethasone was combined with estrogens, we observed a marked reduction of the effects at the protein expression level that prevented us from distinguishing between treated and control animals. However this result is not surprising, because a crosstalk between glucocorticoids and estrogens is known to occur at different levels, generating opposite effects (Tsai *et al*., 2007).

The β-agonists enhance growth efficiency by increasing the rate of gain, decreasing feed consumption, and increasing the amount of skeletal muscle tissue. Muscle growth induced by β-agonists is associated with a substantial

change in fibres' properties towards a fast-contracting phenotype, which involved the whole muscle architecture (Burniston *et al*., 2007). With this respect, our findings on the combined treatment with dexamethasone and clenbuterol contradict the alterations usually observed after administration of only clenbuterol. Indeed we found a protein expression pattern that is very similar to that obtained by treating animals with dexamethasone alone, with the exception that some protein displayed a higher fold-change with respect to controls.

In summary, the results obtained using the 2D-DIGE approach, demonstrated that this technique is useful to simultaneously evaluate a variety of proteins as potential indirect markers of illicit pharmacological treatments. However, these putative biomarkers must be tested using other approaches and other animal sets in order to be definitively validated. Thus, at present, this study represents a first step towards the development of screening tests based on the detection of the biological effects (at the protein level) of illicit treatments.Two major strategies can be envisaged for validation studies: antibody-based techniques, and proteomic-based approaches.

Western blot and ELISA have been for a long time the most powerful methods for quantitative assessments and the identification of biomarkers. Indeed, antibody-based assays (such as ELISA or antibody microarrays) are currently the most widely used methods for quantitative biomarker measurement. Recent studies using proteomics and protein arrays, however, have demonstrated that antibody specificity is often lacking (Haab and Zhou, 2004; MacBeath, 2002), and considerable care must be taken in biomarkers validation by antibody-based methods (Ackermann and Berna, 2007). Another limit of antibody-based analysis is that adequate antibodies are not easily developed for use in ELISA kits. Additionally, homogeneous protein standards need to be carefully generated, validated and quantified for immuno-assays (Barker, 2003). The limited specificity and antibody availability, coupled with recent advances in MS technology, is stimulating the development of quantitative MS-based techniques for protein and peptide validation (Anderson and Hunter, 2006; Kuhn *et al*., 2004). LC-MS/MS of small molecules is already used for routine assays,

including metabolite screening and multiple drug analysis (Streit *et al*., 2002). As for proteins, if quantification of only a selected subset is desired, peptides derived from these proteins can be targeted by a technique called multiple reaction monitoring (MRM). As already mentioned, this requires specialized mass spectrometers (named triple quadrupole, or QQQ), which consist of a selection quadrupole (Q1) for the precursor ion, a collision cell quadrupole (Q2), and a selection quadrupole (Q3) for the analysis of the generated fragments. They are set to exclusively monitor predetermined precursor-to-fragment transitions in rapid succession. This technique is rapidly becoming the method of choice to monitor the presence and the quantity of selected peptides (Wolf-Yadlin *et al*., 2007; Kitteringham *et al*., 2009).

Since a specific antibody does not need to be developed for MRM, this technique can be quickly used to verify candidate biomarkers in controlled subsets of samples and to shorten the advance to validation stages. A clear advantage of MRM is that it can process up to 200 transitions, equivalent to approximately 50 target proteins, using 1-2 µg of the peptide mixture. As for the limits of this technique, it must be mentioned that the detection of low-abundance proteins (in the pg/ml range) is unattainable with current MRM, and the throughput of such experiments primarily depends on the operation time of nano-LC. In addition, quantification using MRM shows considerable experimental variation between runs, primarily caused by sample handling and technical instability. Several attempts have been applied to reduce run-to-run variations improving MRM operations. To minimize technical variability, highly concentrated samples should be substantially diluted, because minute errors in pipetting can lead to wide variations. The distinguishable internal-standard (an isotope-labelled synthetic peptide) should be spiked into each sample at the beginning of the analysis, so that sample handling can be monitored at all stages of preparation (e.g., high-abundance protein depletion, digestion and desalting). Additionally, the internal standard peptide should be spiked into the final peptide mixture before peptide injection for mass spectrometry. The spiked internal standard can thus be used to correct for the variation of ion-spray efficiency. The most tedious procedure in MRM is determining the transitions for target proteins, a crucial step to obtain good measurements of target peptides

and high specificity. For this reason, 3 transitions, that are specific to a given peptide, for at least 2 peptides for protein, should be determined. To this end, software programs that allow researchers to spend less time and effort in determining such transitions, were developed (PeptideAtlas, MRMAtlas).

Despite the above listed limits in quantification, MRM can be useful in biomarker development. In a first (identification) step, crude lists of biomarker candidates can be obtained from a representative set of samples using comparative profiling techniques, such as 2DE, differential labelling (e.g., iTRAQ), and LC-MS/MS. Subsequently, to verify the list of potential biomarkers in individual samples, MRM would be the inevitable choice when no appropriate antibody is available. Use of MRM in biomarker development can also enhance the identification of post-translational modifications, such as phosphorylation and glycosylation, which are difficult tasks for antibody-based systems (Mayya *et al*., 2006; Hulsmeier *et al*., 2007).

In summary, MRM could be useful in diagnostics to detect altered physiological states, such as differential protein expression following pharmacological treatments. Indeed, the potential applicability of MRM is growing thanks to the rapid evolution of MS technology, which continuously generates remarkable innovations in workflow, software, hardware and reagents. Therefore, we believe that a MRM-based approach could be a suitable choice to validate the proteins (or a subset of them) that we found to be differentially expressed between control and treated bulls as actual biologic marker of illicit treatments.

AKNOWLEDGEMENTS

I would like to take the opportunity to thank all the people who have helped me during my PhD work. In particular my thanks go to:

Catia Sorgato, my professor and supervisor. Thank you for giving me the possibility to do this research, for having confidence in me, and encouraging me to realise my potentiality.

Peter James, my co-supervisor abroad, for the opportunity to join his group, for involving me in several different projects, and for the MS touch. Thank you for the patience, your great sense of humor, and for the funny meetings outside the department.

Alessandro Bertoli, my mentor, whose contribution has been fundamental for my work and skills. I appreciate your ability to create a great atmosphere inside and outside the lab (evening lab meetings), and I thank you for always keeping open your office door.

Giancarlo Biancotto for the keen interest and fruitful collaboration on the bovine project, and for consistent discussions and feedback.
The IZSVE for the support during the PhD course, in particular: Igino, Roberto, and, Giandomenico, Cristina, Luca, Giulia, Valentino, Giovanni, Andrea, Federica and the rest of SC2 group for introducing me to the field of "illicits".

Marilina Massimino for teaching me how to cope with mice and cell cultures, for being always positive, especially when starting new projects, and for the good times outside the lab.

My fellow PhD students Cristian, Filippo and Angela for collaboration and great times inside and outside the lab. Thanks to the incredible sense of humor of you all. The other Italians I met during my periods abroad: Paolo, Salvatore, and Giorgio for teaching me a lot of tricks, for the time spent between gym and sauna, and for the Italian coffee.

The "Swedish" PhD students Paolo, Sofia, Åsa, Lynn, Maria, and Kristofer for conversation, running and fun times during dinners and parties. All the people of the Immuno-/Protein-technology group, in particular: Morten, Fredrik, Niclas, Mats, Karin, Liselotte, Ulrika B, Ulrika A, Céline, Tommie for the time we spent together during breaks, for many useful inputs, and for the fantastic efficiency.

The reason of my life Caterina, for love and support, always. Mum, Dad, Paola, Luca, and my family who supported me during these years, and all my friends.

REFERENCES

Ackermann BL, Berna MJ. Coupling immunoaffinity techniques with MS for quantitative analysis of low-abundance protein biomarkers. Expert Rev Proteomics. 2007; 4(2): 175-186.

Aebersold R, Mann M. Mass spectrometry-based proteomics. Nature. 2003; 422: 198-207.

Aebersold R. A mass spectrometric journey into protein and proteome research. J Am Soc Mass Spectrom. 2003; 14(7): 685-695.

Aguzzi A, Baumann F, Bremer J. The prion's elusive reason for being. Annu Rev Neurosci. 2008; 31: 439-477.

Aguzzi A, Calella AM. Prions: protein aggregation and infectious diseases. Physiol Rev. 2009; 89(4): 1105-1152.

Alban A, David SO, Bjorkesten L, Andersson C, Sloge E, Lewis S, Currie I. A novel experimental design for comparative two-dimensional gel analysis: two-dimensional difference gel electrophoresis incorporating a pooled internal standard. Proteomics. 2003; 3: 36-44.

Albini S, Puri PL. SWI/SNF complexes, chromatin remodeling and skeletal myogenesis: it's time to exchange! Exp Cell Res. 2010; 316: 3073-3080.

Allinson TM, Parkin ET, Turner AJ, Hooper NM. ADAMs family members as amyloid precursor protein alpha-secretases. J Neurosci Res. 2003; 74: 342-352.

Alper T. Does the agent of scrapie replicate without nucleic acid? Nature. 1967; 214(5090): 764-766.

Amthor H, Huang R, McKinnell I, Christ B, Kambadur R, Sharma M, Patel K. The regulation and action of myostatin as a negative regulator of muscle development during avian embryogenesis. Dev Biol. 2002; 251(2): 241-257.

Anderson NL, Hunter CL. Quantitative mass spectrometric multiple reaction monitoring assays for major plasma proteins. Molecular and Cellular Proteomics. 2006; 5: 573-588.

Andréoletti O, Simon S, Lacroux C, Morel N, Tabouret G, Chabert A, Lugan S, Corbière F, Ferré P, Foucras G, Laude H, Eychenne F, Grassi J, Schelcher F. PrPSc accumulation in myocytes from sheep incubating natural scrapie. Nat Med. 2004; 10(6): 591-593.

Angers RC, Browning SR, Seward TS, Sigurdson CJ, Miller MW, Hoover EA, Telling GC. Prions in skeletal muscles of deer with chronic wasting disease. Science. 2006; 311(5764): 1117.

Antignac JP, Monteau F, Negriolli J, Andrè F, Le Bizec B. Application of hyphenated mass spectrometric techniques to the determination of corticosteroid residues in biological matrices. Chromatographia 2004; 59: S13-S22.

Arnold L, Henry A, Poron F, Baba-Amer Y, van Rooijen N, Plonquet A, Gherardi RK, Chazaud B. Inflammatory monocytes recruited after skeletal muscle injury switch into antiinflammatory macrophages to support myogenesis. J Exp Med. 2007; 204(5): 1057-1069.

Barker PE. Cancer biomarker validation: standards and process: roles for the National Institute of Standards and Technology (NIST). Annals of the New York Academy of Sciences 2003; 983: 142-150.

Basler K, Oesch B, Scott M, Westaway D, Walchli M, Groth DF, McKinley MP, Prusiner SB, Weissmann C. Scrapie and cellular PrP isoforms are encoded by the same chromosomal gene. Cell. 1986; 46(3): 417-428.

Belanto JJ, Diaz-Perez SV, Magyar CE, Maxwell MM, Yilmaz Y, Topp K, Boso G, Jamieson CH, Cacalano NA, Jamieson CA. Dexamethasone induces dysferlin in myoblasts and enhances their myogenic differentiation. Neuromuscul Disord. 2010; 20(2): 111-121.

Bellinger-Kawahara C, Diener TO, McKinley MP, Groth DF, Smith DR, Prusiner SB. Purified scrapie prions resist inactivation by procedures that hydrolyze, modify, or shear nucleic acids. Virology. 1987; 160(1): 271-274.

Bosque PJ, Ryou C, Telling G, Peretz D, Legname G, DeArmond SJ, Prusiner SB. Prions in skeletal muscle. Proc Natl Acad Sci USA. 2002; 99(6): 3812-3817.

Bounhar Y, Zhang Y, Goodyer CG, LeBlanc A. Prion protein protects human neurons against Bax-mediated apoptosis. J Biol Chem. 2001; 276(42): 39145-39149.

Brandner S, Raeber A, Sailer A, Blättler T, Fischer M, Weissmann C, Aguzzi A. Normal host prion protein (PrPC) is required for scrapie spread within the central nervous system. Proc Natl Acad Sci USA. 1996; 93(23): 13148-13151.

Brown DR, Qin K, Herms JW, Madlung A, Manson J, Strome R, Fraser PE, Kruck T, von Bohlen A, Schulz-Schaeffer W, Giese A, Westaway D, Kretzschmar H. The cellular prion protein binds copper in vivo. Nature. 1997; 390(6661): 684-687.

Buckingham M, Bajard L, Chang T, Daubas P, Hadchouel J, Meilhac S, Montarras D, Rocancourt D, Relaix F. The formation of skeletal muscle: from somite to limb. J Anat. 2003; 202(1): 59-68.

Burniston JG, McLean L, Beynon RJ, Goldspink DF. Anabolic effects of a non-myotoxic dose of the beta2-adrenergic receptor agonist clenbuterol on rat plantaris muscle. Muscle Nerve. 2007; 35(2): 217-223.

Büeler H, Fischer M, Lang Y, Bluethmann H, Lipp HP, DeArmond SJ, Prusiner SB, Aguet M, Weissmann C. Normal development and behaviour of mice lacking the neuronal cell-surface PrP protein. Nature. 1992; 356, 577-582.

Cabane C, Englaro W, Yeow K, Ragno M, Derijard B. Regulation of C2C12 myogenic terminal differentiation by MKK3/p38-pathway. Am. J. Physiol. Cell Physiol. 2003; 284: C658–C666.

Cantiello M, Carletti M, Dacasto M, Martin PG, Pineau T, Capolongo F, Gardini G, Nebbia C. Cytochrome P450 inhibition profile in liver of veal calves administered a combination of 17beta-estradiol, clenbuterol, and dexamethasone for growth-promoting purposes. Food Chem Toxicol. 2008; 46(8): 2849-5285.

Cantini M, Giurisato E, Radu C, Tiozzo S, Pampinella F, Senigaglia D, Zaniolo G, Mazzoleni F, Vittiello L. Macrophage-secreted myogenic factors: a promising tool for greatly enhancing the proliferative capacity of myoblasts in vitro and in vivo. Neurol Sci. 2002; 23: 189-194.

Cardone F, Thomzig A, Schulz-Schaeffer W, Valanzano A, Sbriccoli M, Abdel-Haq H, Graziano S, Pritzkow S, Puopolo M, Brown P, Beekes M, Pocchiari M. PrPTSE in muscle-associated lymphatic tissue during the preclinical stage of mice infected orally with bovine spongiform encephalopathy.J Gen Virol. 2009; 90(Pt 10): 2563-2568.

Caughey B, Brown K, Raymond GJ, Katzenstein GE, Thresher W. Binding of the protease-sensitive form of PrP (prion protein) to sulfated glycosaminoglycan and congo red. J Virol. 1994; 68(4): 2135-2141. Erratum in: J Virol. 1994; 68(6): 4107.

Caughey B, Raymond GJ. The scrapie-associated form of PrP is made from a cell surface precursor that is both protease- and phospholipase-sensitive. J Biol Chem. 1991; 266(27): 18217-18223.

Chargé SB, Rudnicki MA. Cellular and molecular regulation of muscle regeneration. Physiol Rev. 2004; 84(1): 209-238.

Chazaud B, Sonnet C, Lafuste P, Bassez G, Rimaniol AC, Poron F, Authier FJ, Dreyfus PA, Gherardi RK. Satellite cells attract monocytes and use macrophages as a support to escape apoptosis and enhance muscle growth. J Cell Biol. 2003; 163(5): 1133-1143.

Chen S, Mangé A, Dong L, Lehmann S, Schachner M. Prion protein as trans-interacting partner for neurons is involved in neurite outgrowth and neuronal survival. Mol Cell Neurosci. 2003; 22(2): 227-233.

Chen SE, Gerken E, Zhang Y, Zhan M, Mohan RK, Li A, Reid MB, Li YP. Role of TNFalpha signaling in regeneration of cardiotoxin-injured muscle. Am J Physiol Cell Physiol. 2005; 289: 1179-87.

Chen SE, Jin B, Li YP. TNFalpha regulates myogenesis and muscle regeneration by activating p38 MAPK. Am J Physiol Cell Physiol. 2007; 292: 1660-1671.

Chiesa R, Pestronk A, Schmidt RE, Tourtellotte WG, Ghetti B, Piccardo P, Harris DA. Primary myopathy and accumulation of PrPSc-like like molecules in peripheral tissues of transgenic mice ex pressing a prion protein insertional mutation. Neurobiol Dis. 2001; 8(2): 279-288.

Chrétien F, Dorandeu A, Adle-Biassette H, Ereau T, Wingertsmann L, Brion F, Gray F. A process of programmed cell death as a mechanisms of neuronal death in prion diseases. Clin Exp Pathol. 1999; 47(3-4): 181-191.

Cohen FE, Pan KM, Huang Z, Baldwin M, Fletterick RJ, Prusiner SB. Structural clues to prion replication. Science. 1994;264(5158): 530-531.

Coitinho AS, Freitas AR, Lopes MH, Hajj GN, Roesler R, Walz R, Rossato JI, Cammarota M, Izquierdo I, Martins VR, Brentani RR. The interaction between prion protein and laminin modulates memory consolidation. Eur J Neurosci. 2006; 24(11): 3255-3264.

Collinge J, Owen F, Poulter M, Leach M, Crow TJ, Rossor MN, Hardy J, Mullan MJ, Janota I, Lantos PL. Prion dementia without characteristic pathology. Lancet. 1990; 336(8706): 7-9.

Cooper RN, Tajbakhsh S, Mouly V, Cossu G, BuckinghamM, Butler-Browne GS. In vivo satellite cell activation via Myf5 andMyoD in regenerating mouse skeletal muscle. J Cell Sci. 1999; 112: 2895–2901.

Cornelison DD, Olwin BB, Rudnicki MA, Wold BJ. MyoD(-/-) satellite cells in single-fiber culture are differentiation defective and MRF4 deficient. Dev Biol. 2000; 224(2): 122-137.

Courtheyn D, Le Bizec B, Brambilla G, De Brabander HF, Cobbaert E, Van de Wiele M, Vercammena J, De Wasch K. Recent developments in the use and abuse of growth promoters. Anal. Chim. Acta. 2002, 473: 71-82.

Cox J, Mann M. Is proteomics the new genomics? Cell. 2007; 130(3): 395-398.

Dayon L, Hainard A, Licker V, Turck N, Kuhn K, Hochstrasser DF, Burkhard PR, Sanchez JC. Relative quantification of proteins in human cerebrospinal fluids by MS/MS using 6-plex isobaric tags. Anal Chem. 2008; 80: 2921-2931.

Dong MW. Tryptic mapping by reversed phase liquid chromatography. Adv Chromatogr. 1992; 32: 21-51.

Dorandeu A, Wingertsmann L, Chrétien F, Delisle MB, Vital C, Parchi P, Montagna P, Lugaresi E, Ironside JW, Budka H, Gambetti P, Gray F. Neuronal apoptosis in fatal familial insomnia. Brain Pathol. 1998; 8(3): 531-537.

dos Ramos FJ. Beta2-agonist extraction procedures for chromatographic analysis. J Chromatogr A. 2000; 880: 69-83.

Dwivedi RC, Spicer V, Harder M, Antonovici M, Ens W, Standing KG, Wilkins JA, Krokhin OV. Practical implementation of 2D HPLC scheme with accurate peptide retention prediction in both dimensions for high-throughput bottom-up proteomics. Anal Chem. 2008; 80: 7036-7042.

Edwards DR, Handsley MM, Pennington CJ. The ADAM metalloproteinases. Mol Aspects Med. 2008; 29: 258-289.

Elliott CT, McEvoy JD, McCaughey WJ, Crooks SRH, Hewitt SA. Improved detection of the β-agonist clenbuterol by analysis of retina extracts. Vet. Rec. 1993b; 132: 301-302.

Eng JK, McCormack AL, Yates JR. An approach to correlate MS/MS data to amino acid sequences in proten database. J Am Soc Mass Spectrom 1994; 5: 976-89.

Fenn JB, Mann M, Meng CK, Wong SF, Whitehouse CM. Electrospray ionization for mass spectrometry of large biomolecules. Science. 1989; 246: 64-71.

Forloni G, Angeretti N, Chiesa R, Monzani E, Salmona M, Bugiani O, Tagliavini F. Neurotoxicity of a prion protein fragment. Nature. 1993 Apr 8;362(6420):543-6.

Fornai F, Ferrucci M, Gesi M, Bandettini di Poggio A, Giorgi FS, Biagioni F, Paparelli A. A hypothesis on prion disorders: are infectious, inherited, and sporadic causes so distinct? Brain Res Bull. 2006; 69(2): 95-100.

Friso G, Kaiser L, Raud J, Wikström L. Differential protein expression in rat trigeminal ganglia during inflammation. Proteomics. 2001; 1: 397-408.

Gauczynski S, Peyrin JM, Haïk S, Leucht C, Hundt C, Rieger R, Krasemann S, Deslys JP, Dormont D, Lasmézas CI, Weiss S. The 37-kDa/67-kDa laminin receptor acts as the cell-surface receptor for the cellular prion protein. EMBO J. 2001; 20(21): 5863-5875.

Gillette MA, Mani DR, Carr SA. Place of pattern in proteomic biomarker discovery. J Proteome Res. 2005; 4: 1143-1154.

Glatzel M, Abela E, Maissen M, Aguzzi A. Extraneural pathologic prion protein in sporadic Creutzfeldt-Jakob disease. N Engl J Med. 2003; 349(19): 1812-1820.

Gopinath SD, Rando TA. Stem cell review series: aging of the skeletal muscle stem cell niche. Aging Cell. 2008; 7(4): 590-598.

Görg A, Drews O, Lück C, Weiland F, Weiss W. 2-DE with IPGs. Electrophoresis. 2009; 30 Suppl 1: S122-132.

Görg A, Weiss W, Dunn MJ. Current two-dimensional electrophoresis technology for proteomics. Proteomics. 2004; 4(12): 3665-3685. Erratum in: Proteomics. 2005; 5(3): 826-827.

Gowik P, Jülicher B, Ladwig M, Behrendt D. Measurement of beta-agonist residues in retinal tissue of food producing animals. Analyst. 2000; 125: 1103-1107.

Graner E, Mercadante AF, Zanata SM, Forlenza OV, Cabral AL, Veiga SS, Juliano MA, Roesler R, Walz R, Minetti A, Izquierdo I, Martins VR, Brentani RR. Cellular prion protein binds laminin and mediates neuritogenesis. Brain Res Mol Brain Res. 2000a; 76(1): 85-92.

Griffith JS. Self-replication and scrapie. Nature. 1967 215(105):1043-4.

Gygi SP, Rist B, Gerber SA, Turecek F, Gelb MH, Aebersold R. Quantitative analysis of complex protein mixtures using isotope-coded affinity tags. Nat Biotechnol. 1999; 17: 994-999.

Haab BB, Zhou H. Multiplexed protein analysis using spotted antibody microarrays. Methods Mol Biol. 2004; 264: 33-45.

Haass C, Selkoe DJ. Soluble protein oligomers in neurodegeneration: lessons from the Alzheimer's amyloid beta-peptide. Nat Rev Mol Cell Biol 2007; 8:101-12.

Hajj GN, Lopes MH, Mercadante AF, Veiga SS, da Silveira RB, Santos TG, Ribeiro KC, Juliano MA, Jacchieri SG, Zanata SM, Martins VR. Cellular prion protein interaction with vitronectin supports axonal growth and is compensated by integrins. J Cell Sci. 2007; 120(Pt 11): 1915-1926.

Han J, Jiang Y, Li Z, Kravchenko VV, Ulevitch RJ. Activation of the transcription factor MEF2C by the MAP kinase p38 in inflammation. Nature. 1997; 386: 296-299.

Hanash S. Disease proteomics. Nature. 2003; 422 :226-232.

Hansen SM, Berezin V, Bock E. Signaling mechanisms of neurite outgrowth induced by the cell adhesion molecules NCAM and N-cadherin. Cell Mol Life Sci. 2008; 65(23): 3809-3821.

Hawke TJ, Garry DJ. Myogenic satellite cells: physiology to molecular biology. J Appl Physiol. 2001; 91(2): 534-551. Erratum in: J Appl Physiol 2001; 91(6): 2414.

Hill AF, Joiner S, Linehan J, Desbruslais M, Lantos PL, Collinge J. Species-barrier-independent prion replication in apparently resistant species. Proc Natl Acad Sci USA. 2000; 97(18): 10248-10253.

Hooper NM. Roles of proteolysis and lipid rafts in the processing of the amyloid precursor protein and prion protein. Biochem Soc Trans. 2005; 33: 335-338.

Huang S, Liang J, Zheng M, Li X, Wang M, Wang P, Vanegas D, Wu D, Chakraborty B, Hays AP, Chen K, Chen SG, Booth S, Cohen M, Gambetti P, Kong Q. Inducible overexpression of wild-type prion protein in the muscles leads to a primary myopathy in transgenic mice. Proc Natl Acad Sci USA. 2007; 104(16): 6800-6805.

Huber LA, Pfaller K, Vietor I. Organelle proteomics: implications for subcellular fractionation in proteomics. Circ Res. 2003; 92: 962-968.

Hulsmeier AJ, Paesold-Burda P, Hennet T. N-glycosylation site occupancy in serum glycoproteins using multiple reaction monitoring liquid chromatography–mass spectrometry. Mol. Cell. Proteomics. 2007; 6(12): 2132-2138.

Hundt C, Peyrin JM, Haïk S, Gauczynski S, Leucht C, Rieger R, Riley ML, Deslys JP, Dormont D, Lasmézas CI, Weiss S. Identification of interaction domains of the prion protein with its 37-kDa/67-kDa laminin receptor. EMBO J. 2001; 20(21): 5876-86.

Istasse L, De Haan V, Van Eenaeme C, Buts B, Baldwin P, Gielen M, Demeyer D, Bienfait JM. Effects of dexamethasone injections on performances in a pair of monozygotic cattle twins. J. Anim. Physiol. Anim. Nutr. 1984; 62: 150-158.

Kabouridis PS. Lipid rafts in T cell receptor signaling. Mol Membr Biol. 2006;23(1): 49-57.

Kalhovde JM, Jerkovic R, Sefland I, Cordonnier C, Calabria E, Schiaffino S, Lømo T. "Fast" and "slow" muscle fibres in hindlimb muscles of adult rats regenerate from intrinsically different satellite cells. J Physiol. 2005; 562(Pt 3): 847-857.

Kanaani J, Prusiner SB, Diacovo J, Baekkeskov S, Legname G. Recombinant prion protein induces rapid polarization and development of synapses in embryonic rat hippocampal neurons in vitro. J Neurochem. 2005; 95(5): 1373-1386.

Karas M, Bachmann D, Bahr U, Hillenkamp F. Matrix assisted ultraviolet laser desorption of non-volatile compounds. Int. J. Mass Spectrom. Ion Proc. 1987; 78: 53-68.

Kim BH, Lee HG, Choi JK, Kim JI, Choi EK, Carp RI, Kim YS. The cellular prion protein (PrPC) prevents apoptotic neuronal cell death and mitochondrial dysfunction induced by serum deprivation. Brain Res Mol Brain Res. 2004; 124(1): 40-50.

Kim MR, Kim CW. Human blood plasma preparation for two-dimensional gel electrophoresis. J Chromatogr B Analyt Technol Biomed Life Sci. 2007; 849: 203-210.

Kitteringham NR, Jenkins RE, Lane CS, Elliott VL, Park BK. Multiple reaction monitoring for quantitative biomarker analysis in proteomics and metabolomics. J. Chromatogr. B Analyt. Technol. Biomed. Life Sci. 2009; 877: 1229-1239.

Klamt F, Dal-Pizzol F, Conte da Frota ML JR, Walz R, Andrades ME, da Silva EG, Brentani RR, Izquierdo I, Fonseca Moreira JC. Imbalance of antioxidant defense in mice lacking cellular prion protein. Free Radic Biol Med. 2001; 30(10): 1137-1144.

Klose J. Protein mapping by combined isoelectric focusing and electrophoresis of mouse tissues. A novel approach to testing for induced point mutations in mammals. Humangenetik. 1975; 26: 231-243.

Kovacs GC, Linleck-Pozza E, Chimelli L, Araujo AQ, Gabbai AA, Strobel T, Glatzel M, Aguzzi A, Budke H. Creutzfeld-Jacob and inclusion body myositis: abundant disease-associated prion protein in muscle. Ann Neurol. 2004; 55(1): 121-125.

Krasemann S, Neumann M, Geissen M, Bodemer W, Kaup FJ, Schulz-Schaeffer W, Morel N, Aguzzi A, Glatzel M. Preclinical deposition of pathological prion protein in muscle of experimentally infected primates. PLoS One. 2010; 5(11): e13906.

Kuhn E, Wu J, Karl J, Liao H, Zolg W, Guild B. Quantification of C-reactive protein in the serum of patients with rheumatoid arthritis using multiple reaction monitoring mass spectrometry and ^{13}C-labeled peptide standards. Proteomics. 2004; 4: 1175-1186.

Laemmli UK. Cleavage of structural proteins during the assembly of the head of bacteriophage T4. Nature. 1970; 227: 680-685.

Lasmézas CI, Deslys JP, Robain O, Jaegly A, Beringue V, Peyrin JM, Fournier JG, Hauw JJ, Rossier J, Dormont D. Transmission of the BSE agent to mice in the absence of detectable abnormal prion protein. Science. 1997; 275(5298): 402-5.

Le Grand F, Rudnicki MA. Skeletal muscle satellite cells and adult myogenesis. Curr Opin Cell Biol. 2007; 19(6): 628-633.

Li YP, Schwartz RJ. TNF-alpha regulates early differentiation of C2C12 myoblasts in an autocrine fashion. FASEB J. 2001; 15: 1413-1415.

Linden R, Martins VR, Prado MA, Cammarota M, Izquierdo I, Brentani RR. Physiology of the prion protein. Physiol Rev. 2008; 88(2): 673-728.

Loboda AV, Krutchinsky AN, Bromirski M, Ens W, Standing KG. A tandem quadrupole /time-of-flight mass spectrometer with a matrix-assisted laser desorption/ionization source: design and performance. Rapid Commun. Mass Spectrom. 2000; 14: 1047-1057.

Lopes MH, Hajj GN, Muras AG, Mancini GL, Castro RM, Ribeiro KC, Brentani RR, Linden R, Martins VR. Interaction of cellular prion and stress-inducible protein 1 promotes neuritogenesis and neuroprotection by distinct signaling pathways. J Neurosci. 2005; 25(49): 11330-11339.

MacBeath G. Protein microarrays and proteomics. Nat Genet. 2002; 32 Suppl: 526-532.

Makarov A. Electrostatic axially harmonic orbital trapping: a highperformance technique of mass analysis. Anal. Chem. 2000; 72: 1156-1162.

Málaga-Trillo E, Sempou E. PrPs: Proteins with a purpose: Lessons from the zebrafish. Prion. 2009; 3(3): 129-133.

Málaga-Trillo E, Solis GP, Schrock Y, Geiss C, Luncz L, Thomanetz V, Stuermer CA. Regulation of embryonic cell adhesion by the prion protein.PLoS Biol. 2009; 7(3): e55.

Mallucci G, Collinge J. Update on Creutzfeldt-Jakob disease. Curr Opin Neurol. 2004; 17(6): 641-647.

Mallucci G, Ratte S, Asante EA, Linehan J, Gowland I, Jefferys JG, Collinge J. Post-natal knockout of prion protein alters hippocampal CA1 properties, but does not result in neurodegeneration. EMBO J. 2002; 21(3): 202-210.

Mann M, Hendrickson RC, Pandey A. Analysis of proteins and proteome by mass spectrometry. Annu Rev Biochem. 2001; 70: 437-473.

Mann M, Wilm MS. Error tolerant identification of peptides in sequence databases by peptide sequence tags. Anal. Chem. 1994; 66: 4390-4399.

Manson JC, Clarke AR, Hooper ML, Aitchison L, McConnell I, Hope J. 129/Ola mice carrying a null mutation in PrP that abolishes mRNA production are developmentally normal. Mol Neurobiol. 1994; 8(2-3): 121-127.

Massimino ML, Ferrari J, Sorgato MC, Bertoli A. Heterogeneous PrPC metabolism in skeletal muscle cells. FEBS Lett. 2006; 580(3): 878-884.

Mauro A. Satellite cell of skeletal muscle fibers. J Biophys Biochem. 1961; 9: 493-495.

Mayya V, Rezual K, Wu L, Fong MB, Han DK. Absolute quantification of multisite phosphorylation by selective reaction monitoring mass spectrometry: determination of inhibitory phosphorylation status of cyclin-dependent kinases. Mol. Cell. Proteomics. 2006; 5(6): 1146-1157.

Mazzanti G, Daniele C, Boatto G, Manca G, Brambilla G, Loizzo A. New beta-adrenergic agonists used illicitly as growth promoters in animal breeding: chemical and pharmacodynamic studies. Toxicology. 2003; 187: 91-99.

McKerracher L, Chamoux M, Arregui CO. Role of laminin and integrin interactions in growth cone guidance. Mol Neurobiol. 1996; 12(2): 95-116.

McLennan NF, Brennan PM, McNeill A, Davies I, Fotheringham A, Rennison KA, Ritchie D, Brannan F, Head MW, Ironside JW, Williams A, Bell JE. Prion protein accumulation and neuroprotection in hypoxic brain damage. Am J Pathol. 2004; 165(1): 227-235.

Medori R, Montagna P, Tritschler HJ, LeBlanc A, Cortelli P, Tinuper P, Lugaresi E, Gambetti P. Fatal familial insomnia: a second kindred with mutation of prion protein gene at codon 178. Neurology. 1992; 42(3 Pt 1): 669-670.

Medzihradszky KF, Campbell JM, Baldwin MA, Falick AM, Juhasz P, Vestal ML, Burlingame AL. The characteristics of peptide collision-induced dissociation using a high performance MALDI-TOF/TOF tandem mass spectrometer. Anal. Chem. 2000; 72: 552-558.

Miele G, Alejo Blanco AR, Baybutt H, Horvat S, Manson J, Clinton M. Embryonic activation and developmental expression of the murine prion protein gene. Gene Expr. 2003; 11(1): 1-12.

Minden JS, Dowd SR, Meyer HE, Stühler K. Difference gel electrophoresis. Electrophoresis. 2009; 30 (Suppl 1): S156-161.

Mitchell AD, Steele NC, Solomon MB, Alila HW, Lindsey TO, Cracknell V. Influence of dietary background on the response of pigs to the beta-adrenergic agonist BRL 47672. J. Anim. Sci. 1994; 72: 1516-1521.

Mitteregger G, Vosko M, Krebs B, Xiang W, Kohlmannsperger V, Nölting S, Hamann GF, Kretzschmar HA. The role of the octarepeat region in neuroprotective function of the cellular prion protein.Brain Pathol. 2007; 17(2): 174-183.

Monnet C, Gavard J, Mège RM, Sobel A. Clustering of cellular prion protein induces ERK1/2 and stathmin phosphorylation in GT1-7 neuronal cells. FEBS Lett. 2004; 576(1-2): 114-118.

Moritz B, Meyer HE. Approaches for the quantification of protein concentration ratios. Proteomics. 2003; 3: 2208-2220.

Mouillet-Richard S, Ermonval M, Chebassier C, Laplanche JL, Lehmann S, Launay JM, Kellermann O. Signal transduction through prion protein. Science, 2000; 289: 1925-1928.

Nazor KE, Seward T, Telling GC. Motor behaviour and neuropathological deficits in mice deficient form normal prion protein expression. Biochim Biophys Acta. 2007; 1772(6): 645-653.

Neuhoff V, Arold N, Taube D, Ehrhardt W. Improved staining of proteins in polyacrylamide gels including isoelectric focusing gels with clear background at nanogram sensitivity using Coomassie Brilliant Blue G-250 and R-250. Electrophoresis. 1988; 9: 255-262.

Nico PB, Lobão-Soares B, Landemberger MC, Marques W Jr, Tasca CI, de Mello CF, Walz R, Carlotti CG Jr, Brentani RR, Sakamoto AC, Bianchin MM. Impaired exercise capacity, but unaltered mitochondrial respiration in skeletal or cardiac muscle of mice lacking cellular prion protein. Neurosci Lett. 2005; 388(1): 21-26.

O'Farrell PH. High resolution two-dimensional electrophoresis of proteins. J Biol Chem. 1975; 250: 4007-21.

Old WM, Meyer-Arendt K, Aveline-Wolf L, Pierce KG, Mendoza A, Sevinsky JR, Resing KA, Ahn NG. Comparison of label-free methods for quantifying human proteins by shotgun proteomics. Mol. Cell. Proteomics. 2005; 4: 1487-1502.

Ong SE, Blagoev B, Kratchmarova I, Kristensen DB, Steen H, Pandey A, Mann M. Stable isotope labeling by amino acids in cell culture, SILAC, as a simple and accurate approach to expression proteomics. Mol. Cell. Proteomics. 2002; 1: 376-386.

Palacios D, Mozzetta C, Consalvi S, Caretti G, Saccone V, Proserpio V, Marquez VE, Valente S, Mai A, Forcales SV, Sartorelli V, Puri PL. TNF/p38α/polycomb signaling to Pax7 locus in satellite cells links inflammation to the epigenetic control of muscle regeneration. Cell Stem Cell. 2010; 7: 455-69.

Pan KM, Baldwin M, Nguyen, Gasset M, Serban A, Groth D, Mehlhorn I, Huang Z, Fletterick RJ, Cohen FE. Conversion of alpha-helices into beta sheet features in the formation of scrapie prion protein. Proc. Natl. Acad. Sci. USA 1993; 90: 10962-10966.

Pan T, Wong BS, Liu T, Li R, Petersen RB, Sy MS. Cell-surface prion protein interacts with glycosaminoglycans. Biochem J. 2002; 368(Pt 1): 81-90.

Parker MH, Seale P, Rudnicki MA. Looking back to the embryo: defining transcriptional networks in adult myogenesis. Nat Rev Genet. 2003; 4(7): 497-507.

Patterson SD, Aebersold RH. Proteomics: the first decade and beyond. Nat. Genet. 2003; 33: 311–323.

Peden AH, Ritchie DL, Head MW, Ironside JW. Detection and localization of PrPSc in the skeletal muscle of patients with variant, iatrogenic, and sporadic forms of Creutzfeldt-Jakob disease. Am J Pathol. 2006; 168(3): 927-935.

Peters PJ, Mironov A Jr, Peretz D, van Donselaar E, Leclerc E, Erpel S, DeArmond SJ, Burton DR, Williamson RA, Vey M, Prusiner SB. Trafficking of prion proteins through a caveolae-mediated endosomal pathway. J Cell Biol. 2003; 162(4): 703-717.

Pradines E, Loubet D, Mouillet-Richard S, Manivet P, Launay JM, Kellermann O, Schneider B. Cellular prion protein coupling to TACE-dependent TNF-alpha shedding controls neurotransmitter catabolism in neuronal cells. J Neurochem. 2009; 110(3): 912-923.

Prestori F, Rossi P, Bearzatto B, Laine J, Necchi D, Diwakar S, Schiffmann SN, Axelrad H, D'Angelo E. Altered neuron excitability and synaptic plasticity in the cerebellar granular layer of juvenile prion protein knock-out mice with impaired motor control. J. Neurosci. 2008; 28: 7091–7103.

Prusiner SB. Prions. Proc. Natl. Acad. Sci. 1998; 95: 13363-13383.

Prusiner SB. Prions: novel infectious pathogens. Adv Virus Res. 1984; 29: 1-56.

Rabilloud T, Strub JM, Luche S, van Dorsselaer A, Lunardi J. A comparison between Sypro Ruby and ruthenium II tris (bathophenanthroline disulfonate) as fluorescent stains for protein detection in gels. Proteomics. 2001; 1: 699-704.

Rabilloud T. Membrane proteins and proteomics: love is possible, but so difficult. Electrophoresis. 2009; 30 Suppl 1: S174-180.

Race R, Chesebro B. Scrapie infectivity found in resistant species. Nature. 1998; 392(6678): 770.

Relaix F, Montarras D, Zaffran S, Gayraud-Morel B, Rocancourt D, Tajbakhsh S, Mansouri A, Cumano A, Buckingham M. Pax3 and Pax7 have distinct and overlapping functions in adult muscle progenitor cells. J Cell Biol. 2006; 172(1): 91-102. Erratum in: J Cell Biol. 2007; 176(1): 125.

Reynolds JEF. Marthindale - The Extra Pharmacopoeia, 1996; 31st edition.

Rieger R, Edenhofer F, Lasmezas CI, Weiss S. The human 37-kDa laminin receptor precursor interacts with the prion protein in eukaryotic cells. Nat Med. 1997; 3(12): 1383-1388.

Riek R, Hornemann S, Wider G, Billeter M, Glockshuber R, Wüthrich K. NMR structure of the mouse prion protein domain PrP(121-321). Nature. 1996; 382(6587): 180-182.

Rogers M, Graham J, Tonge RP. Statistical models of shape for the analysis of protein spots in two-dimensional electrophoresis gel images. Proteomics. 2003; 3: 887-896.

Ross PL, Huang YN, Marchese JN, Williamson B, Parker K, Hattan S, Khainovski N, Pillai S, Dey S, Daniels S, Purkayastha S, Juhasz P, Martin S, Bartlet-Jones M, He F, Jacobson A, Pappin DJ. Multiplexed protein quantitation in Saccharomyces cerevisiae using amine-reactive isobaric tagging reagents. Mol. Cell. Proteomics. 2004; 3: 1154-1169.

Safar J, Roller PP, Gajduesek DC, Gibbs CJ Jr. Thermal stability and conformational transitions of scrapie amyloid (prion) protein correlate with infectivity. Protein Sci. 1993; 2: 2206-2216.

Samaia HB, Brentani RR. Can loss-of-function prion-related diseases exist? Mol Psychiatry. 1998; 3(3): 196-197.

Santoni V, Molloy M, Rabilloud T. Membrane proteins and proteomics: un amour impossible? Electrophoresis. 2000; 21: 1054-1070.

Santuccione A, Sytnyk V, Leshchyns'ka I, Schachner M. Prion protein recruits its neuronal receptor NCAM to lipid rafts to activate p59Fyn and to enhance neurite outgrowth. J Cell Biol. 2005; 169(2): 341-354.

Schmalbruch H, Lewis DM. Dynamics of nuclei of muscle fibers and connective tissue cells in normal and denervated rat muscles. Muscle Nerve. 2000; 23(4): 617-626.

Schmitt-Ulms G, Legname G, Baldwin MA, Ball HL, Bradon N, Bosque PJ, Crossin KL, Edelman GM, DeArmond SJ, Cohen FE, Prusiner SB. Binding of neural cell adhesion molecules (N-CAMs) to the cellular prion protein. J Mol Biol. 2001; 314(5): 1209-1225.

Schneider B, Mutel V, Pietri M, Ermoval M, Mouillet-Richard S, Kellermann O. NADPH oxidase and extracellular regulated kinases1/2 are targets of prions protein signalling in neuronal and nonneuronal cells. Proc Natl Acad Sci U S A. 2003; 100(23): 13326-13331.

Schwartz JC, Senko MW, Syka JE. A two-dimensional quadrupole ion trap mass spectrometer. J Am Soc Mass Spectrom. 2002; 13(6): 659-669.

Scigelova M, Makarov A. Orbitrap mass analyzer-overview and applications in proteomics. Proteomics. 2006; 6 (Suppl 2): 16-21.

Seale P, Sabourin LA, Girgis-Gabardo A, Mansouri A, Gruss P, Rudnicki MA. Pax7 is required for the specification of myogenic satellite cells. Cell. 2000; 102(6): 777-786.

Serra C, Palacios D, Mozzetta C, Forcales SV, Morantte I, Ripani M, Jones DR, Du K, Jhala US, Simone C, Puri PL. Functional interdependence at the chromatin level between the MKK6/ p38 and IGF1/PI3K/AKT pathways during muscle differentiation. Mol Cell. 2007; 28: 200-213.

Serrano AL, Baeza-Raja B, Perdiguero E, Jardí M, Muñoz-Cánoves P. Interleukin-6 is an essential regulator of satellite cell-mediated skeletal muscle hypertrophy. Cell Metab. 2008; 7(1): 33-44.

Shaw J, Rowlinson R, Nickson J, Stone T, Sweet A, Williams K, Tonge R. Evaluation of saturation labelling two-dimensional difference gel electrophoresis fluorescent dyes. Proteomics. 2003; 3(7): 1181-1195.

Shyu WC, Lin SZ, Chiang MF, Ding DC, Li KW, Chen SF, Yang HI, Li H. Overexpression of PrPC by Adenovirus-mediated gene targeting reduces ischemic injury in a stroke rat model. J Neurosci. 2005; 25(39): 8967-8977.

Simone C, Forcales SV, Hill DA, Imbalzano AN, Latella L, Puri PL. p38 pathway targets SWI-SNF chromatin-remodeling complex to muscle-specific loci. Nat Genet. 2004; 36: 738-743.

Simons K, Ikonen E. Functional rafts in cell membranes. Nature. 1997; 387(6633): 569-572.

Smith CK II, Janney MJ, Allen RE. Temporal expression of myogenic regulatory genes during activation, proliferation, and differentiation of rat skeletal muscle satellite cells. J Cell Physiol. 1994; 159: 379-385.

Sparkes RS, Simon M, Cohn VH, Fournier RE, Lem J, Klisak I, Heinzmann C, Blatt C, Lucero M, Mohandas T. Assignment of the human and mouse prion protein genes to homologous chromosomes. Proc Natl Acad Sci U S A. 1986; 83(19): 7358-7362.

Spudich A, Frigg R, Kilic E, Kilic U, Oesch B, Raeber A, Bassetti CL, Hermann DM. Aggravation of ischemic brain injury by prion protein deficiency: role of ERK-1/-2 and STAT-1. Neurobiol Dis. 2005; 20(2): 442-449.

Steele AD, Lindquist S, Aguzzi A. The prion protein knockout mouse: a phenotype under challenge. Prion. 2007;1(2): 83-93.

Steele AD, Zhou Z, Jackson WS, Zhu C, Auluck P, Moskowitz MA, Chesselet MF, Lindquist S. Context dependent neuroprotective properties of prion protein (PrP). Prion. 2009; 3(4): 240-249.

Stolker AA, Brinkman UA. Analytical strategies for residue analysis of veterinary drugs and growth-promoting agents in food-producing animals--a review. J Chromatogr A. 2005; 1067(1-2): 15-53.

Streit F, Armstrong VW, Oellerich M. Rapid liquid chromatography-tandem mass spectrometry routine method for simultaneous determination of sirolimus, everolimus, tacrolimus, and cyclosporin A in whole blood. Clinical Chemistry. 2002; 48: 955-958.

Stuermer CA, Langhorst MF, Wiechers MF, Legler DF, Von Hanwehr SH, Guse AH, Plattner H. PrPc capping in T cells promotes its association with the lipid raft proteins reggie-1 and reggie-2 and leads to signal transduction. FASEB J. 2004; 18(14): 1731-1733.

Taylor DR, Hooper NM. The prion protein and lipid rafts. Mol Membr Biol. 2006; 23(1): 89-99.

Taylor DR, Parkin ET, Cocklin SL, Ault JR, Ashcroft AE, Turner AJ, Hooper NM. Role of ADAMs in the ectodomain shedding and conformational conversion of the prion protein. J Biol Chem 2009; 284: 22590-22600.

Ten Broek RW, Grefte S, Von den Hoff JW. Regulatory factors and cell populations involved in skeletal muscle regeneration. J Cell Physiol. 2010; 224(1): 7-16.

Thompson A, Schäfer J, Kuhn K, Kienle S, Schwarz J, Schmidt G, Neumann T, Johnstone R, Mohammed AK, Hamon C. Tandem mass tags: a novel quantification strategy for comparative analysis of complex protein mixtures by MS/MS. Anal Chem. 2003; 75: 1895-1904.

Thomzig A, Schulz-Schaeffer W, Kratzel C, Mai J, Beekes M. Preclinical deposition of pathological prion protein PrPSc in muscles of hamsters orally exposed to scrapie. J Clin Invest. 2004; 113(10): 1465-1472.

Tidball JG, Berchenko E, Frenette J. Macrophage invasion does not contribute to muscle membrane injury during inflammation. J Leukoc Biol. 1999; 65: 492-498.

Tidball JG, Wehling-Henricks M. Macrophages promote muscle membrane repair and muscle fibre growth and regeneration during modified muscle loading in mice in vivo. J Physiol. 2007; 578(Pt 1): 327-336.

Tidball JG. Inflammatory cell response to acute muscle injury. Med Sci Sports Exerc. 1995; 27(7): 1022-1032.

Tsai WJ, McCormick KM, Brazeau DA, Brazeau GA. Estrogen effects on skeletal muscle insulin-like growth factor 1 and myostatin in ovariectomized rats. Exp Biol Med (Maywood). 2007; 232(10): 1314-1325.

Unlü M, Morgan ME, Minden JS. Difference gel electrophoresis: a single gel method for detecting changes in protein extracts. Electrophoresis. 1997; 18: 2071-2077.

Uptain SM, Lindquist S. Prions as protein-based genetic elements. Annu Rev Microbiol. 2002; 56: 703-741.

Vardy ER, Catto AJ, Hooper NM. Proteolytic mechanisms in amyloid-beta metabolism: therapeutic implications for Alzheimer's disease. Trends Mol Med. 2005; 11: 464-472.

Vey M, Pilkuhn S, Wille H, Nixon R, DeArmond SJ, Smart EJ, Anderson RG, Taraboulos A, Prusiner SB. Subcellular colocalization of the cellular and scrapie prion proteins in caveolae-like membranous domains. Proc Natl Acad Sci USA. 1996; 93(25): 14945-9.

Villalta SA, Nguyen HX, Deng B, Gotoh T, Tidball JG. Shifts in macrophage phenotypes and macrophage competition for arginine metabolism affect the severity of muscle pathology in muscular dystrophy. Hum Mol Genet. 2009; 18: 482-496.

Wagner K, Miliotis T, Marko-Varga G, Bischoff R, Unger KK. An automated on-line multidimensional HPLC system for protein and peptide mapping with integrated sample preparation. Anal Chem. 2002; 74: 809-820.

Wang X, Wu H, Zhang Z, Liu S, Yang J, Chen X, Fan M, Wang X. Effects of interleukin-6, leukemia inhibitory factor, and ciliary neurotrophic factor on the proliferation and differentiation of adult human myoblasts. Cell Mol Neurobiol. 2008; 28: 113–124.

Watt NT, Hooper NM. The prion protein and neuronal zinc homeostasis. Trends Biochem Sci 2003; 28: 406-410.

Weise J, Crome O, Sandau R, Schulz-Schaeffer W, Bähr M, Zerr I. Upregulation of cellular prion protein (PrPC) after focal cerebral ischemia and influence of lesion severity. Neurosci Lett. 2004; 372(1-2): 146-150.

Weise J, Doeppner TR, Müller T, Wrede A, Schulz-Schaeffer W, Zerr I, Witte OW, Bähr M. Overexpression of cellular prion protein alters postischemic Erk1/2 phosphorylation but not Akt phosphorylation and protects against focal cerebral ischemia. Restor Neurol Neurosci. 2008; 26(1): 57-64.

Weise J, Sandau R, Schwarting S, Crome O, Wrede A, Schulz-Schaeffer W, Zerr I, Bähr M. Deletion of cellular prion protein results in reduced Akt activation, enhanced postischemic caspase-3 activation, and exacerbation of ischemic brain injury. Stroke. 2006; 37(5): 1296-1300.

Weissmann C, Flechsig E. PrP knock-out and PrP transgenic mice in prion research. Br Med Bull. 2003; 66: 43-60.

Westermeier R, Marouga R. Protein detection methods in proteomics research. Biosci Rep. 2005; 25: 19-32.

Wilkins MR, Sanchez JC, Gooley AA, Appel RD, Humphery-Smith I, Hochstrasser DF, Williams KL. Progress with proteome projects: why all proteins expressed by a genome should be identified and how to do it. Biotechnol Genet Eng Rev. 1996; 13: 19-50.

Wolf-Yadlin A, Hautaniemi S, Lauffenburger DA, White FM. Multiple reaction monitoring for robust quantitative proteomic analysis of cellular signaling networks. Proc. Natl. Acad. Sci. USA. 2007; 104: 5860-5865.

Wu Z, Woodring PJ, Bhakta KS, Tamura K, Wen F, Feramisco JR, Karin M, Wang JY, Puri PL. p38 and extracellular signal-regulated kinases regulate the myogenic program at multiple steps. Mol Cell Biol. 2000; 20: 3951-3964.

Zammit PS, Golding JP, NagataY, Hudon V, Partridge TA, Beauchamp JR. Muscle satellite cells adopt divergent fates: a mechanism for self-renewal? J. Cell Biol. 2004; 166: 347-357.

Zammit PS, Partridge TA, Yablonka-Reuveni Z. The skeletal muscle satellite cell: the stem cell that came in from the cold. J Histochem Cytochem. 2006; 54(11): 1177-1191.

Zanata SM, Lopes MH, Mercadante AF, Hajj GN, Chiarini LB, Nomizo R, Freitas AR, Cabral AL, Lee KS, Juliano MA, de Oliveira E, Jachieri SG, Burlingame A, Huang L, Linden R, Brentani RR, Martins VR. Stress-inducible protein 1 is a cell surface ligand for cellular prion that triggers neuroprotection. EMBO J. 2002; 21(13): 3307-3316.

Zanusso G, Vattemi G, Ferrari S, Tabaton M, Pecini E, Cavallaro T, Tomelleri G, Filosto M, Tonin P, Nardelli E, Rizzuto N, Monaco S. Increased expression of the normal cellular isoform of prion protein in inclusion-body myositis, inflammatory myopathies and denervation atrophy. Brain Pathol. 2001; 11(2): 182-189.

Zhan M, Jin B, Chen SE, Reecy JM, Li YP. TACE release of TNFalpha mediates mechanotransduction induced activation of p38 MAPK and myogenesis. J Cell Sci. 2007; 120: 692-701.

Zhang CC, Steele AD, Lindquist S, Lodish HF. Prion protein is expressed on long-term repopulating hematopoietic stem cells and is important for their self-renewal. Proc Natl Acad Sci USA. 2006; 103(7): 2184-2189.